X-ray microscopy

Slides: https://tinyurl.com/y5kdrxxo

Chris Jacobsen

Argonne Distinguished Fellow
Advanced Photon Source
Argonne National Laboratory
Argonne, Illinois, USA

Professor, Department of Physics & Astronomy; Applied Physics; Chemistry of Life Processes Institute
Northwestern University
Evanston, Illinois, USA

NU web page:
http://xrm.phys.northwestern.edu

Support: Basic Energy Sciences, US Department of Energy; National Institutes of Health

The refractive index

- Damped, driven harmonic oscillator

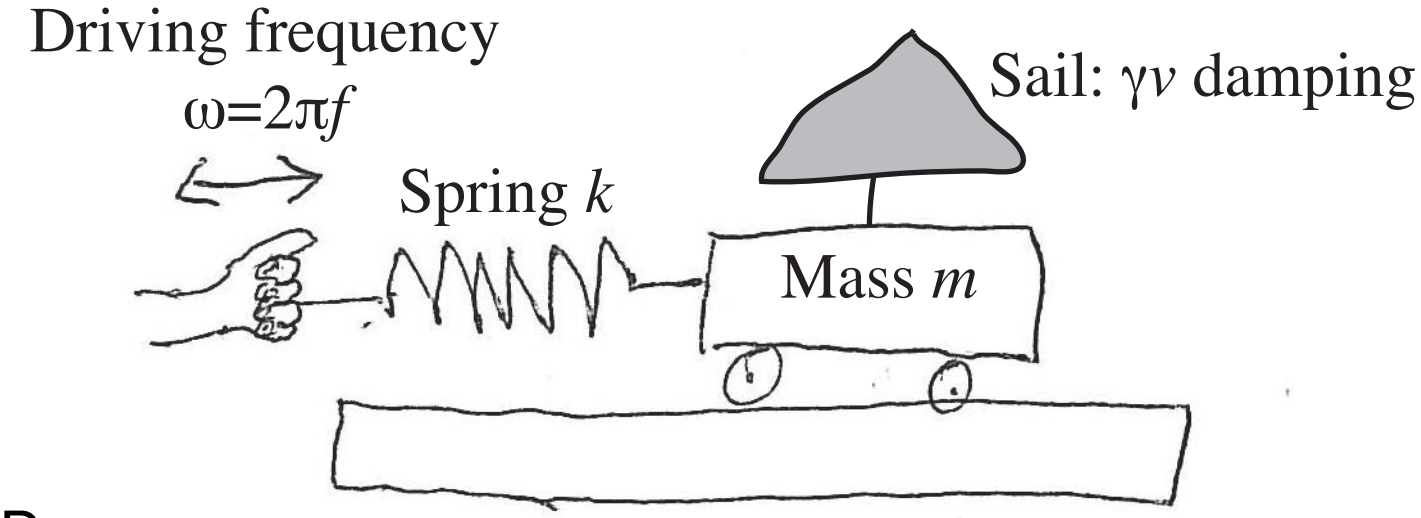

- D
- Driven: incident electromagnetic wave ω
- Harmonic oscillator: electronic quantum state with energy

$$\hbar\omega = \hbar\sqrt{k/m}$$

Damped, driven harmonic oscillator

- Single resonance: absorption peak, phase shift across resonance

$$Q = \omega_0/\gamma$$

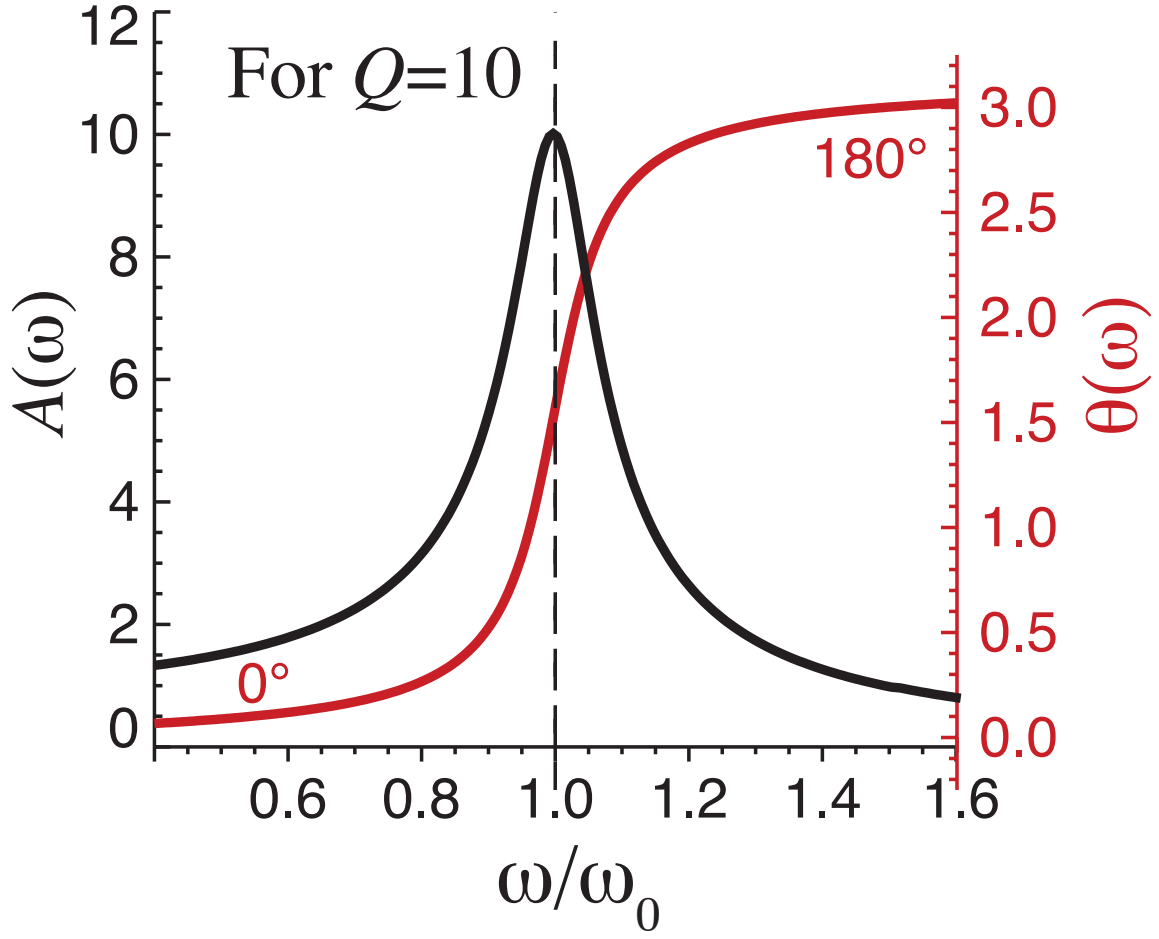

X-rays: the high frequency limit?

What's the dividing line between low and high frequency limits of refractive index? At what frequency are most of the oscillators?

Plasmon frequency

$\omega_p=(4\pi c^2 n_a r_e)^{1/2}$

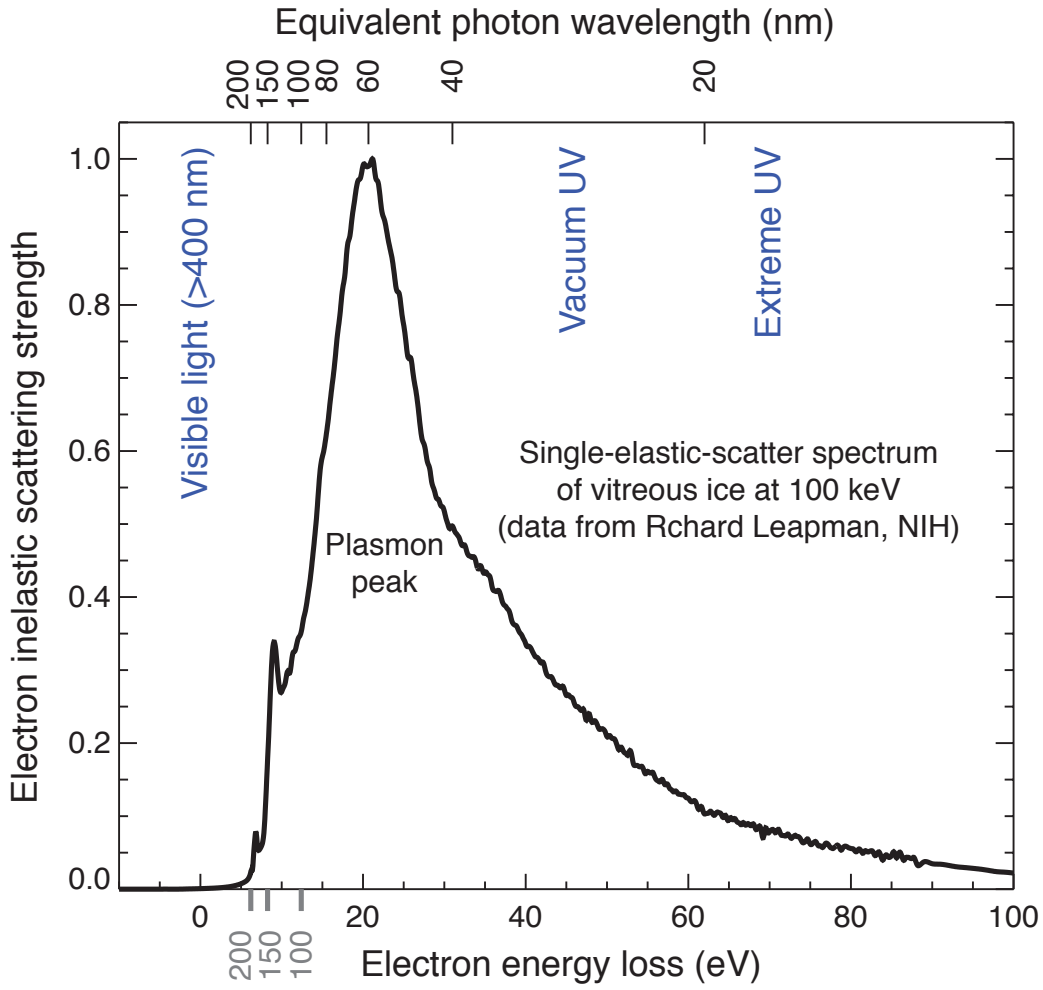

Mysteries of the x-ray refractive index

Write refractive index as

$$n = 1 - \frac{n_a r_e}{2\pi}\lambda^2(f_1 + if_2)$$

$$= 1 - \alpha\lambda^2(f_1 + if_2)$$

where n_a=# atoms/volume, and

r_e=2.818x10^{-15} m is the classical radius of the electron. Assumes exp[$-i(kx-\omega t)$] for forward propagation.

Also written as n=1-δ-iβ

Phase velocity is

$$v_p = \frac{\omega}{k} \simeq c(1 + \alpha\lambda^2 f_1)$$

Group velocity is

$$v_g = \frac{d\omega}{dk} \simeq c(1 - \alpha\lambda^2 f_1)$$

86 A. Einstein, [Nr. 9/12.

Lassen sich Brechungsexponenten der Körper für Röntgenstrahlen experimentell ermitteln?

Von A. Einstein.

(Eingegangen am 21. März 1918.)

Vor einigen Tagen erhielt ich von Herrn Prof. A. KÖHLER (Wiesbaden) eine kurze Arbeit[1]), in welcher eine auffallende Erscheinung bei Röntgenaufnahmen geschildert ist, die sich bisher nicht hat deuten lassen. Die reproduzierten Aufnahmen — zumeist menschliche Gliedmaßen darstellend — zeigen an der Kontur einen hellen Saum von etwa 1 mm Breite, in welchem die Platte heller bestrahlt zu sein scheint als in der (nicht beschatteten) Umgebung des Röntgenbildes.

Ich möchte die Fachgenossen auf diese Erscheinung hinweisen und beifügen, daß die Erscheinung wahrscheinlich auf Totalreflexion beruht. Nach der klassischen Dispersionstheorie müssen wir erwarten, daß der Brechungsexponent n für Röntgenstrahlen nahe an 1 liegt, aber im allgemeinen doch von 1 verschieden ist. n wird kleiner bzw. größer als 1 sein, je nachdem der Einfluß derjenigen Elektronen auf die Dispersion überwiegt, deren Eigenfrequenz kleiner oder größer ist als die Frequenz der Röntgenstrahlen. Die Schwierigkeit einer Bestimmung von n liegt darin, daß $(n-1)$ sehr klein ist (etwa 10^{-5}). Es ist aber leicht einzusehen, daß bei nahezu streifender Inzidenz der Röntgenstrahlen im Falle $n<1$ eine nachweisbare Totalreflexion auftreten muß.

X-ray refractive index

Refractive index of $n=1-\alpha\lambda^2(f_1+if_2)$

Real part of oscillator strength f_1 tends towards atomic number Z

Imaginary part of oscillator strength f_2 declines as E^{-2}

Phase exp[$-ink$] is advanced relative to vacuum by $2\pi\alpha\lambda f_1$

Intensity is decreased as exp[$-4\pi\alpha\lambda f_2$]

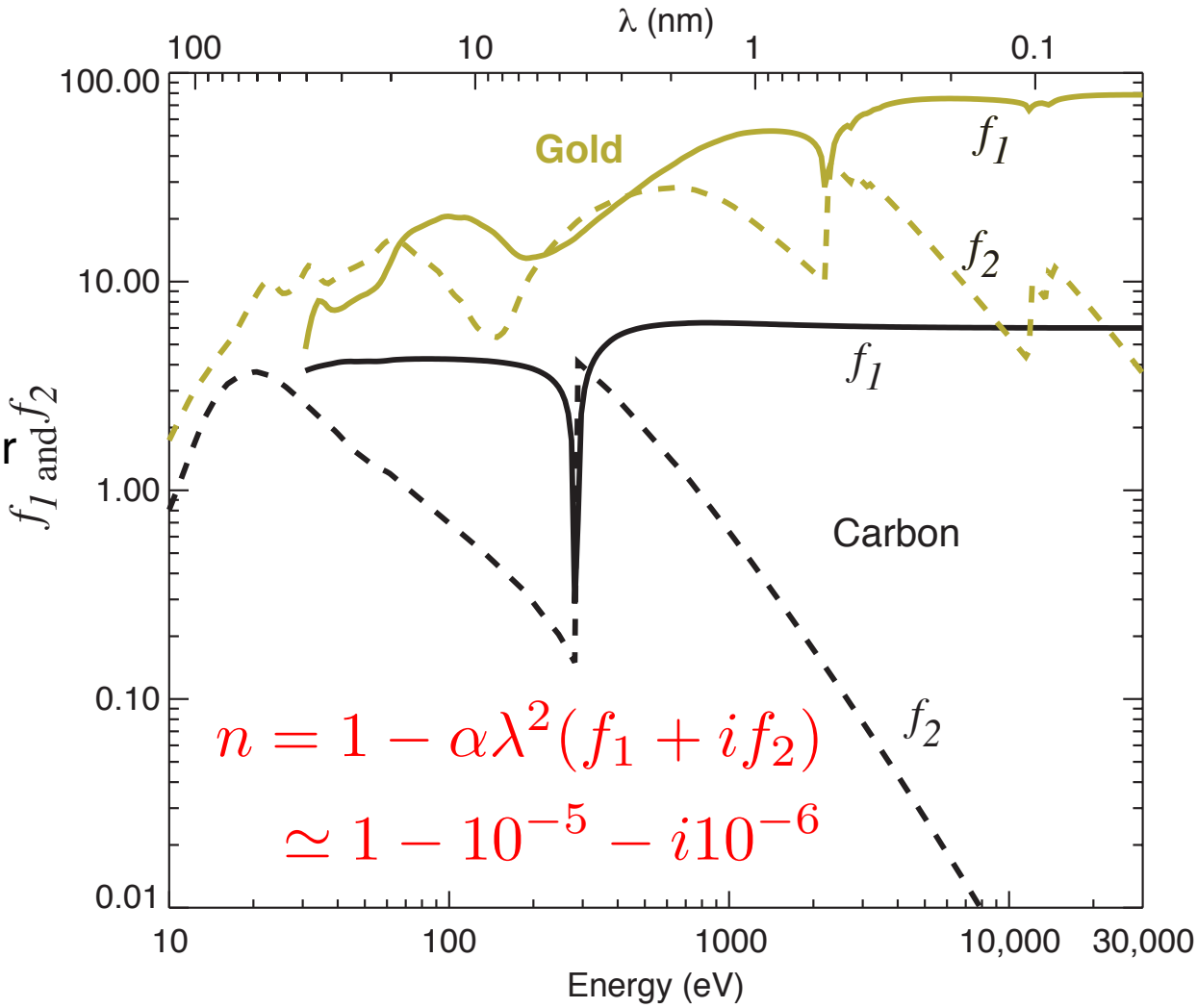

Data from http://henke.lbl.gov/optical_constants/

X rays in media

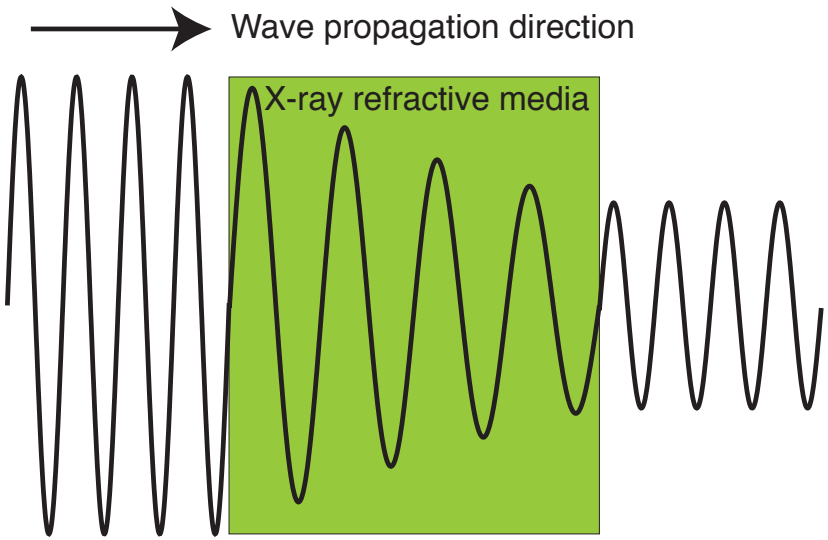

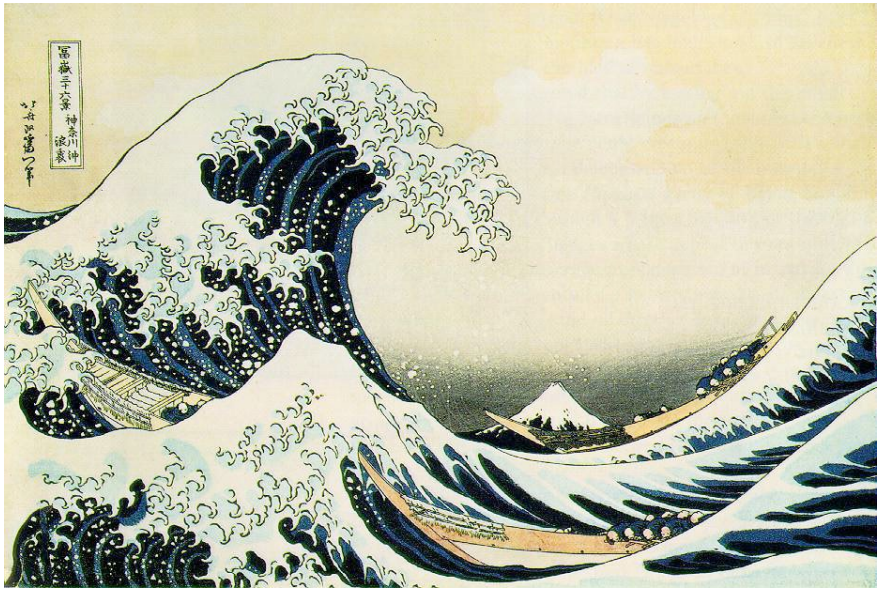

X-ray refraction

Larsson, Siegbahn, and Waller, *Naturwis*. **12**, 1212 (1924)

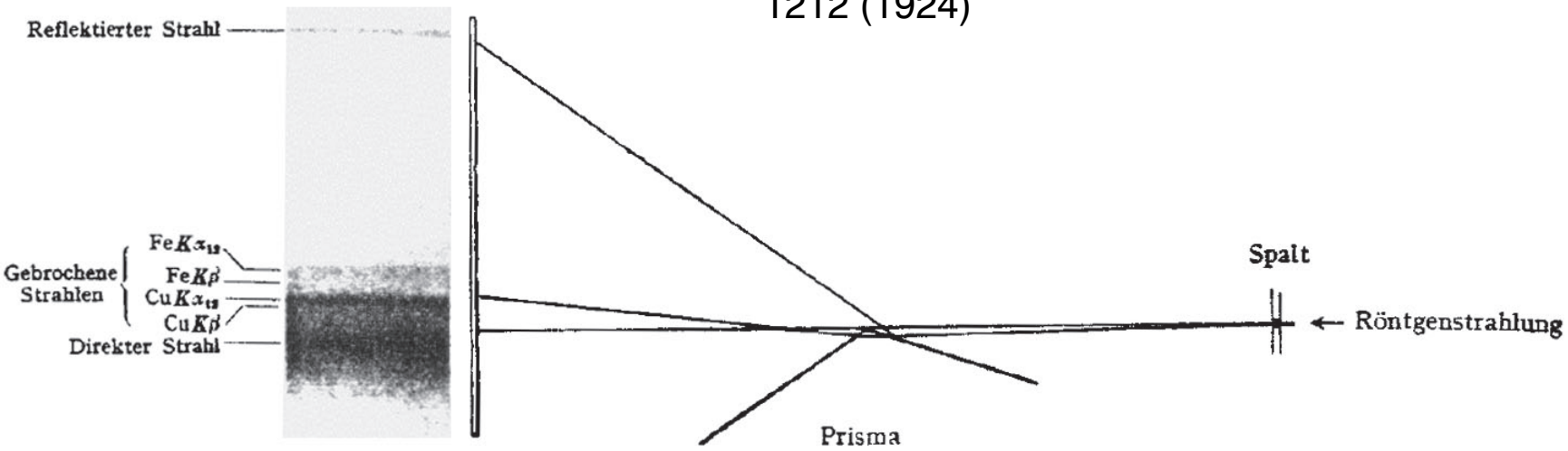

X-ray mirrors use total *internal* reflection!

- Total internal reflection happens when θ_1=90° in $n_1\sin\theta_1=n_2\sin\theta_2$, or $\theta_2=\text{asin}(n_1/n_2)$.

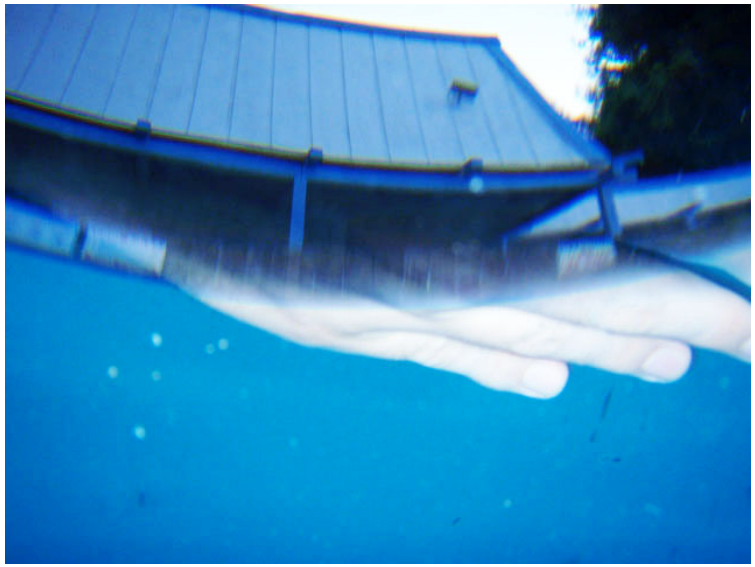

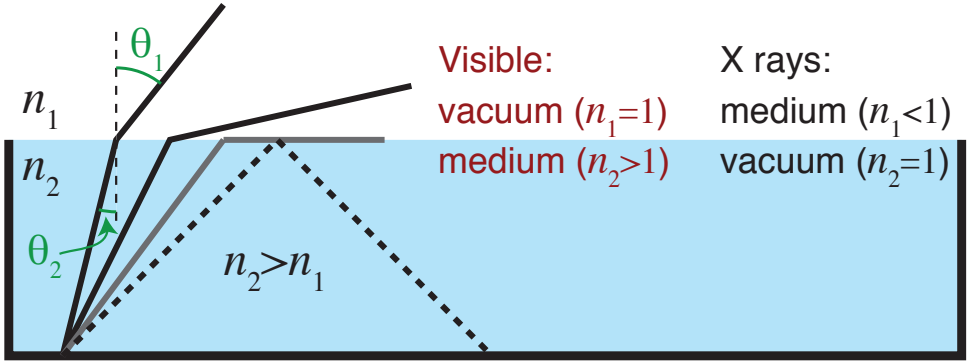

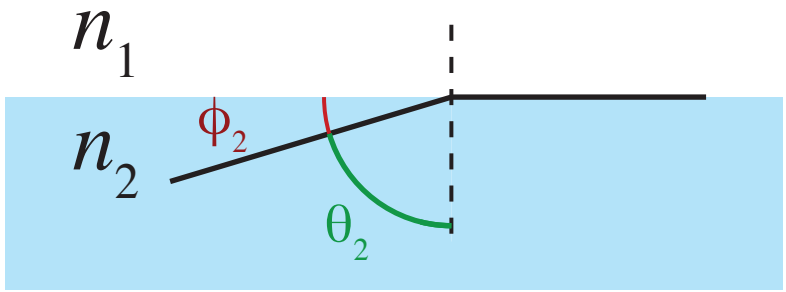

- Switch from angle θ_2 relative to normal incidence, to angle ϕ_2 relative to grazing incidence, or $\sin(\theta_2)=\cos(90°-\phi_2)=\sin(\phi_2)$
- We then have $n_1=n_2\sin(\phi_2)$ or with n_2=1 and $\sin(\phi_2)\approx1-(\phi_2)^2/2$ we have a grazing incidence critical angle of $\phi_2=\lambda(2\alpha f_1)^{1/2}$
- Note diffraction resolution limit of ϕ_2/λ is (almost) independent of wavelength!

Paul Kirkpatrick and Albert Baez, 1948

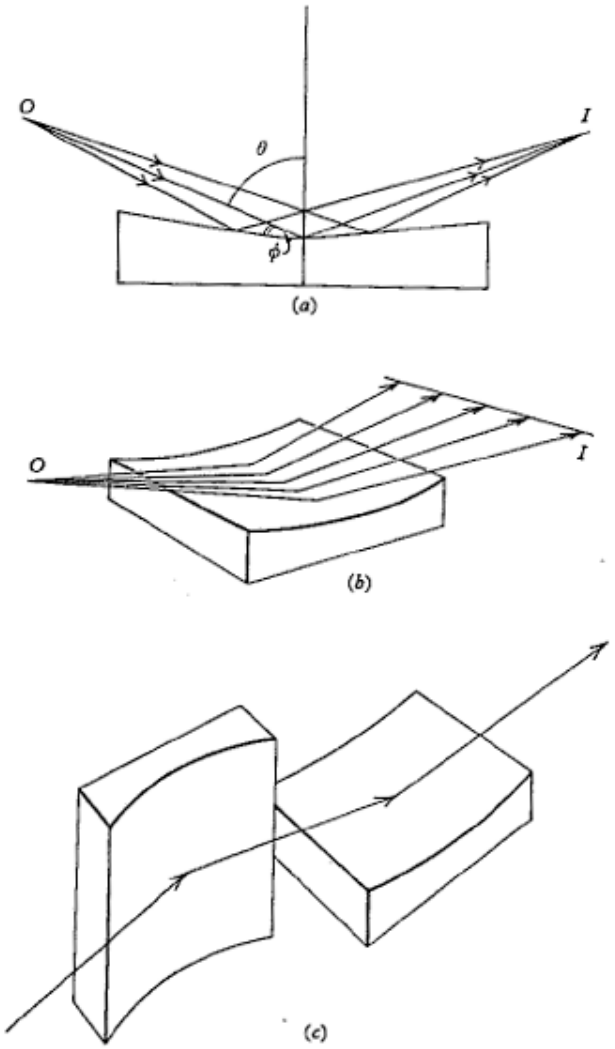

Fig. 1.2. Reflexion X-ray microscopy. (*a*) and (*b*) X-rays diverging from a source *O* are focused by a cylindrical surface to form an astigmatic image *I*; (*c*) arrangement of two cylindrical mirrors for eliminating astigmatism. (Kirkpatrick & Pattee, 1953.)

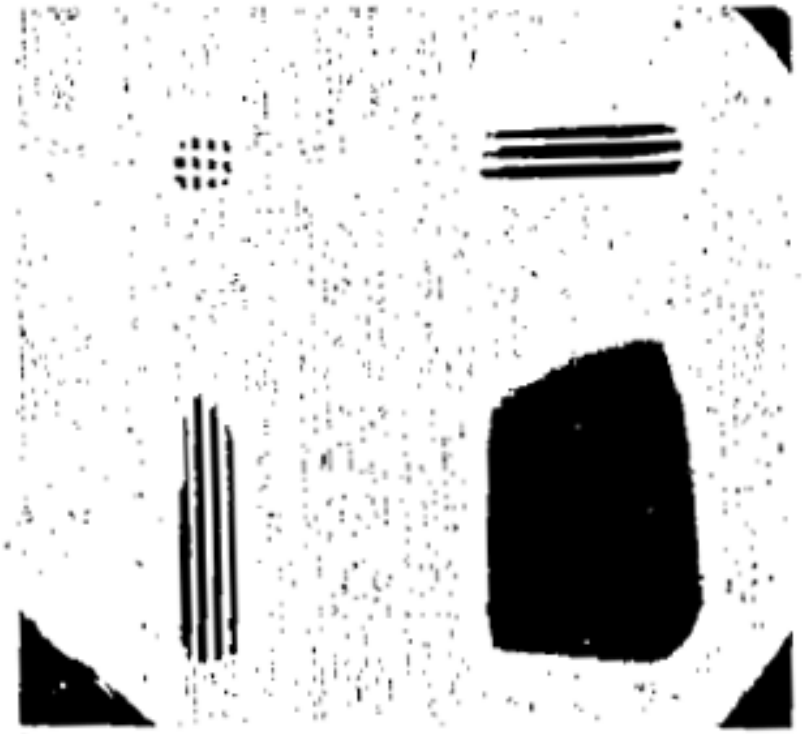

FIG. 12. Pattern produced by mirrors arranged as in Fig. 11. Object was a monel screen having 350 meshes per linear inch. In addition to the full image of the screen two partial images, each formed by one mirror, and a large spot caused by direct radiation appear above.

SCIENTIFIC AMERICAN

Established 1845

CONTENTS FOR MARCH 1949 VOLUME 180, NUMBER 3

Kirkpatrick and Pattee, 1953

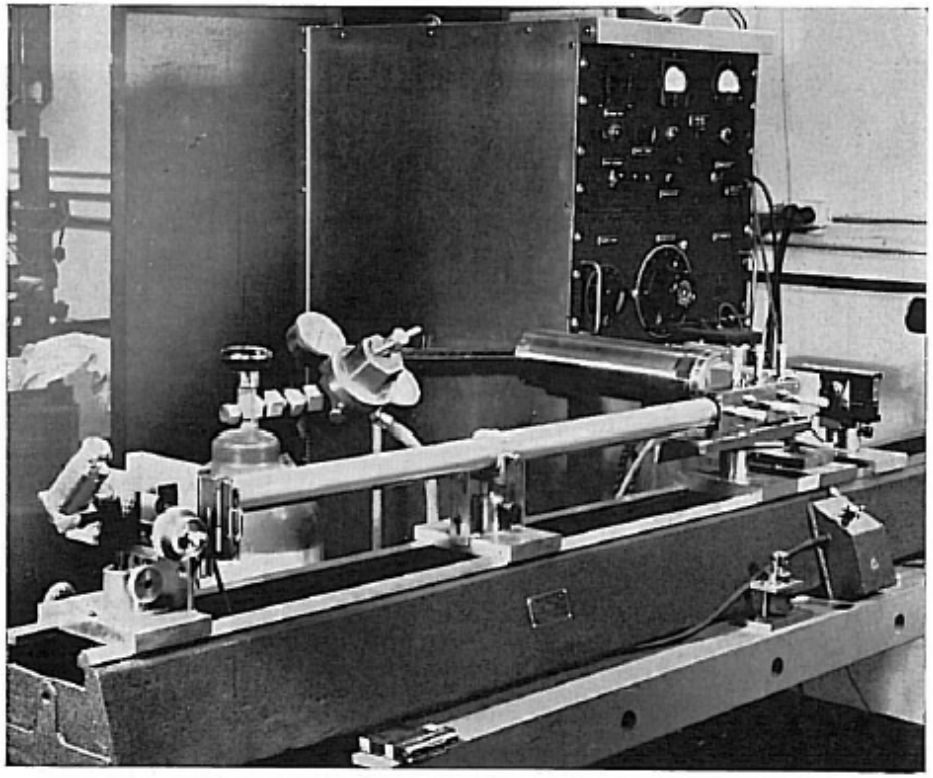

Reflexion X-ray microscope of Kirkpatrick and Pattee, incorporating two pairs of mirrors. (Kirkpatrick & Pattee, 1953.)

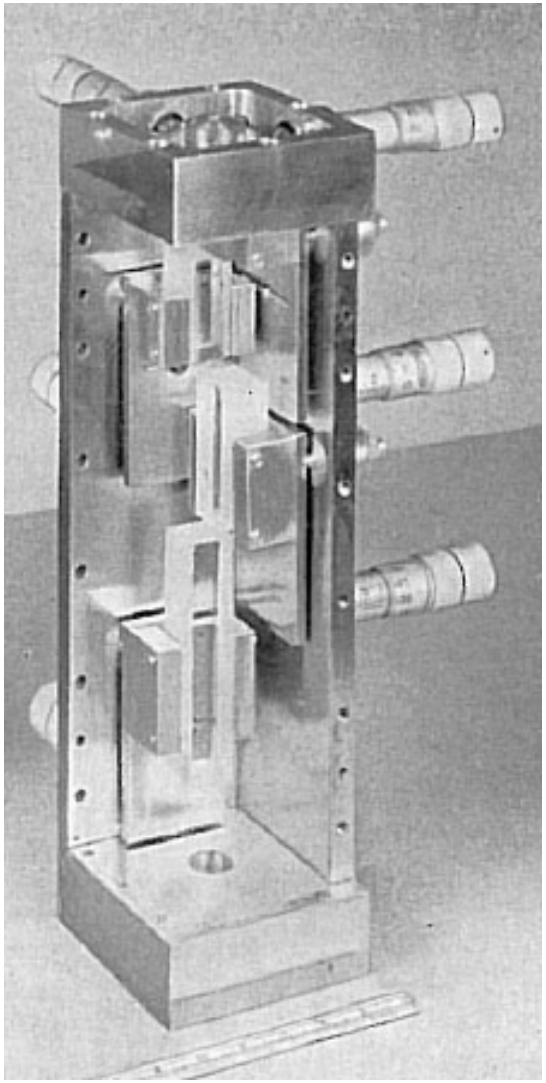

Improving the figure and roughness of mirrors

- Data provided by Lahsen Assoufid, head of the Optics Group at the APS

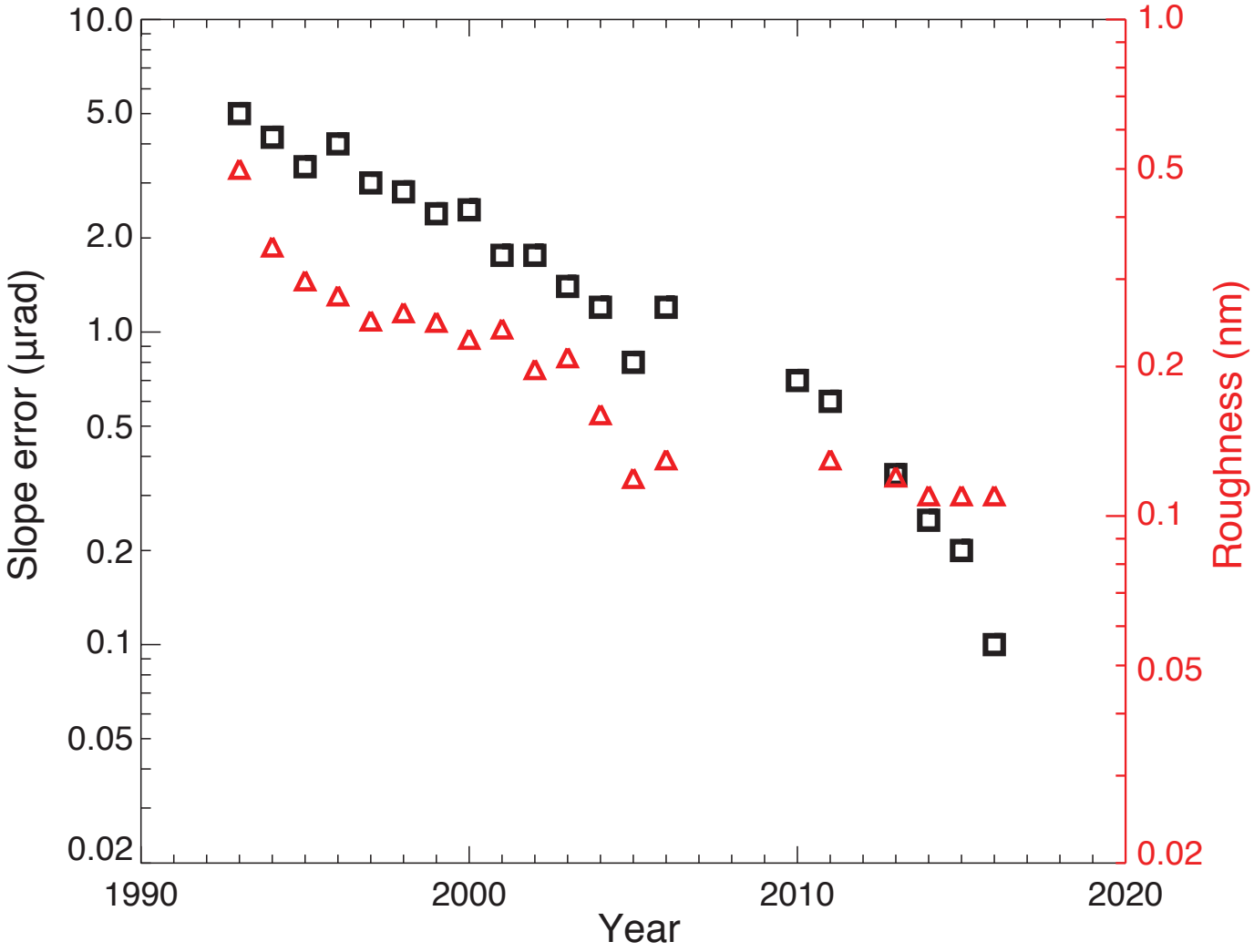

Nanofocusing with multilayer-coated KB mirrors

- da Silva, Pacureanu, Yang, Bohic, Morawe, Barrett, and Cloetens, *Optica* **4**, 492 (2017)
- FWHM of 12.0 nm (H) and 12.6 nm (V) at 17 keV

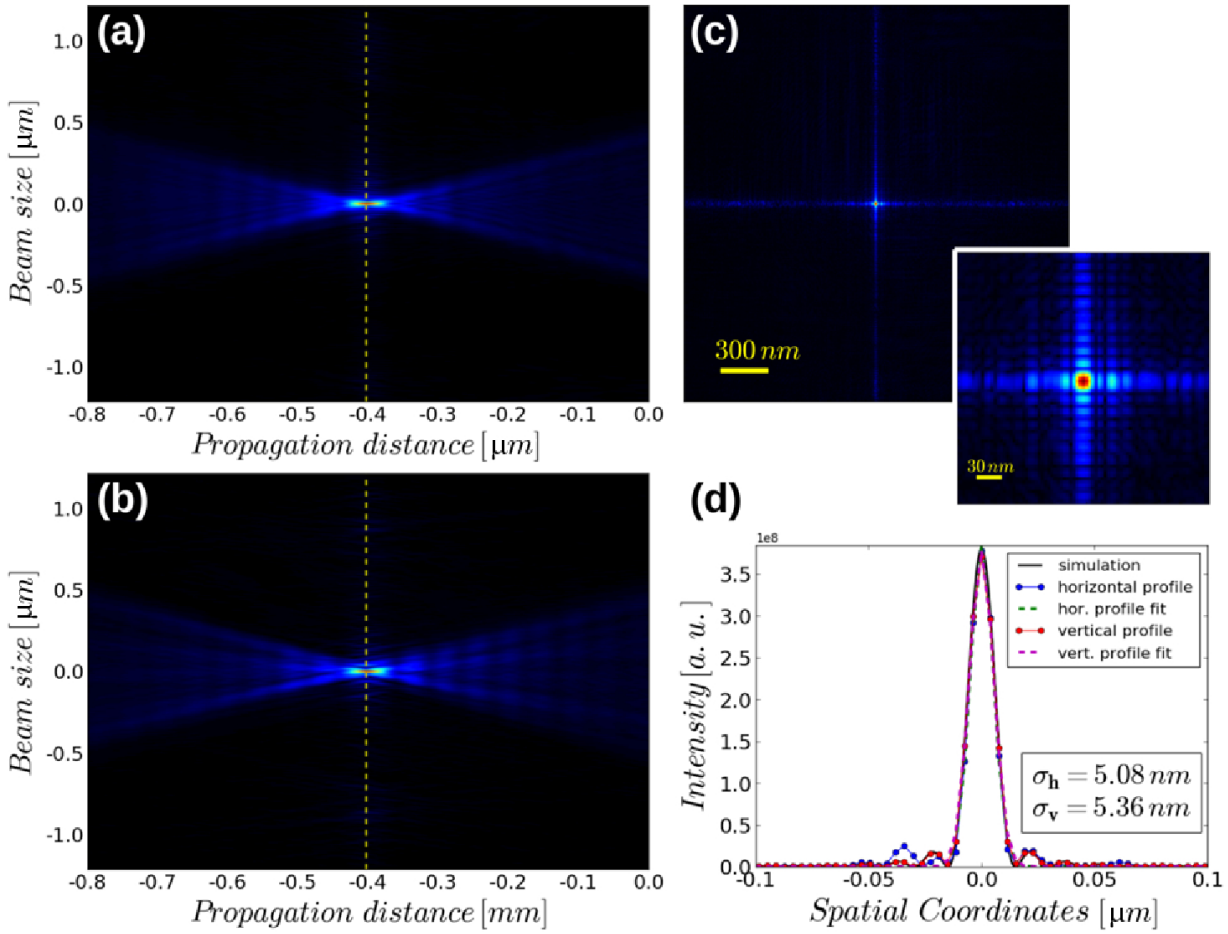

Compound refractive lenses

- Röntgen tried to make lenses, but found no focusing.
- Focal length of one lens is long – so combine many lenses! Tomie; Snigirev *et al.*, *Nature* **384**, 49 (1996); Lengeler *et al.*, *J. Synch. Rad.* **9**, 119 (2002).
- Resolution approaching 60 nm at 5-10 keV with parabolic beryllium lenses.
- Refractive lenses are especially good at 20 keV and higher.

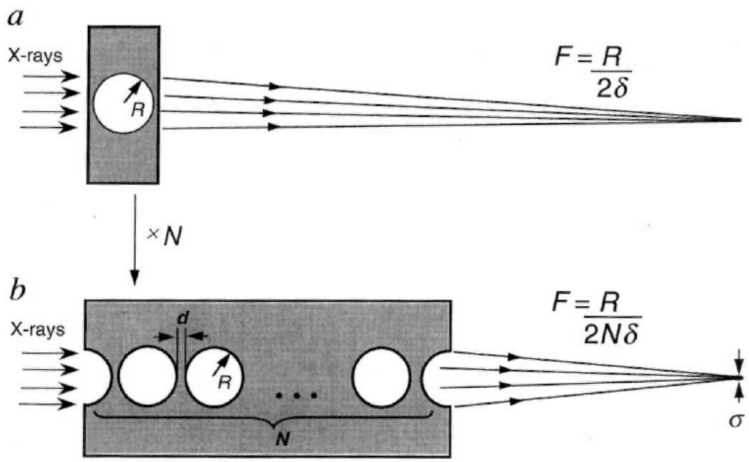

Compound refractive lenses at Universität Aachen

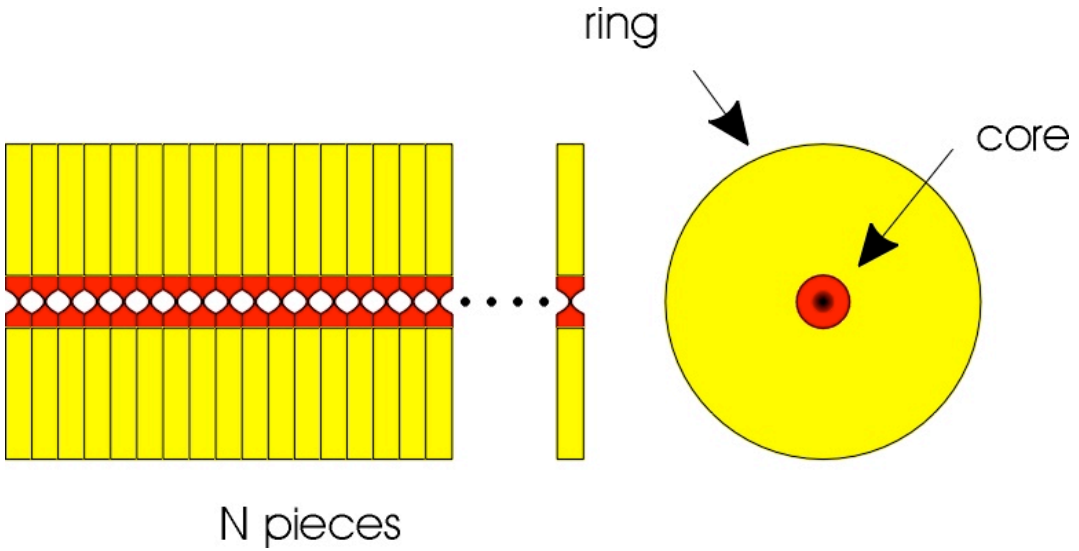

Diffractive focusing: Fresnel zone plates

- Fresnel zone construction: block out (or phase shift) every other $\lambda/2$
- Largest diffraction angle is given by outermost (finest) zone width dr_N as $\theta=\lambda/(2dr_N)$
- Rayleigh resolution is $0.61\ \lambda/(\theta)=1.22dr_N$
- Zones must be positioned to ~1/3 width over diameter (10 nm in 100 μm, or $1:10^4$)
- Diameters tend to be ~100 μm, and focal lengths tend to be ~1 mm at 300 eV and few cm at 10 keV.

Diameter *d*, outermost zone width dr_N, focal length *f*, wavelength λ:

$$d\ dr_N = f\ \lambda$$

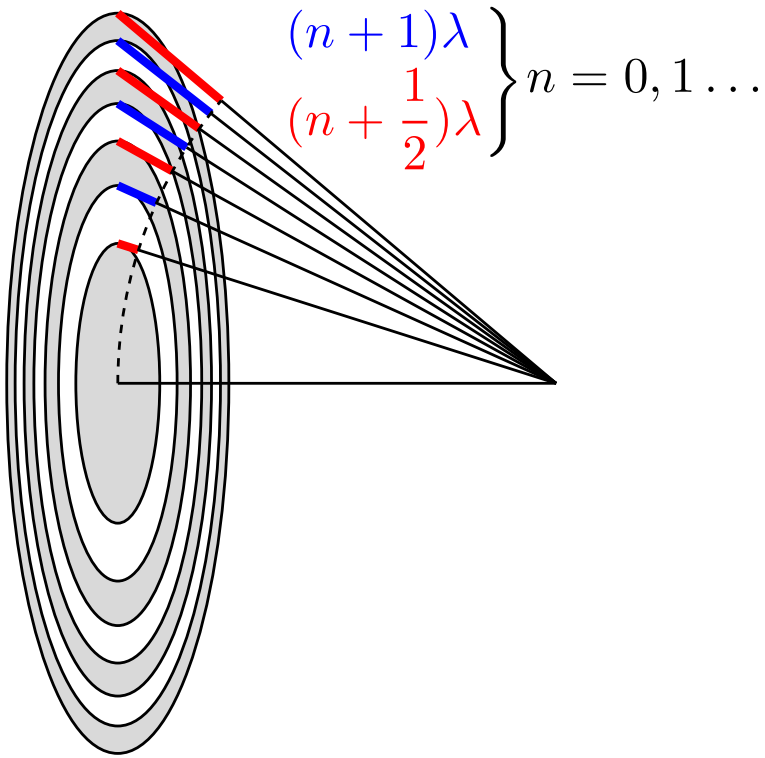

X-ray focusing: Fresnel zone plates

- Diffractive optics: radially varied grating spacing
- Largest diffraction angle is given by outermost (finest) zone width dr_N as $\theta=\lambda/(2dr_N)$
- Rayleigh resolution is $0.61\ \lambda/(\theta)=1.22dr_N$
- Zones must be positioned to ~1/3 width over diameter (10 nm in 100 μm, or $1:10^4$)
- Diameters tend to be ~100 μm, and focal lengths tend to be ~1 mm at 300 eV and few cm at 10 keV.

Diameter d, outermost zone width dr_N, focal length f, wavelength λ:

$$d\ dr_N = f\ \lambda$$

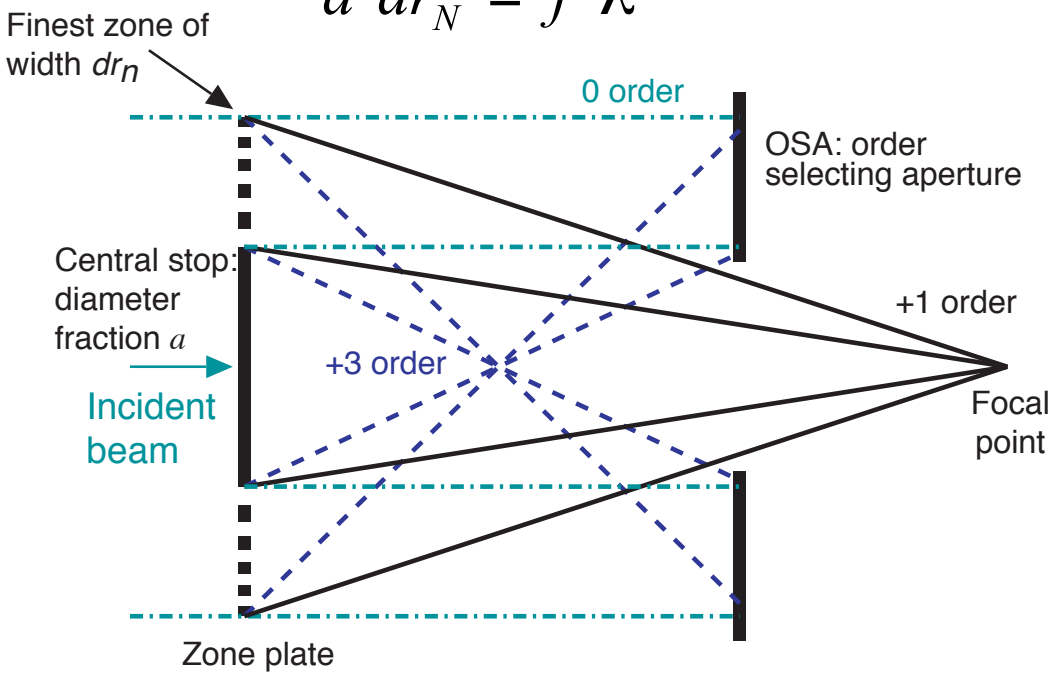

Central stop and order sorting aperture (OSA) to isolate first order focus

Zone plate efficiency and thickness

For binary zones, 1:1 mark:space ratio.
See Kirz, *J. Opt. Soc. Am.* **64**, 301 (1974)

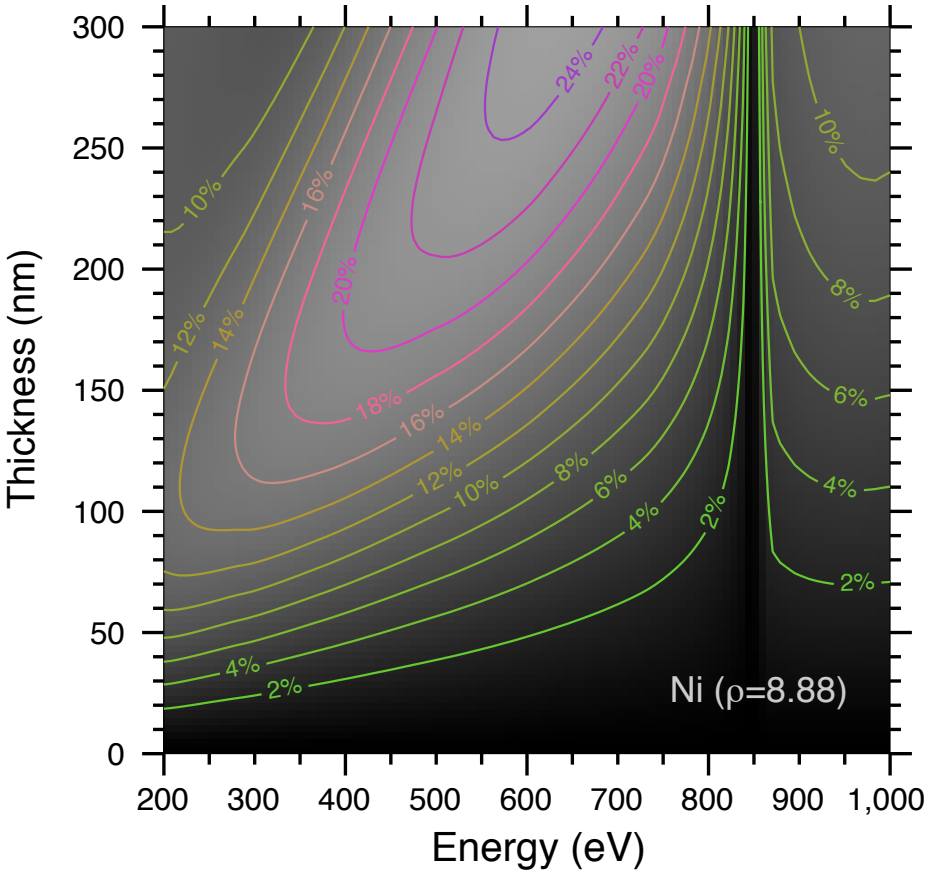

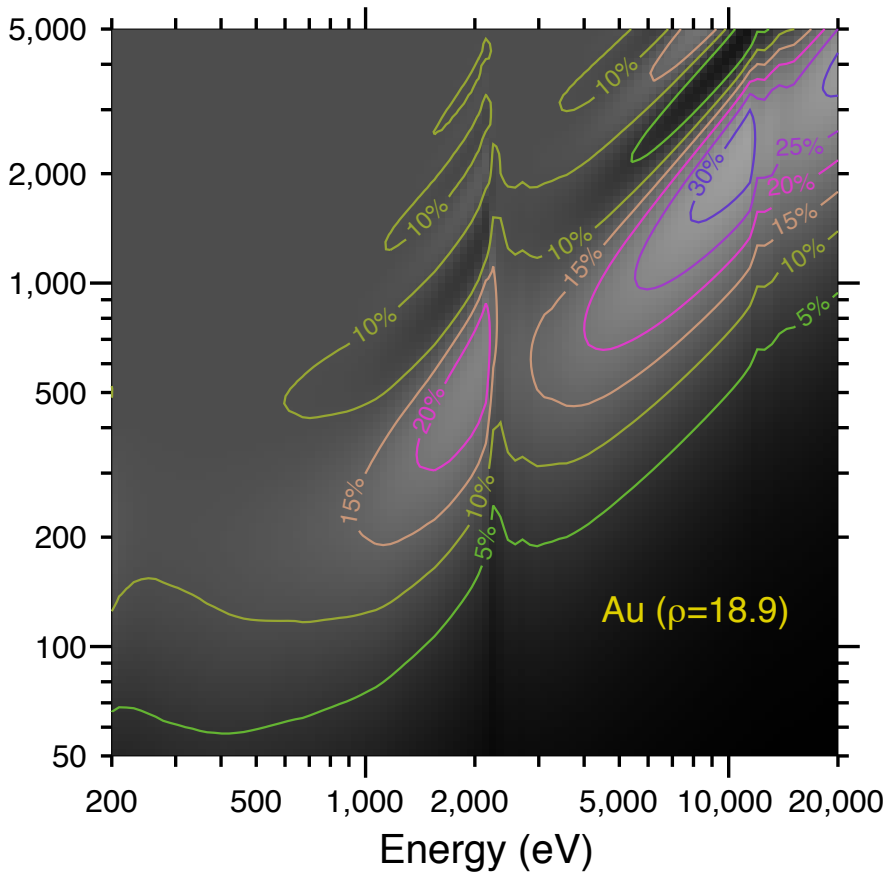

Zone plates by electron beam lithography

- Electron beam lithography: produces the finest possible structures (other than what nature can be persuaded to make by itself)
  - Example: JEOL JBX-9300FS: 1 nA into 4 nm spot, 1.2 nm over 500 μm, 100 keV
- Electrons scatter within resist, so highest resolution is only within ~100 nm thickness.
- Use directional etching methods like reactive ion etching for thick structures

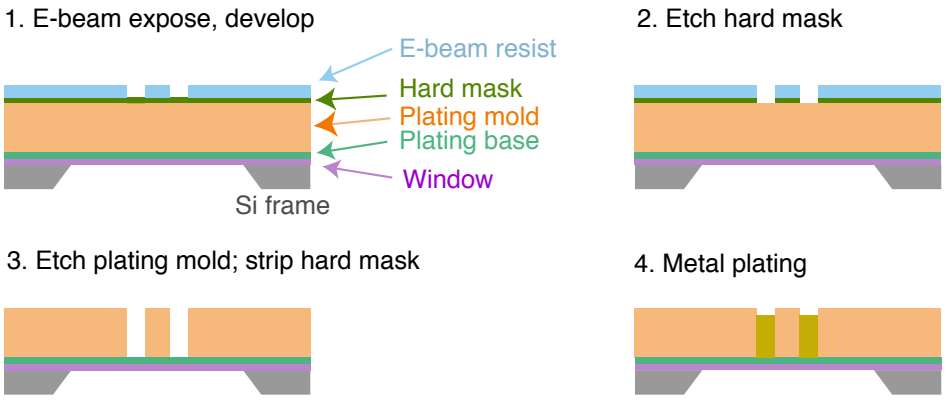

A. Stein and JBX-9300FS

Improving single zone plates: zone doubling

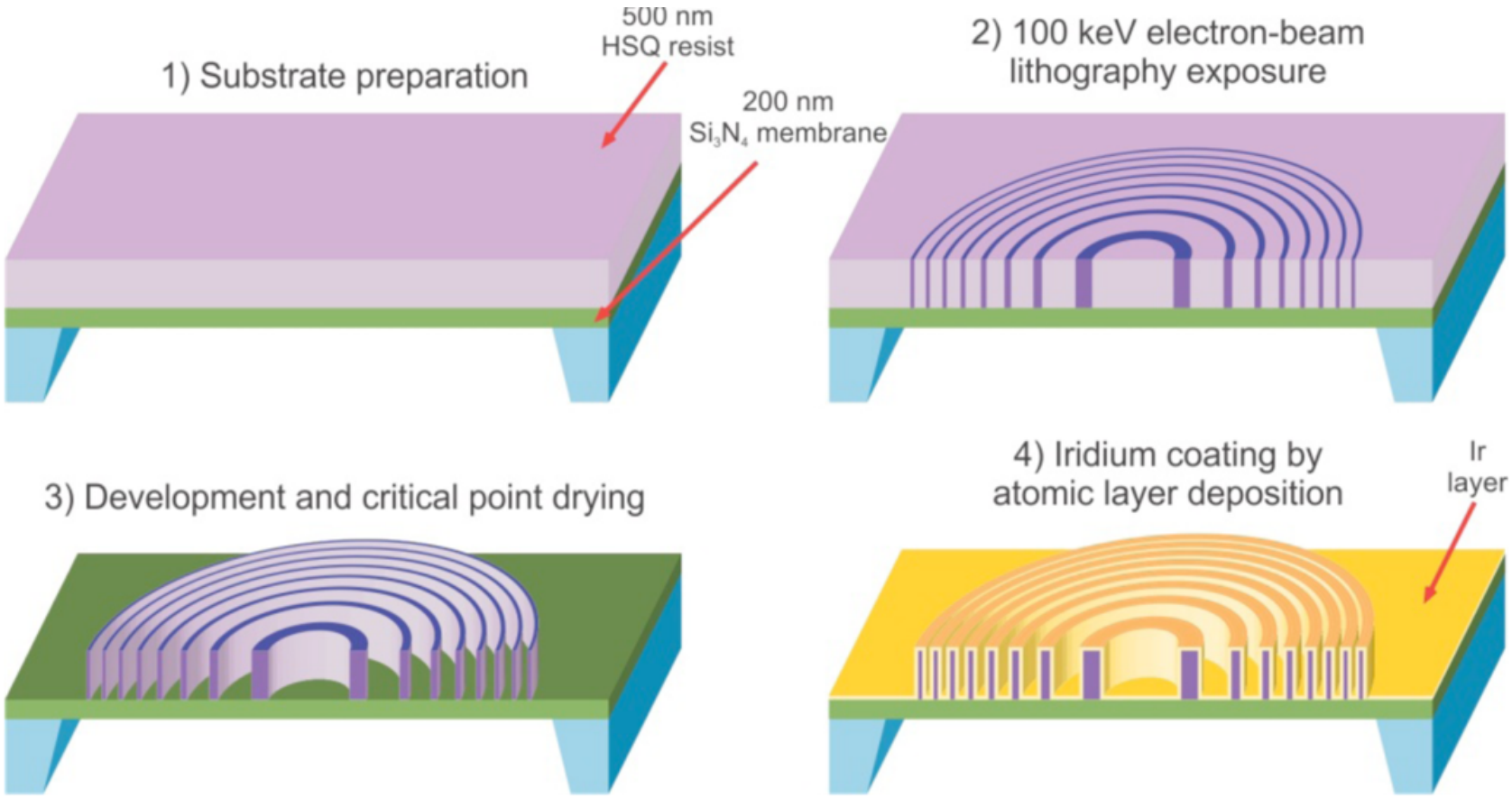

Jefimovs *et al.*, *Phys. Rev. Lett.* **99**, 264801 (2007).

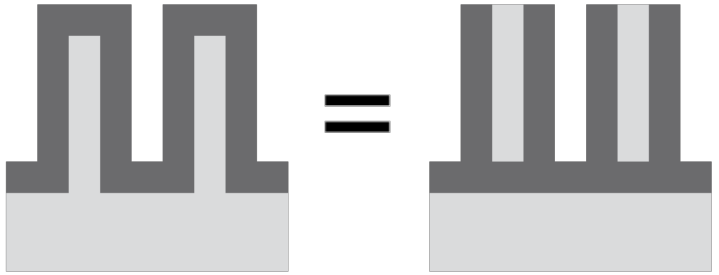

Fresnel zone plates for x-ray nanofocusing

14 nm zone width in Pt, up to 8 μm tall (aspect ratio=500). 6% efficient at 20 keV in preliminary tests; resolution tests underway.

Kenan Li, M. Wojcik, R. Divan, L. Ocola, B. Shi, D. Rosenmann, and C. Jacobsen, *J. Vac. Sci. Tech. B* (Nov. 2017)

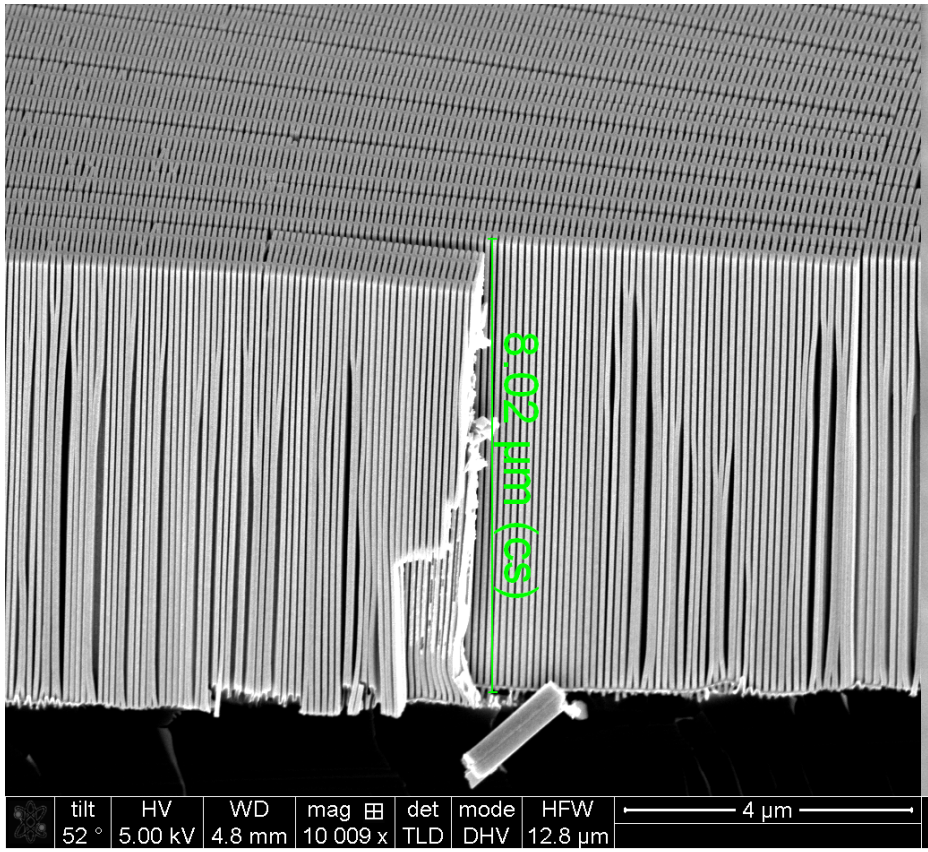

Metal-assisted chemical etching of silicon and atomic layer deposition to produce Pt zones.
14 nm wide zones that are 8 μm tall!
Aspect ratio>500

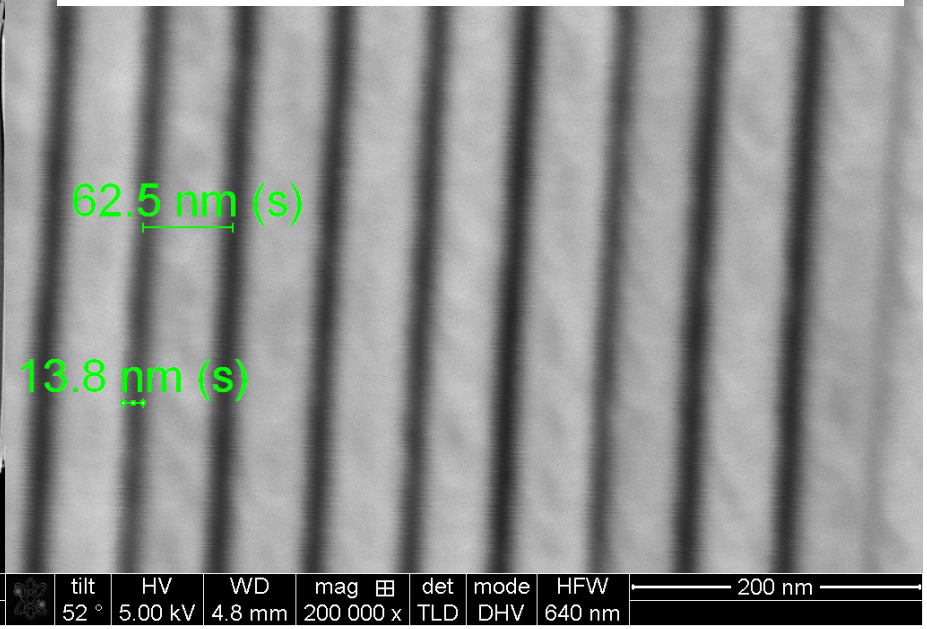

Recent APS/CNM/NU results: off the charts, on a log scale!

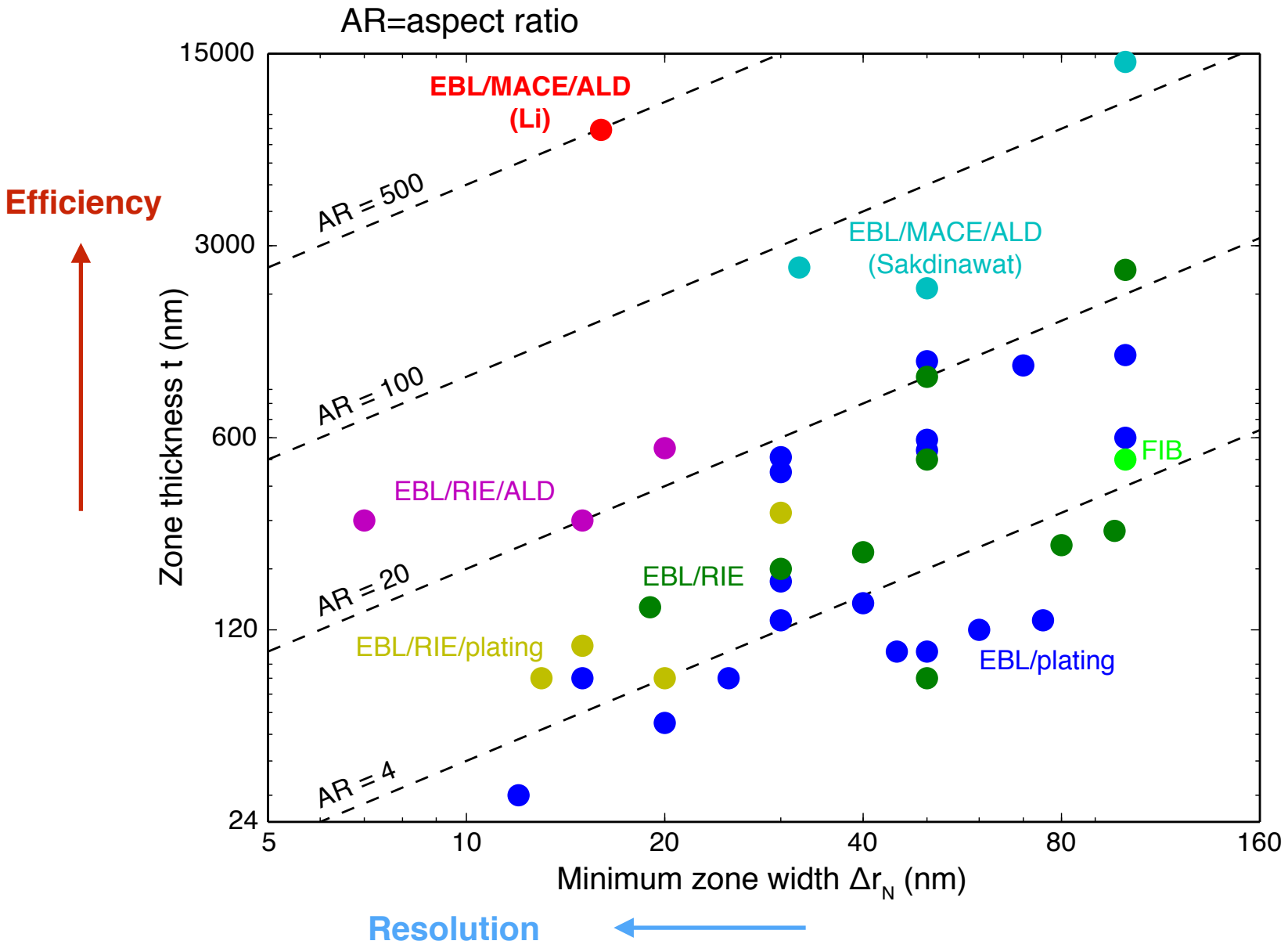

Recent tests at Brookhaven Lab

- 14 nm FWHM probe size at 12 keV, with 10^8 photons/second in the focus
- Northwestern University: Kenan Li, Sajid Ali, Chris Jacobsen
- Argonne Lab: Michael Wojcik
- Brookhaven Lab: Xiaojing Huang, Hanfei Yan, Yong Chu, Ajith Pattammattel, Evgueni Nazaretski

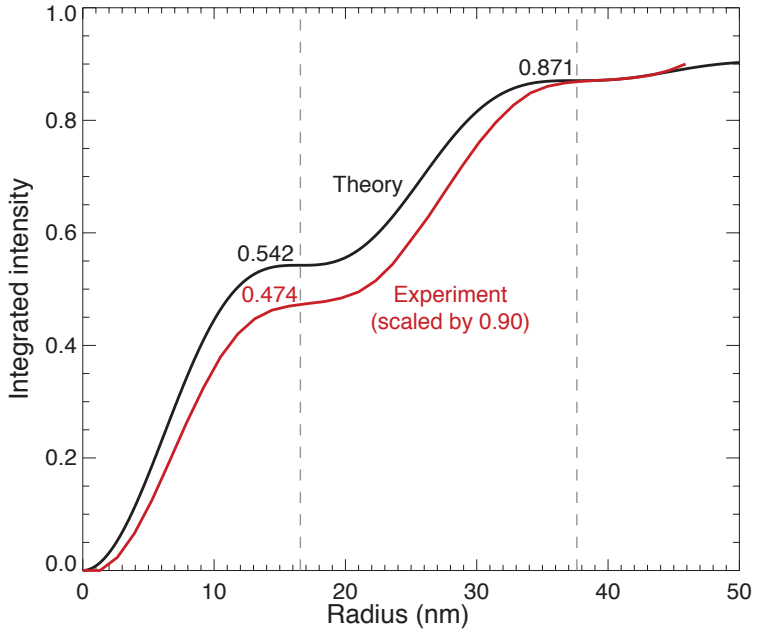

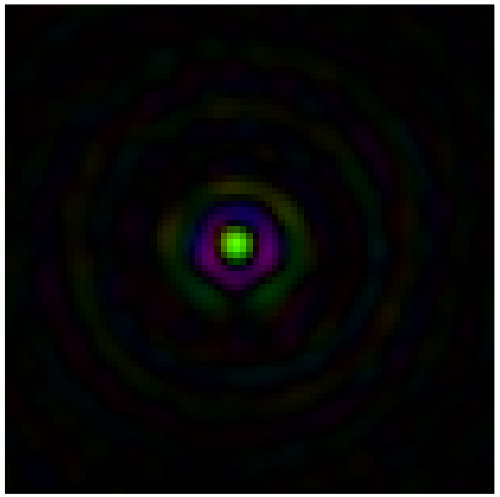

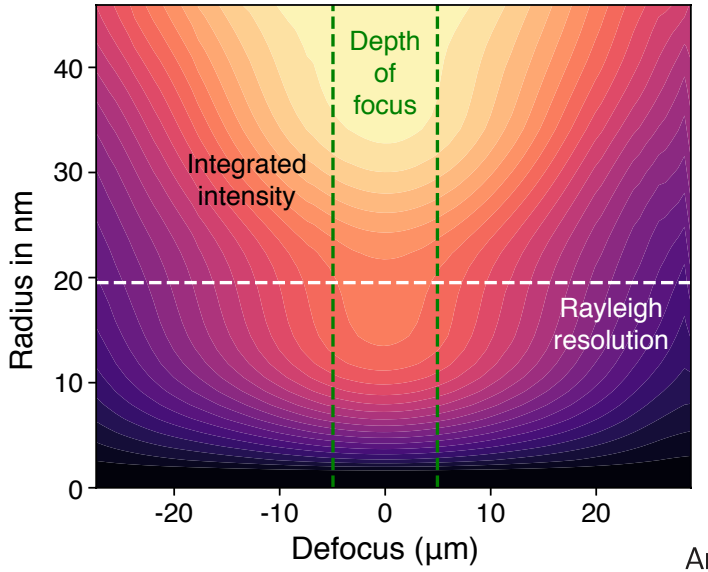

X-ray nanofocusing approaches are improving

- Visible light microscopy: better than 30 nm using centroid of Rayleigh blur of sparse/ switchable emitters
- Electron microscopy: aberration-corrected microscopes reach below 0.1 nm resolution
- X-ray microscopy: reaching 10 nm resolution for demonstrations on robust samples

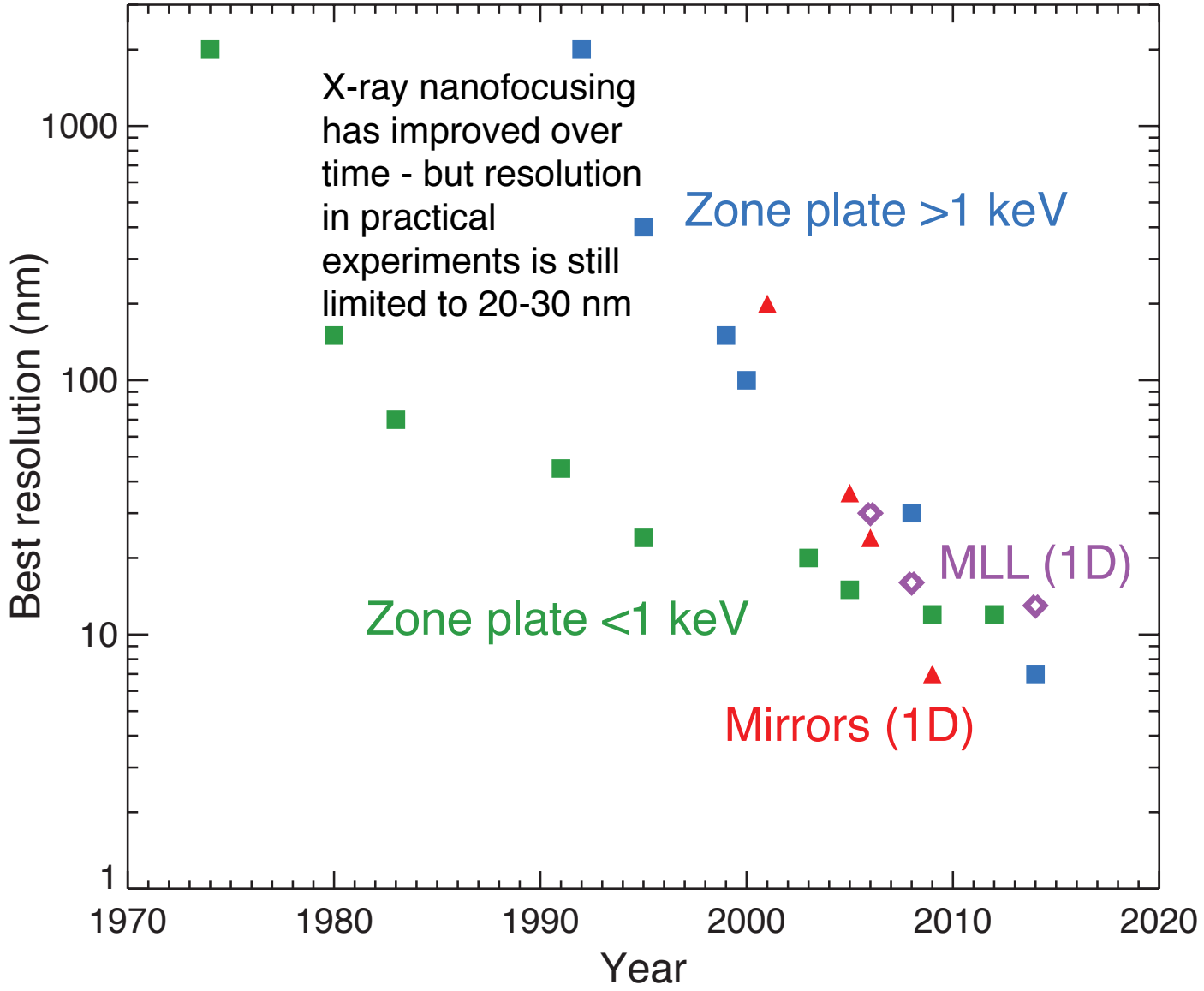

Zone plate microscopes

Full-field: transmission x-ray microscope (TXM)

- Incoherent illumination; works well with a bending magnet or a laboratory source
- Inefficient zone plate is *after* the sample (higher radiation dose)
- Faster (pixels in parallel)
- If zone plate condensers are used as monochromators, poor spectral resolution
- Transmission or reflection imaging

TXM: transmission x-ray microscope

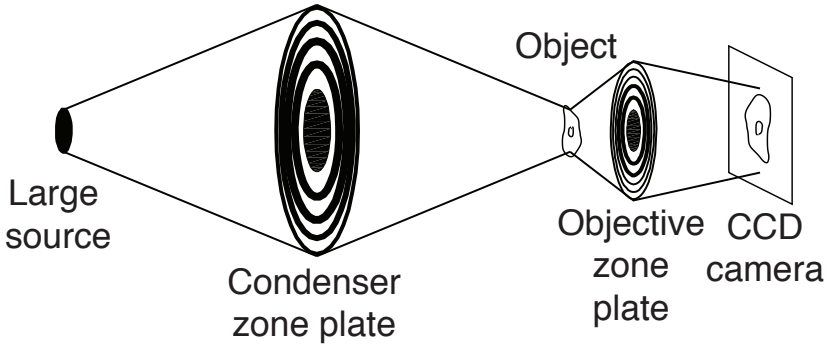

Scanning transmission x-ray microscope (STXM)

- Coherent illumination; works best with an undulator
- Inefficient zone plate is *before* the sample (lower radiation dose)
- Slower (pixels one-by-one)
- Unlimited field of view and magnification (scanning stages)
- Better suited to high resolution monochromators
- Flexible modalities: fluorescence etc.

STXM: scanning transmission x-ray microscope

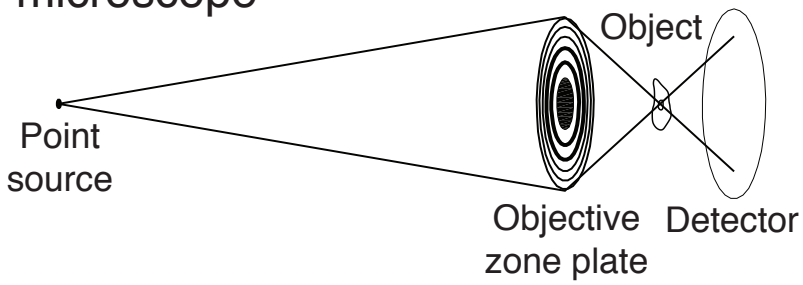

Nanofocusing requires coherent illumination

- Full-width, full-angle phase space of a diffraction limited lens with numerical aperture θ: (2θ)·(2·0.61λ/θ)=2.44λ
- Thus need to limit source phase space to ~λ both in x and y

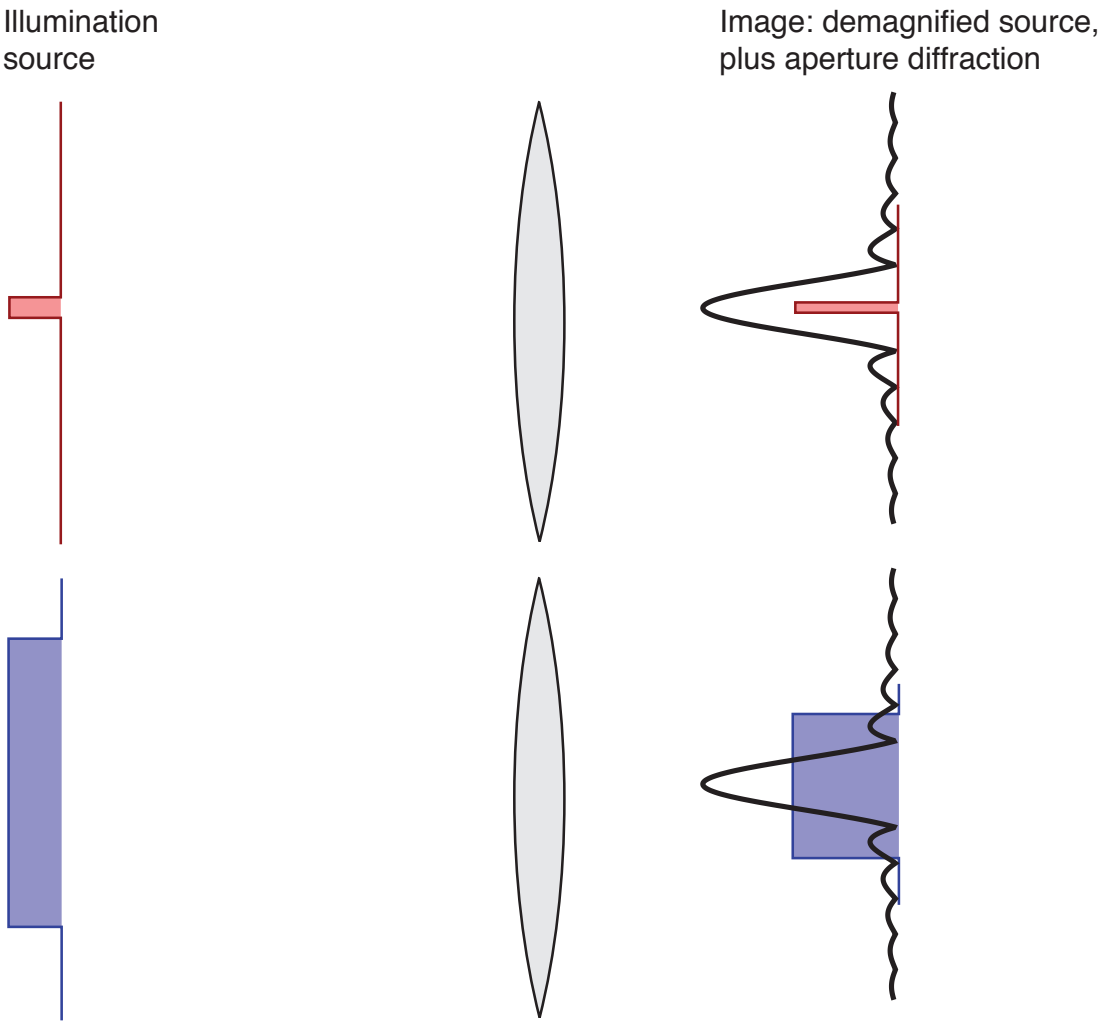

Controlling spatial coherence

- Spatial filter: pinhole at the focus of a lens. Passes only the spatially coherent fraction of an incident beam.
- X-ray beamlines: image the source to a secondary position with an aperture, for a flux-versus-coherence tradeoff.

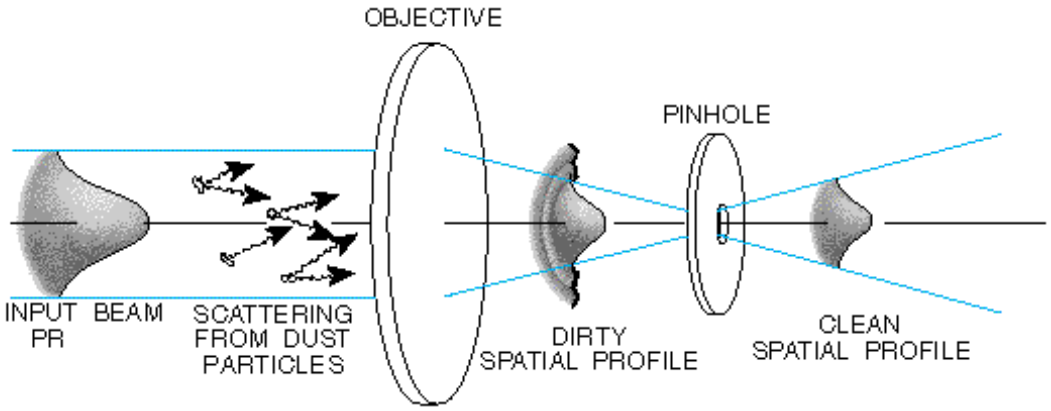

Diagram, photo from Newport catalog

Phase space area and probe focus

How close must p=(source diameter)•(optic's full subtended angle) be to λ? $p \approx 1 \cdot \lambda$ works pretty well!

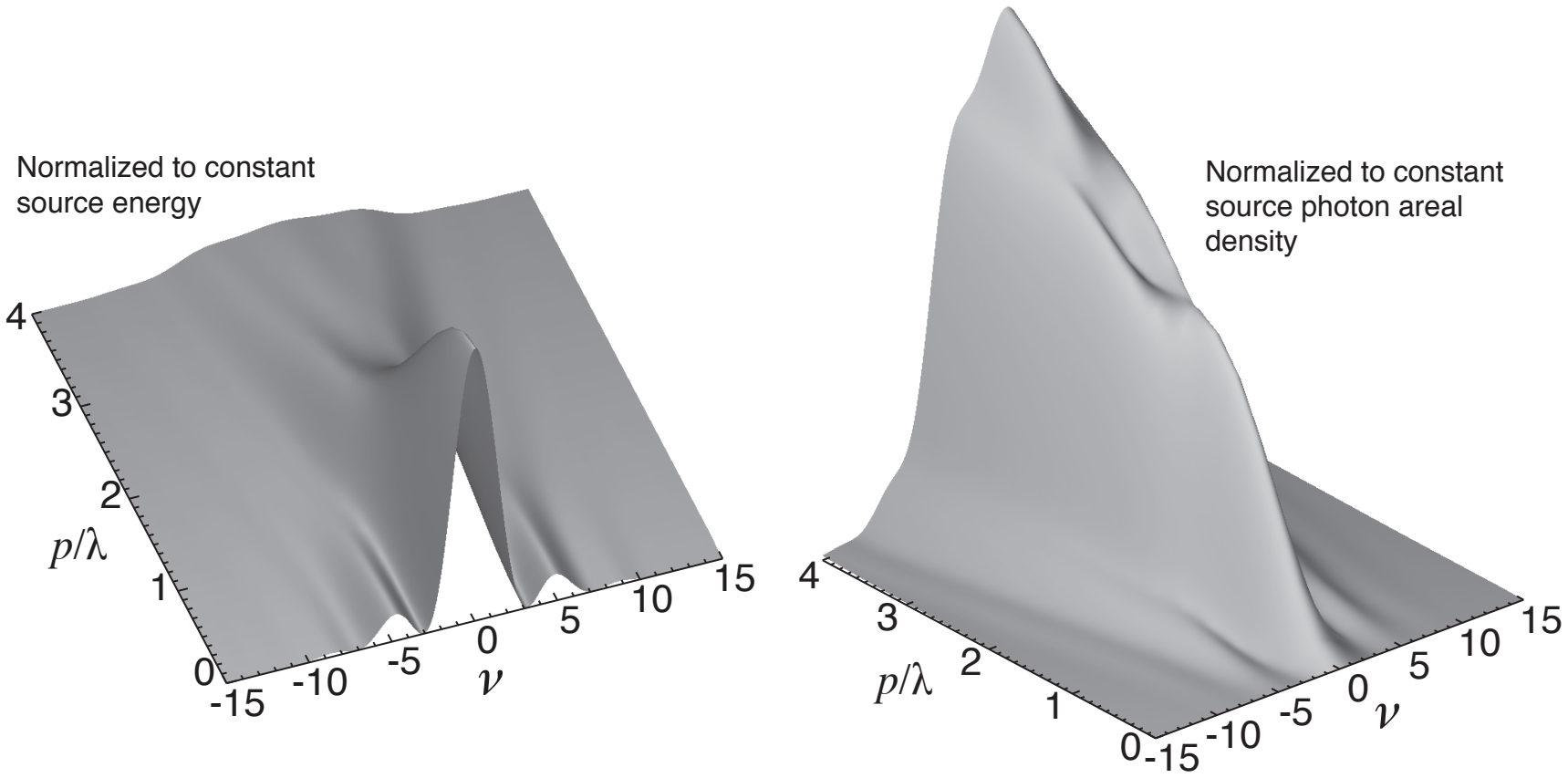

Effect on point spread function PSF (50% central stop)

Jacobsen *et al.*, *Ultramicroscopy* **47**, 55 (1992); Winn *et al.*, *J. Synch. Rad.* **7**, 395 (2000).

How to limit modes?

- Approach 1: distance, with a single nanofocusing optic.
  - Need to demagnify the source size in one step; for a fixed focal length (thus working distance) optic, you need a longer beamline.
  - Example: 40 μm to 20 nm in 200/0.1 meters. Total length: **200 m**.
  - For an optic with fixed diameter (and thus numerical aperture, and resolution), you have no flux-versus-resolution tradeoff.

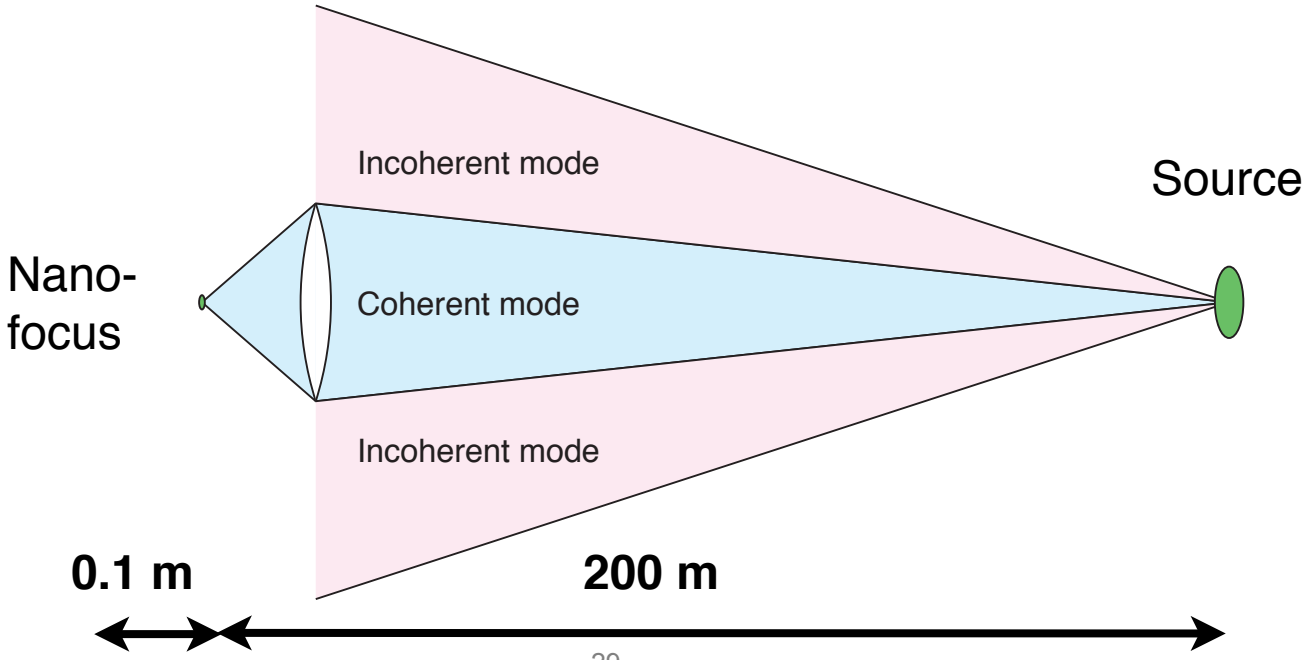

How to limit modes?

- Approach 2: aperture at an intermediate focus.
  - Two-stage demagnification means you can work with a shorter beamline!
  - Example: demagnify source size from 40 μm to 4 μm in 30/3 meters, then 4 μm to 20 nm in 20/0.1 meters. Total length 30+3+20=**53 m**.
  - You can adjust your intermediate aperture and have a flux-versus-resolution tradeoff.

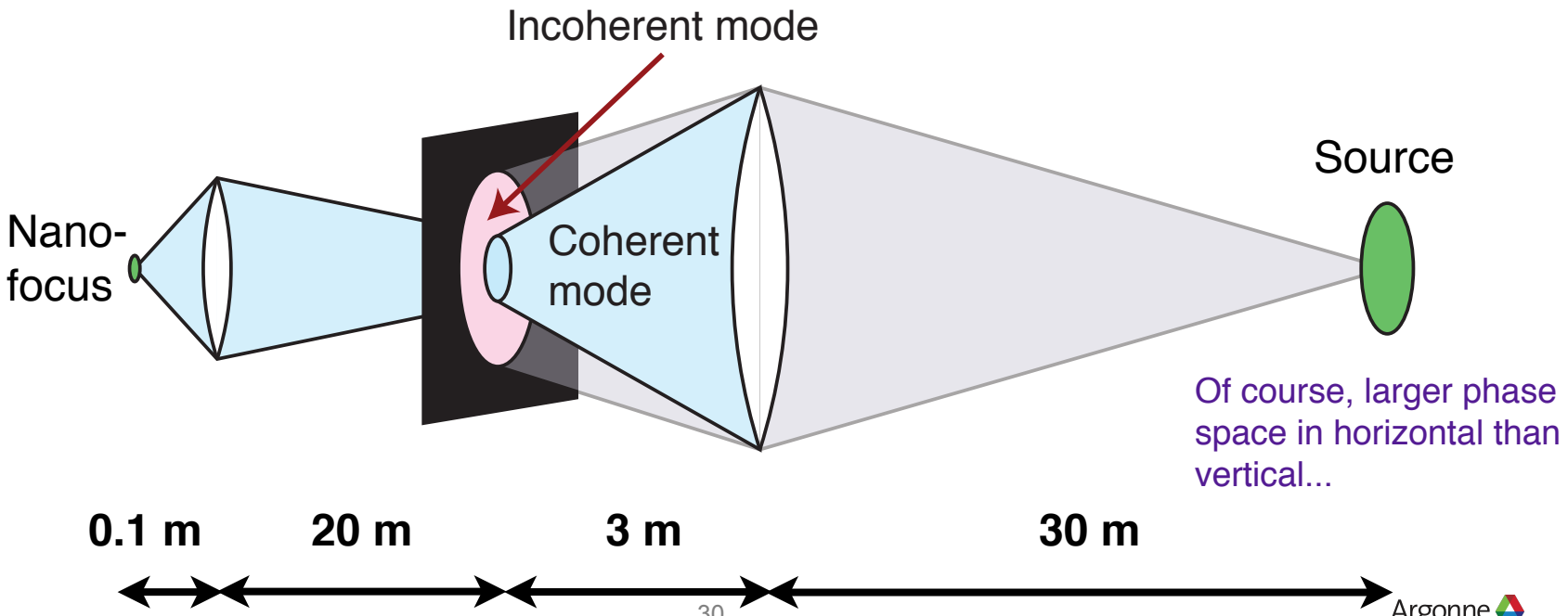

2D imaging with Stony Brook STXMs

2D imaging is moderately useful but...

- Cannot track fluroescently-labeled proteins in living cells
- Resolution is inferior to cryoEM, though do not need to section
- Best utility may lie beyond simple 2D imaging

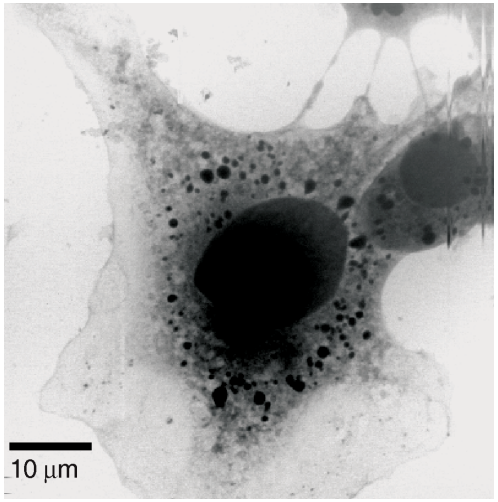

NIL 8 fibroblast (wet, fixed): Oehler *et al.*

Human sperm (unfixed): Wirick, Fleckenstein, Sheynkin *et al.*

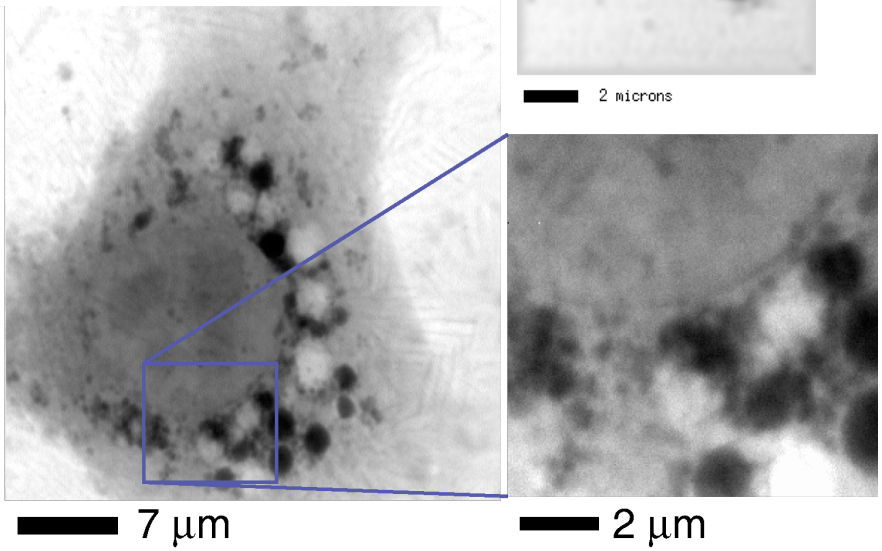

Fibroblast (frozen hydrated): Maser *et al.*, *J. Micros.* **197**, 68 (2000)

Anilao, Philippines, 17-Oct-2010

Energy scales

- Chemistry: C-H bond is 104 kcal/mol or 435 kJoules/mol:

$$(435\frac{\mathrm{kJ}}{\mathrm{mol}})\cdot(\frac{10^3\ \mathrm{J}}{\mathrm{kJ}})\cdot(\frac{1\ \mathrm{eV}}{1.602\times10^{-19}\ \mathrm{J}})\cdot(\frac{1}{6.02\times10^{23}\ \mathrm{molecules/mol}})$$

  or E=4.5 eV/molecule.

- Photon wavelength associated with 4.5 eV is

$$E=\frac{hc}{\lambda}=\frac{1240\ \mathrm{eV}\cdot\mathrm{nm}}{\lambda}$$

  or λ=275 nm.

- More broadly, chemical bonds involve 300-900 kJ/mol, or 3-9 eV/molecule, or 130-400 nm light.
- Bohr model:

$$E=-E_0\frac{Z^2}{n^2}=-13.6\ \mathrm{eV}\,\frac{Z^2}{n^2}$$

Absorption edges

Lambert-Beer law: linear absorption coefficient μ

$$I = I_0 e^{-\mu(E)\cdot t} = I_0 e^{-D(E)}$$

This coefficient makes a jump at specific elemental absorption edges!

This example: 0.1 μm protein in water

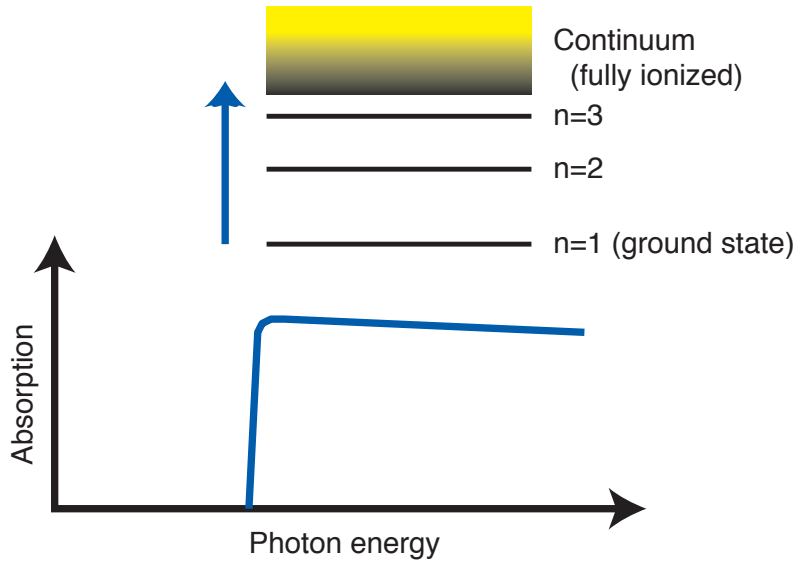

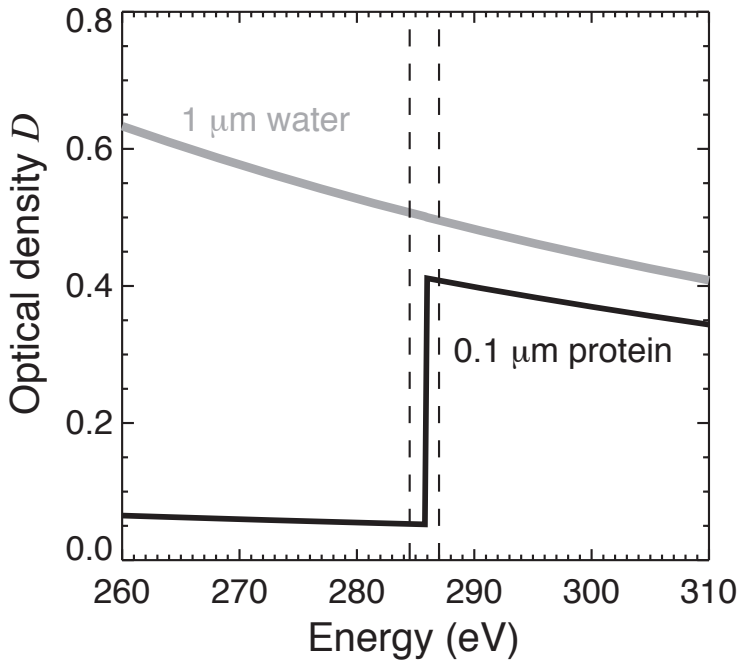

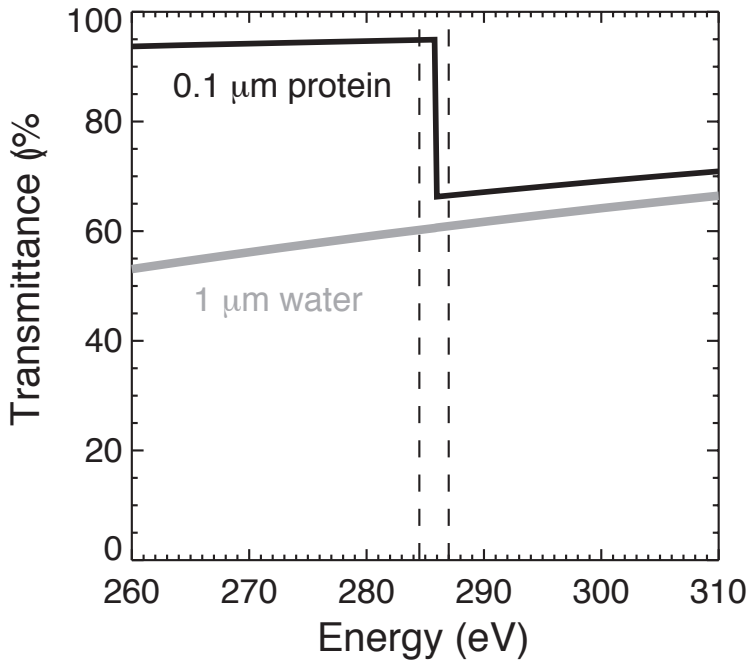

X-ray microscopy of colloids

- U. Neuhäusler (Stony Brook/Göttingen), S. Abend (Kiel), G. Lagaly (Kiel), C. Jacobsen (Stony Brook), *Colloid and Polymer Science* **277**, 719 (1999).
- Emulsion: water, oil droplets, clay, and layered double hydroxides (LDH).
- "Caged" part of oil droplet remains fixed; "uncaged" part can disperse.

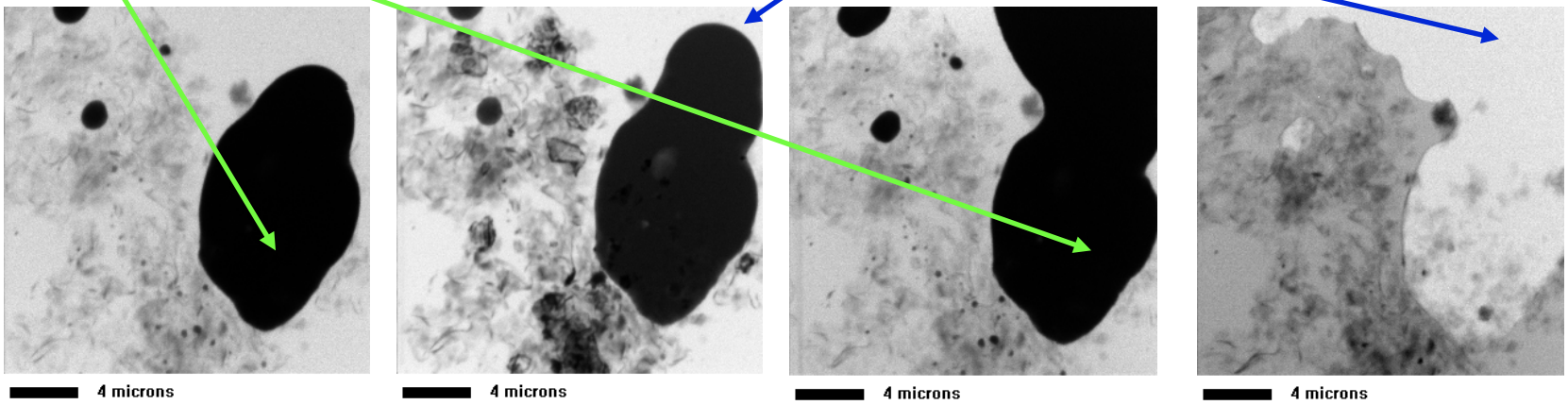

346 eV: calcium weakly absorbing. Clays and LDHs absorb equally

352.3 eV: calcium strongly absorbing. Calcium-rich LDHs are highlighted.

290 eV: carbon strongly absorbing

284 eV: carbon (oil drop) weakly absorbing

Near-edge absorption fine structure (NEXAFS) or

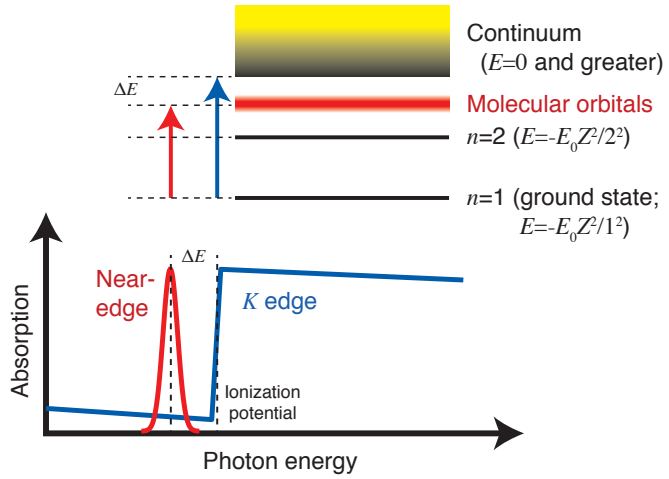

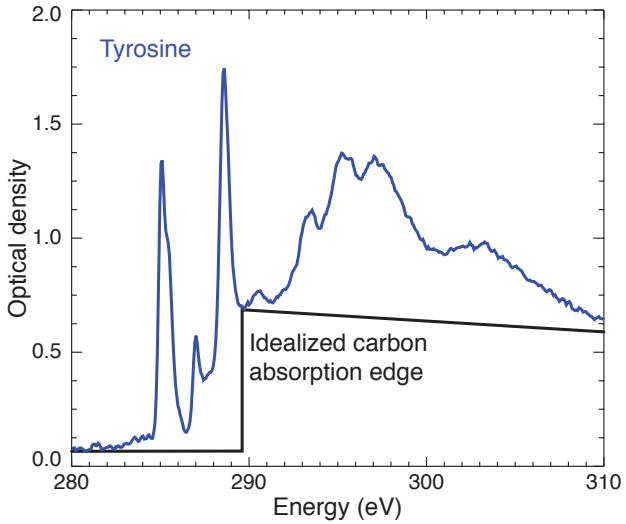

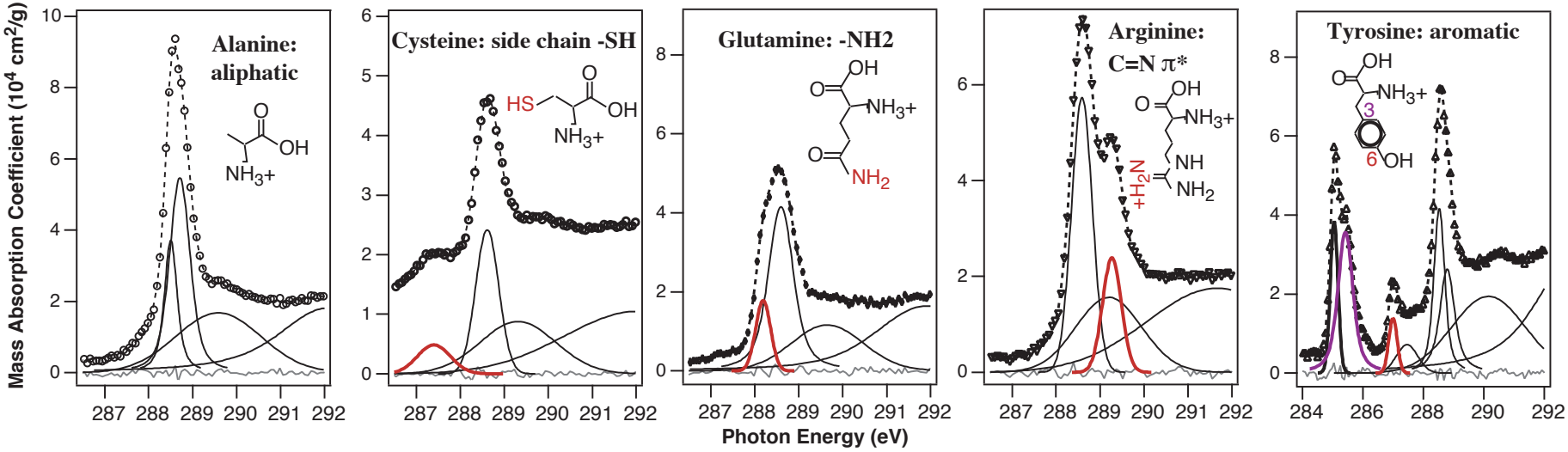

Amino acids example: K. Kaznacheyev *et al.*, *J. Phys. Chem.* **A 106**, 3153 (2002)

Cluster analysis: Lu in hæmatite

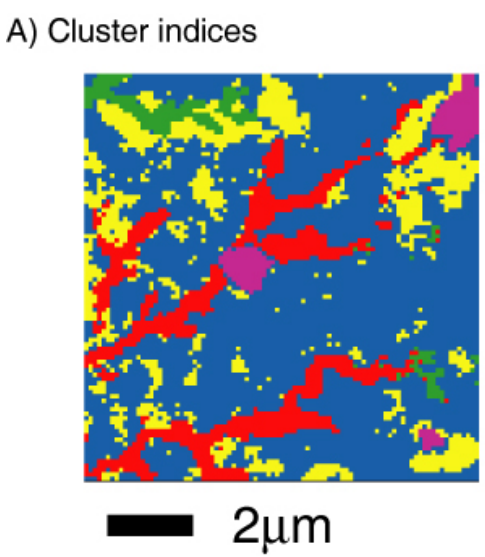

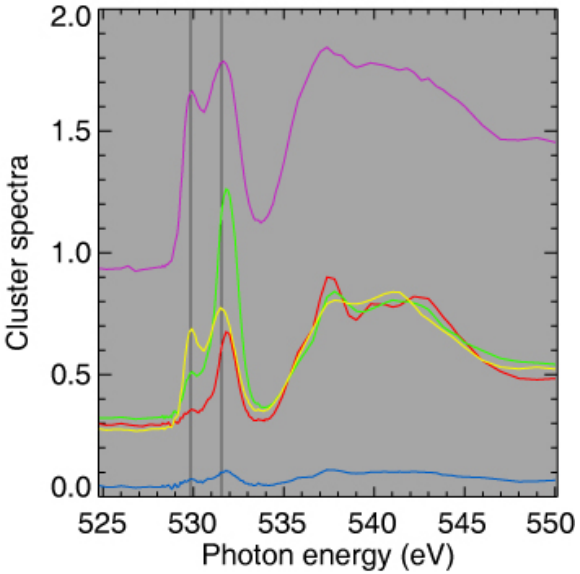

cluster 1

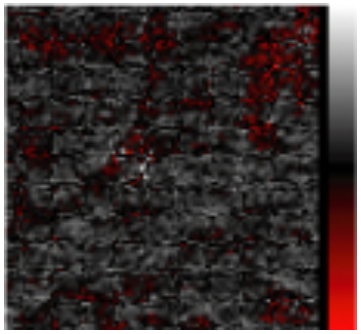

cluster 2

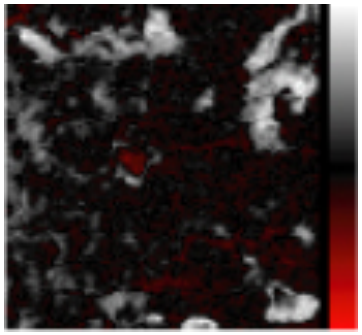

- Lu as a stand-in for Am in nuclear wastes; hæmatite can be a groundwater colloid that increases transport rate 1000x
- Oxygen XANES shows two different incorporation phases of Lu in hæmatite (clusters 2 and 5)
- Lerotic, Jacobsen, Schäfer, Vogt, *Ultramic*. **100**, 35 (2004)

cluster 3

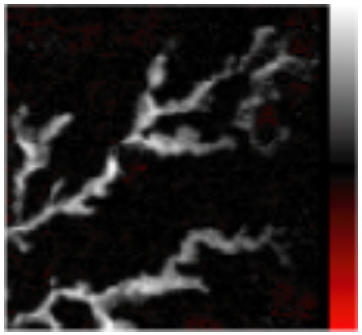

cluster 4

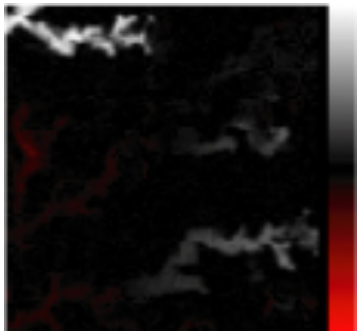

cluster 5

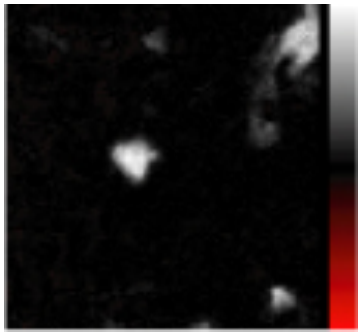

Organic carbon in soils: C-XANES

Lehma

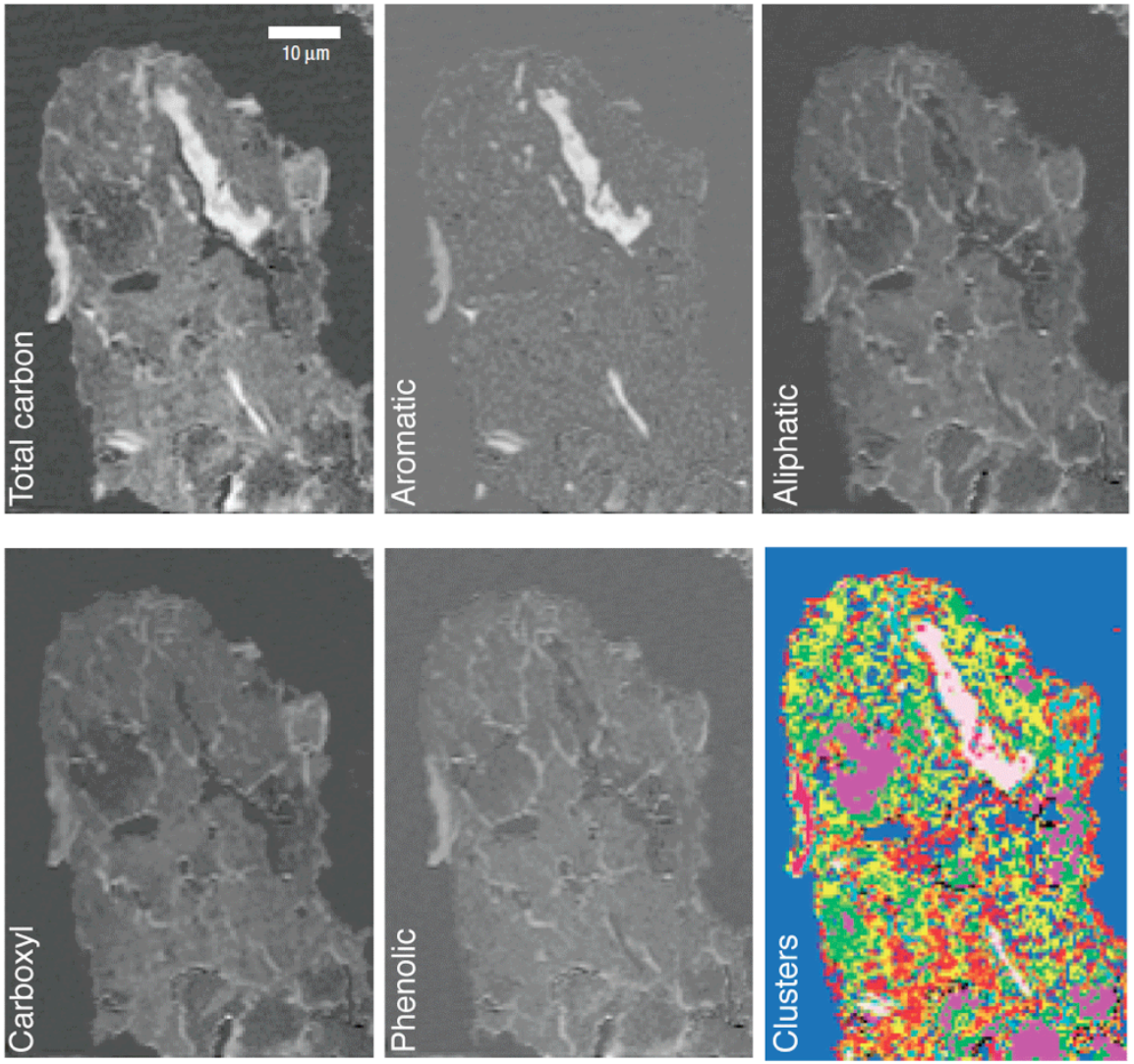

J. Lehmann, D. Solomon, J. Kinyangi, L. Dathe, S. Wirick, and C. Jacobsen, *Nature Geoscience* **1**, 238 (2008)

Optimization techniques in spectromicroscopy analysis

Global cost function F:

$$F(\mu, t) = ||D - \mu \cdot t||_2^2 + \lambda_{\text{sparse}}||t||_1 + \lambda_{\text{sim}}||\mu - \mu_{\text{cluster}}||_2^2$$

- Data matching: reconstruction from spectra μ and images t should match optical density data D.
- Sparseness: maximize the separation of features in the images t. The L_1 norm provides a good measure of sparseness.
- Similarity: keep the spectra μ similar to those found in regions of the sample (μ_{cluster}).
- The regularization parameters λ are like a currency exchange rate to put all the costs on the same scale; increase λ until data matching error begins to grow significantly.
- Partial derivatives of each cost guide iterative solutions.
- Mak, M. Lerotic, H. Fleckenstein, S. Vogt, S. Wild, S. Leyffer, Y. Sheynkin, and C. Jacobsen, *Faraday Discussions* **171**, 357 (2014).

Finding a global minimum cost

- Search space over regularizers to find global cost minimum, while maximizing sparseness and cluster spectra similarity.
- R. Mak, PhD thesis, Northwestern University, 2014

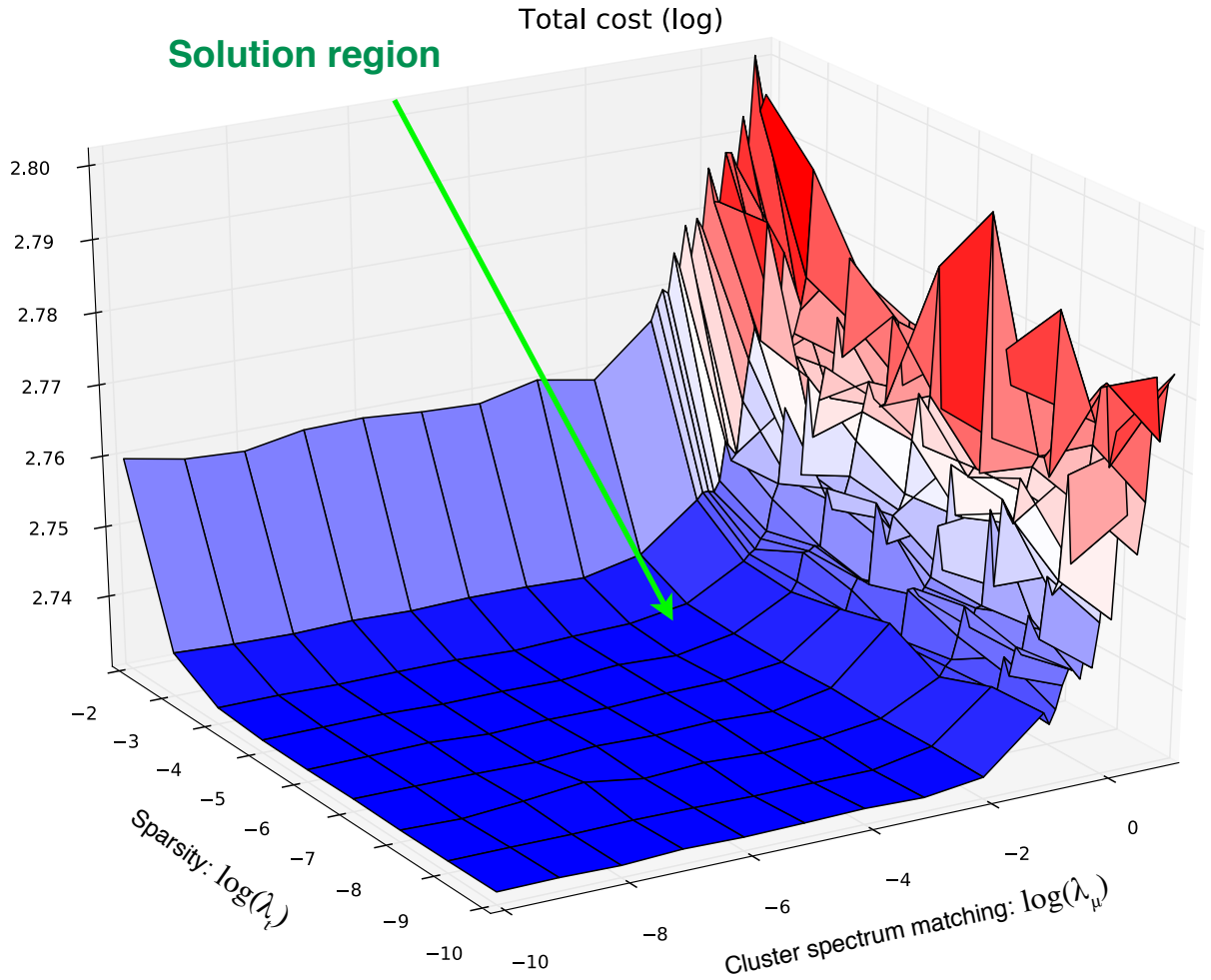

Optimized analysis

Faraday Discussions

Cite this: DOI: 10.1039/c4fd00023d

PAPER View Article Online View Journal

Non-negative matrix analysis for effective feature extraction in X-ray spectromicroscopy

Rachel Mak,[a] Mirna Lerotic,[b] Holger Fleckenstein,[c] Stefan Vogt,[d] Stefan M. Wild,[e] Sven Leyffer,[e] Yefim Sheynkin[f] and Chris Jacobsen*[dag]

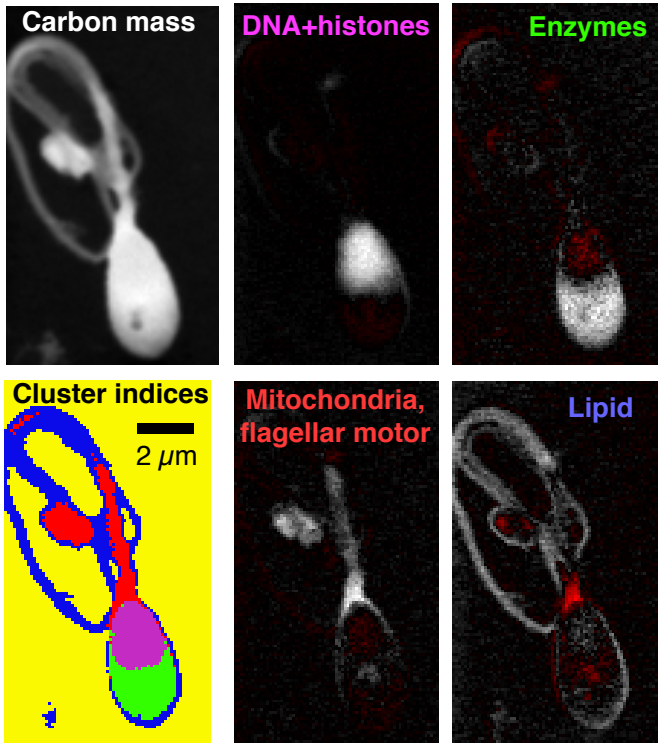

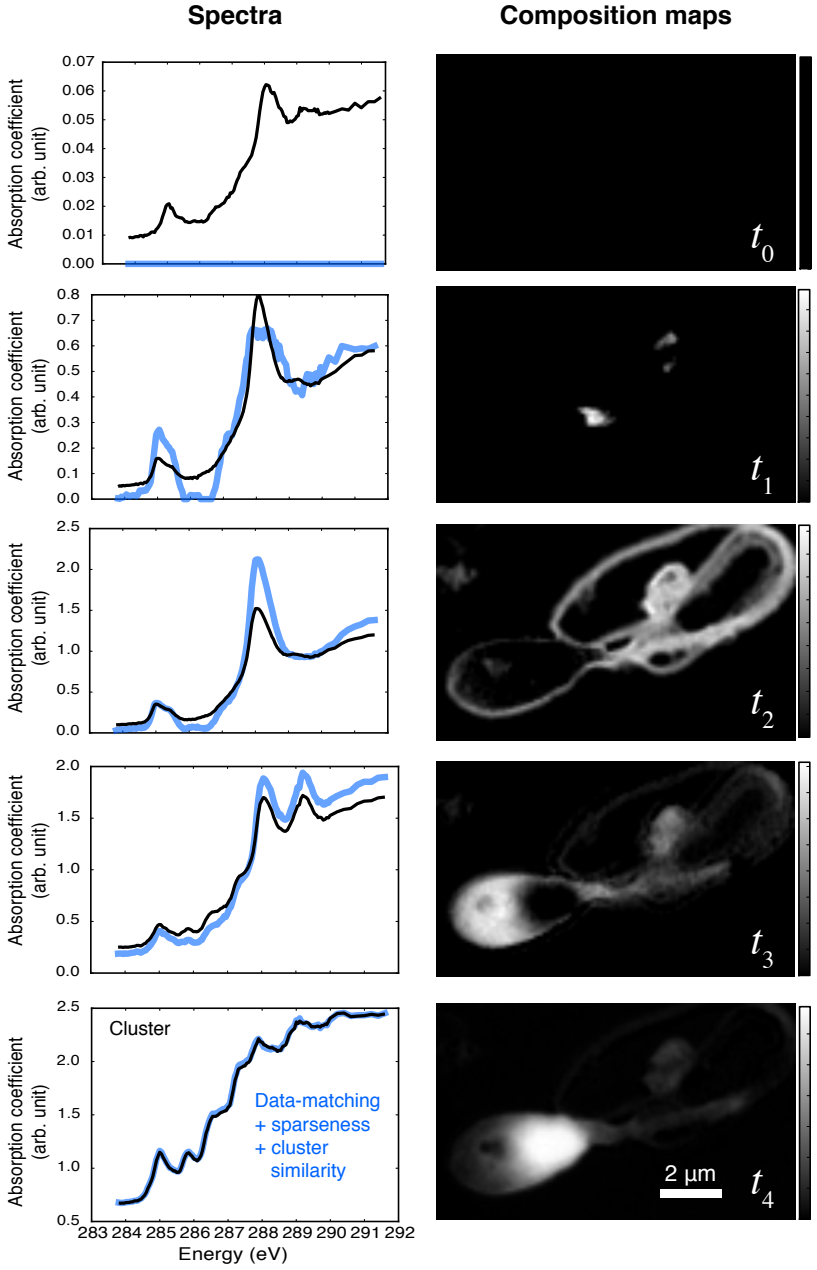

Argonne NATIONAL LABORATORY

Optimization: better chemistry, no negatives!

- Optimization eliminates residual unphysical errors (negative optical density) in analysis results.
- Subtle changes in spectra - can also “tweak” solution starting from spectral standards.

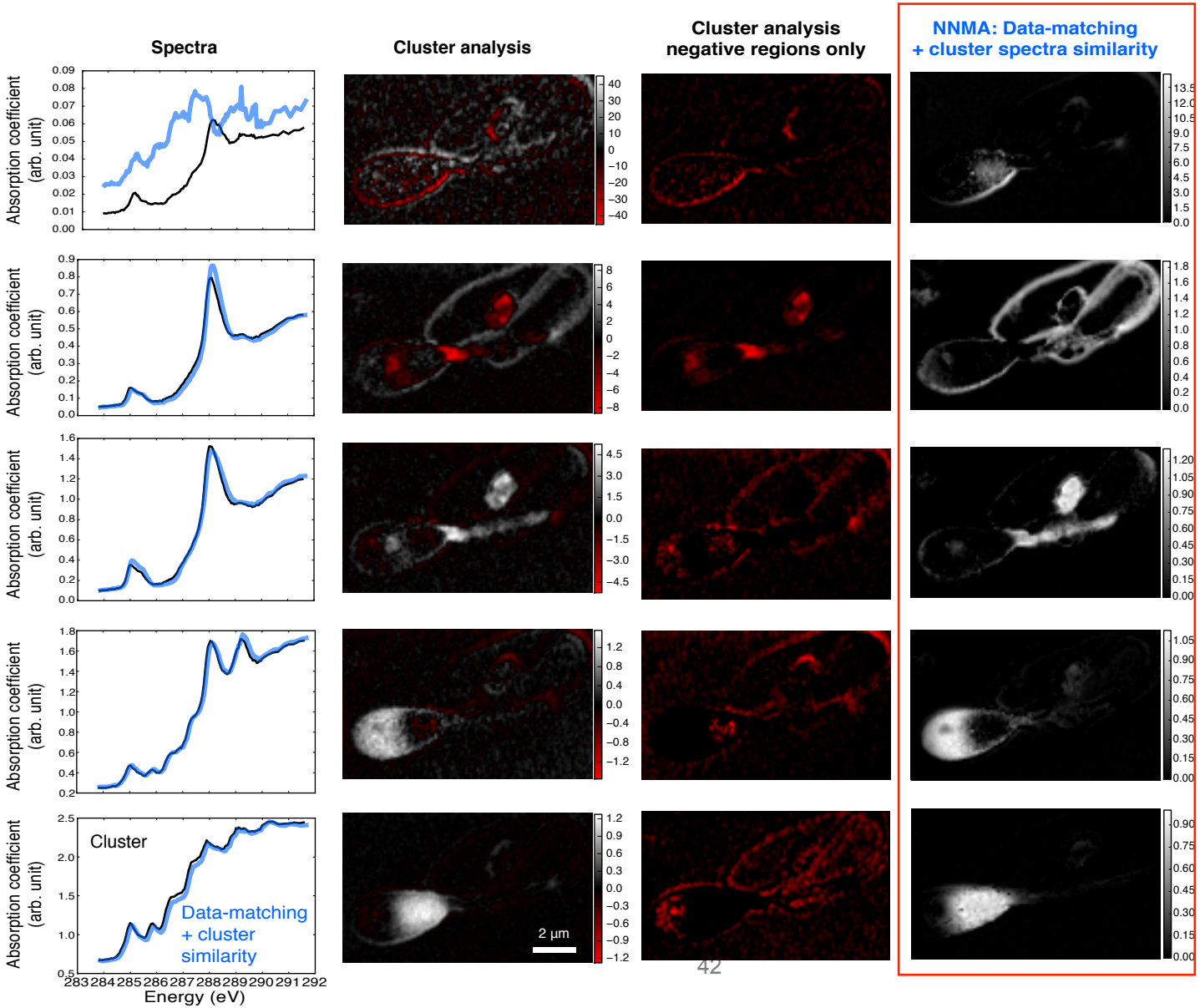

Protamine variations in histones?

Lipid membrane and tail

Flagellar motor + mitochondria

Enzymes triggering egg penetration

DNA packed in histones

Argonne NATIONAL LABORATORY


Silverman Hall
Northwestern University
H
Li
Na
Mg
K
Ca
Mn
Fe
Co
Cu
Zn
Mo
Tc
Ag
Pt
C
N
O
F
P
S
As
Gd

X-ray fluorescence microscopy

- Energy dispersive detectors: 3.65 eV per electron-hole pair separation in Si.
- 10 keV photon produces 2740 electrons. Fluctuations: $(2740)^{1/2}$=52, so uncertainty is (52/2740)*10,000 eV=190 eV.
- Detector at 90°: minimize elastic scattering.

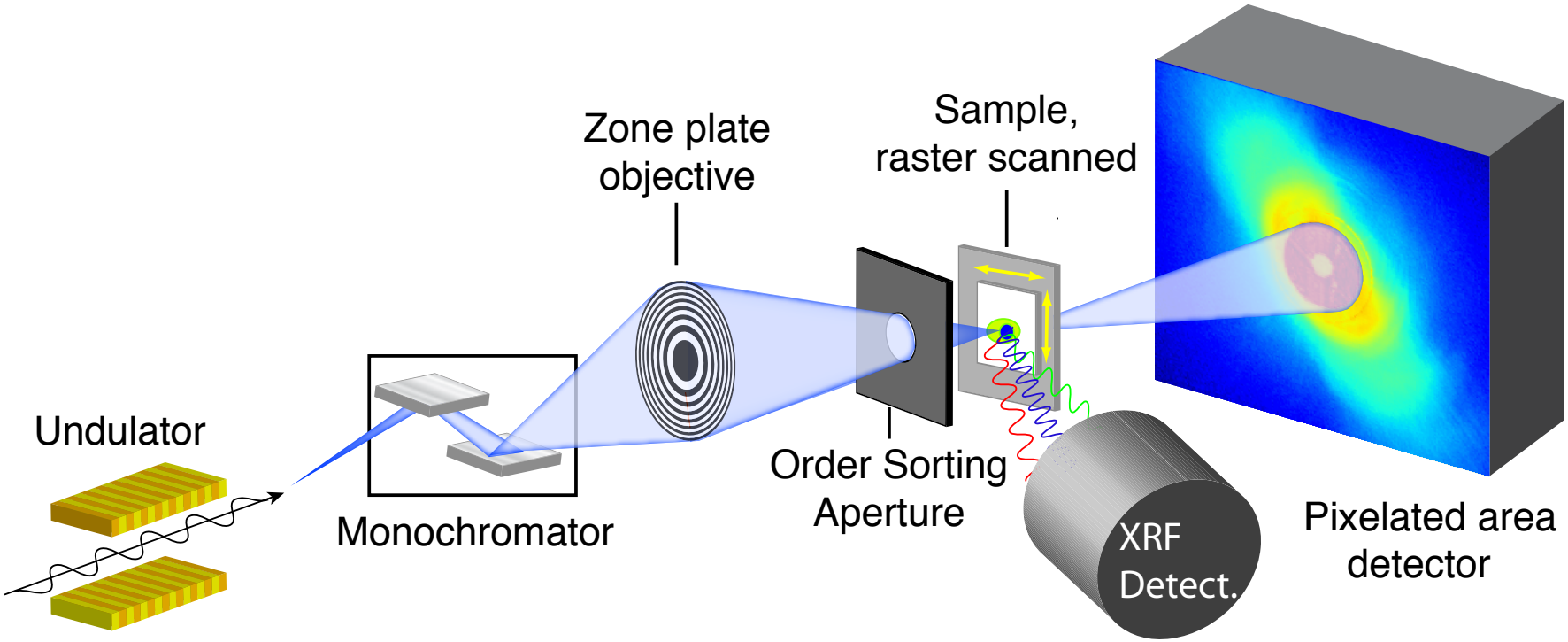

Fluorescence yield

Fluorescence yield ω=fraction of time you get a fluorescent photon rather than an Auger electron

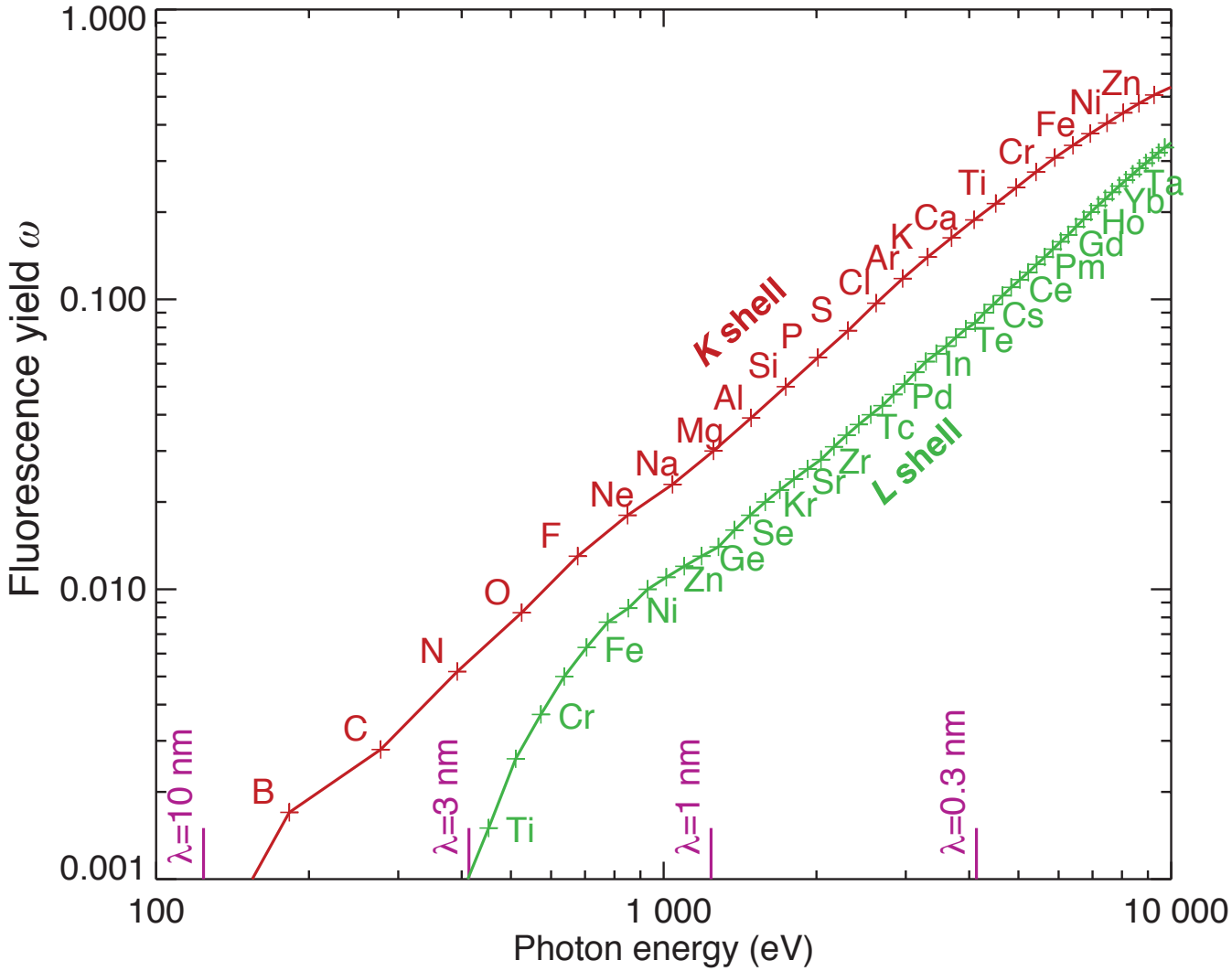

Fluorescence detector response to a 8 keV photon

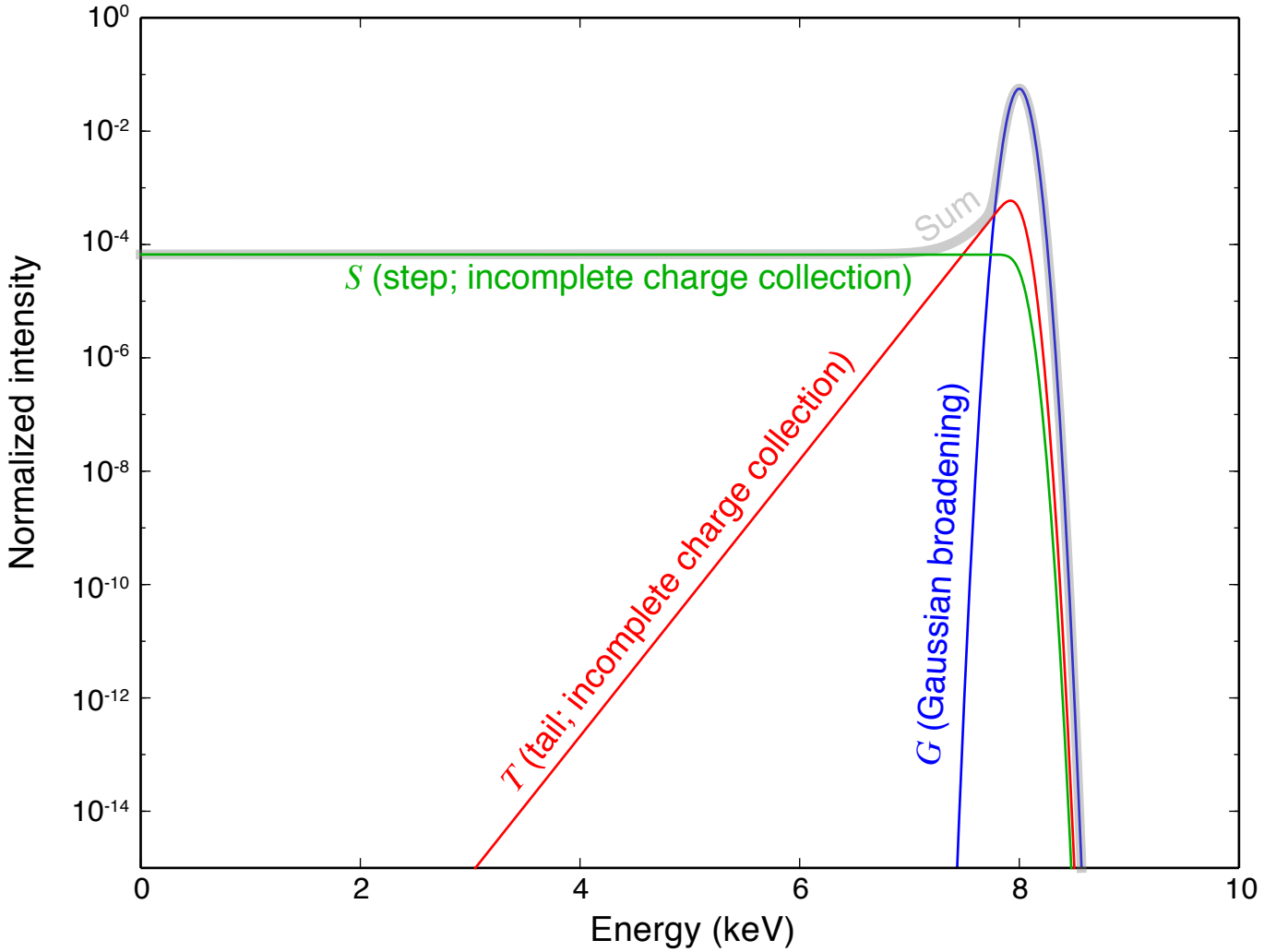

Van Grieken and Markowicz, *Handbook of X-ray Spectrometry* (CRC Press, 2001).
This plot from Sun, Gleber, Jacobsen, Kirz, and Vogt, *Ultramicroscopy* **152**, 44 (2015)

Example calculated x-ray spectrum

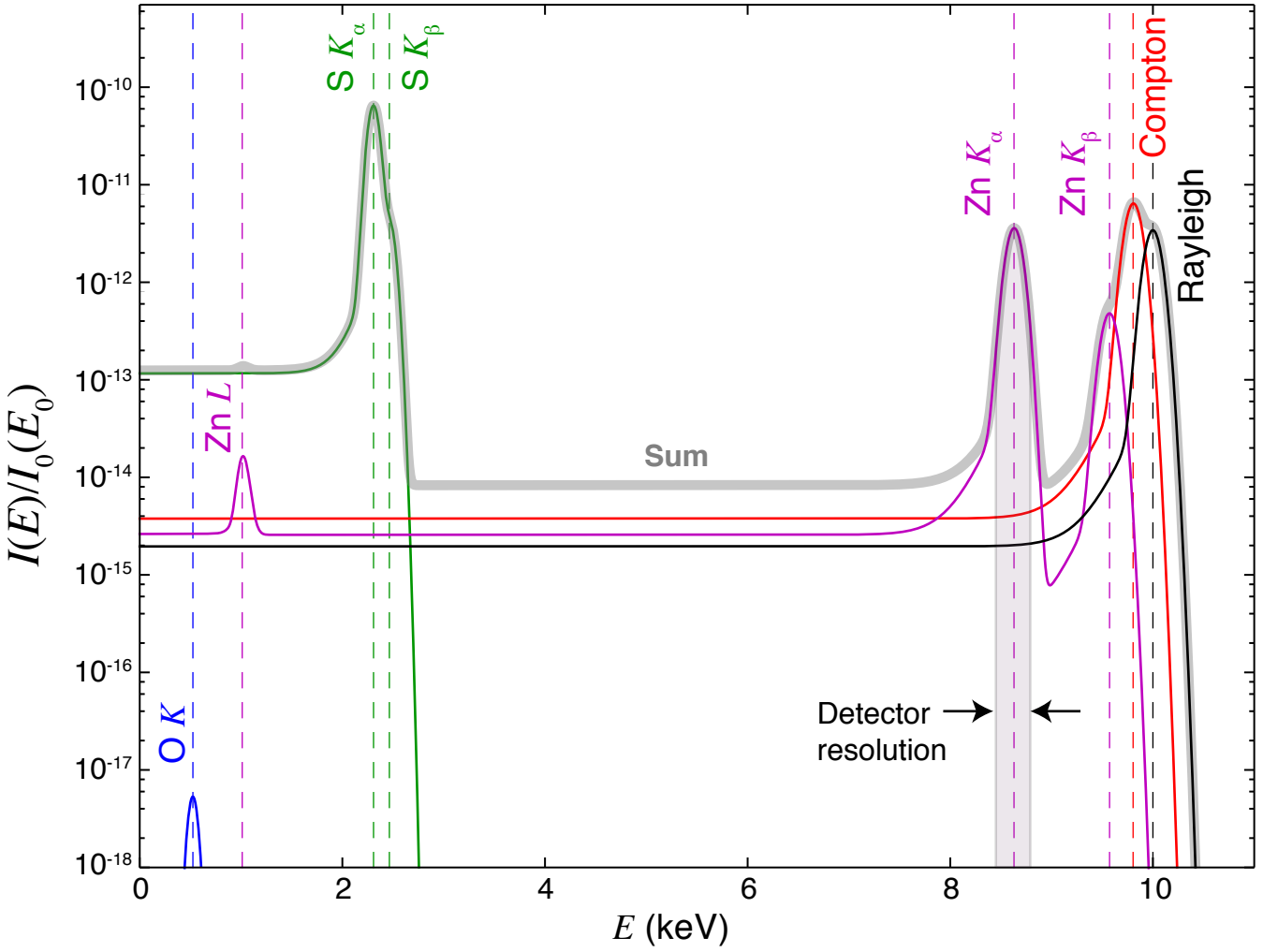

Sun, Gleber, Jacobsen, Kirz, and Vogt, *Ultramicroscopy* **152**, 44 (2015)

X-ray interaction cross sections

- There are no cloudy days for X rays!

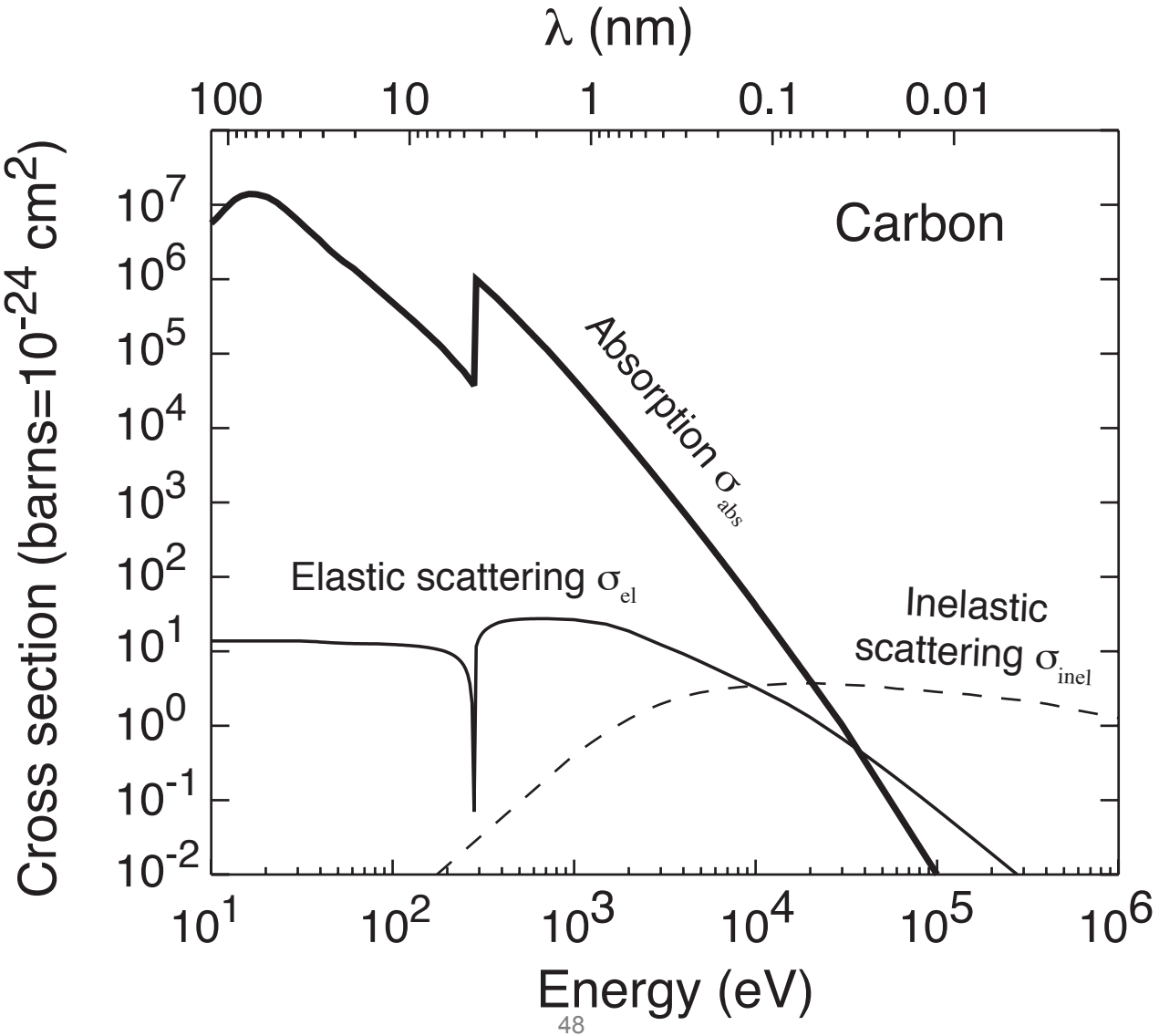

Detector geometries vary!

- Elastic and Compton scattering profiles have angular dependencies

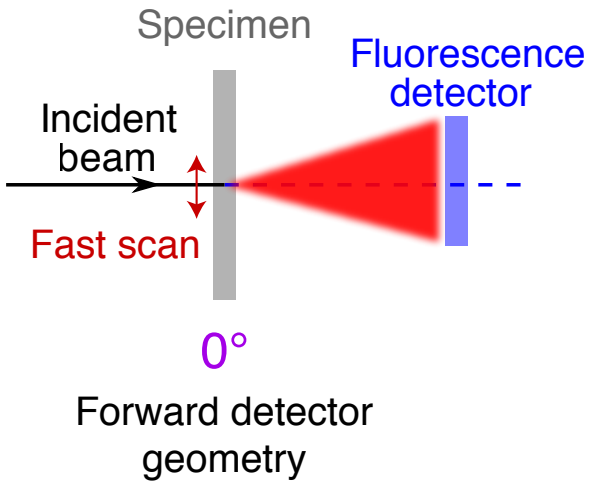

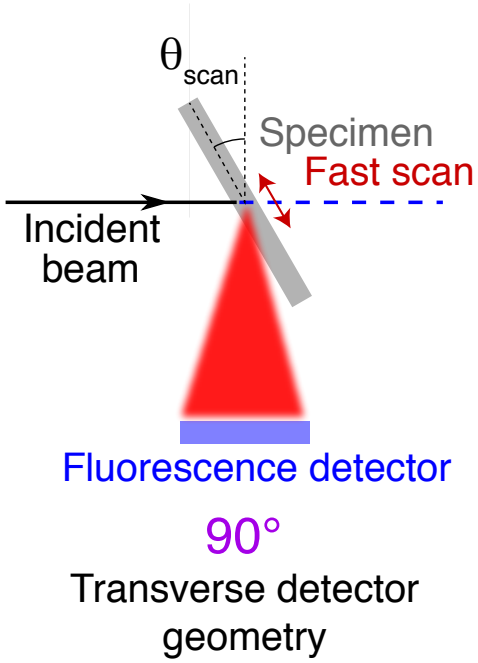

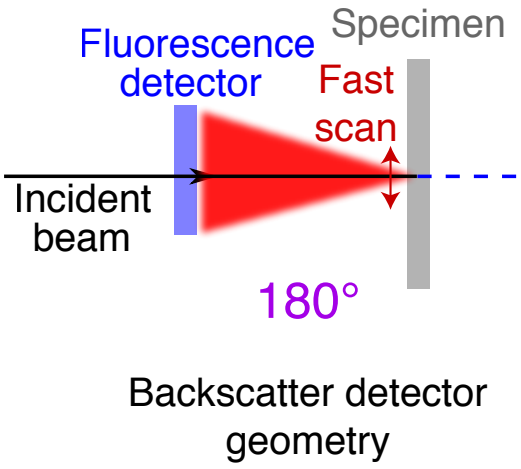

Sun, Gleber, Jacobsen, Kirz, and Vogt, Ultramicroscopy 152, 44 (2015)

Sensitivity for two detector geometries

- Bio sample with 0.01% Zn in a 20 nm thick protein layer within ice/water, using 10 keV photons.
- Vortex: solid angle fraction is 0.0034.
- Maia in backscatter geometry.

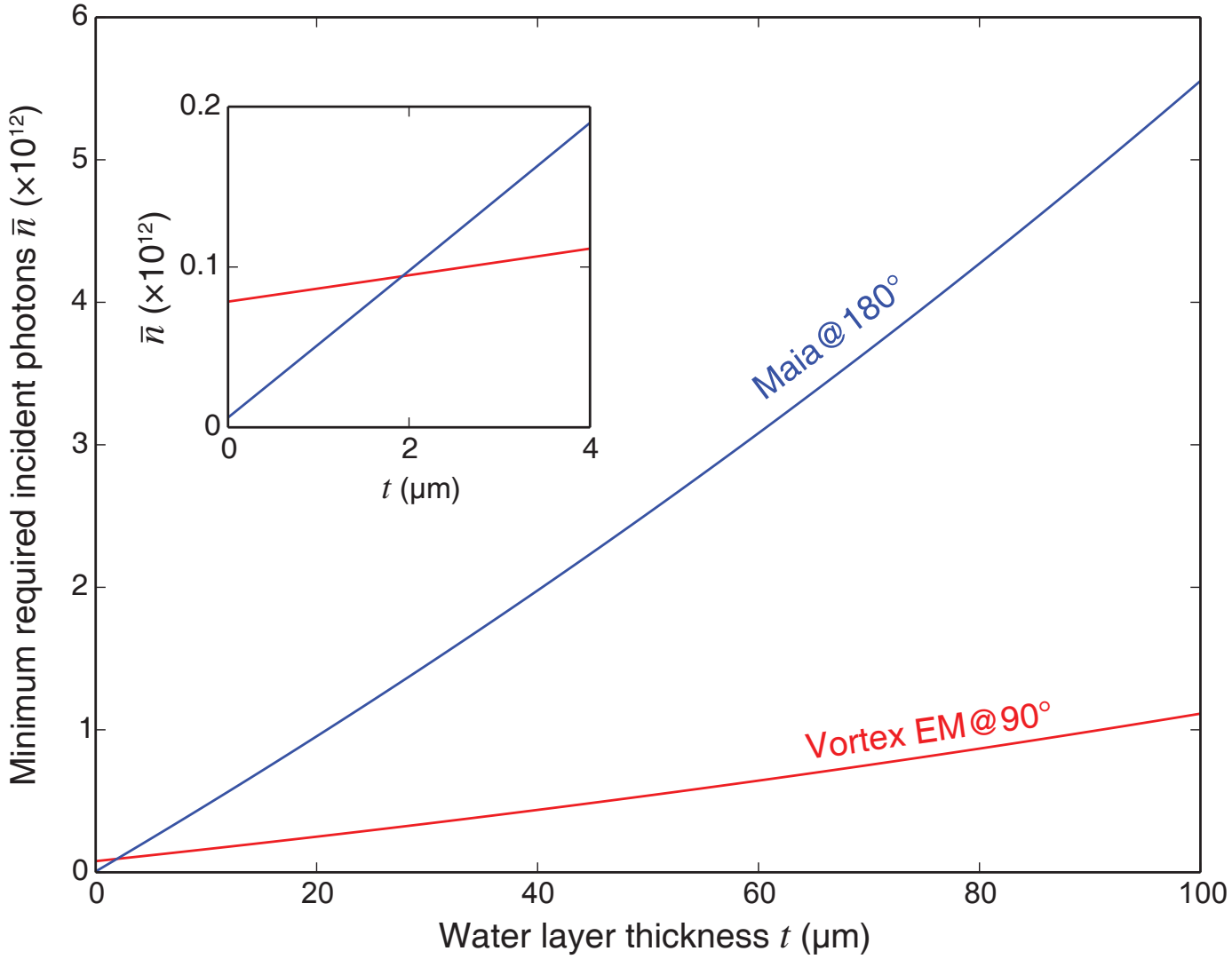

Sun, Gleber, Jacobsen, Kirz, and Vogt, *Ultramicroscopy* **152**, 44 (2015)

Exciting x-ray fluorescence

X rays and protons produce a dramatically lower continuum background, increasing sensitivity (but proton microprobes induce much more damage)

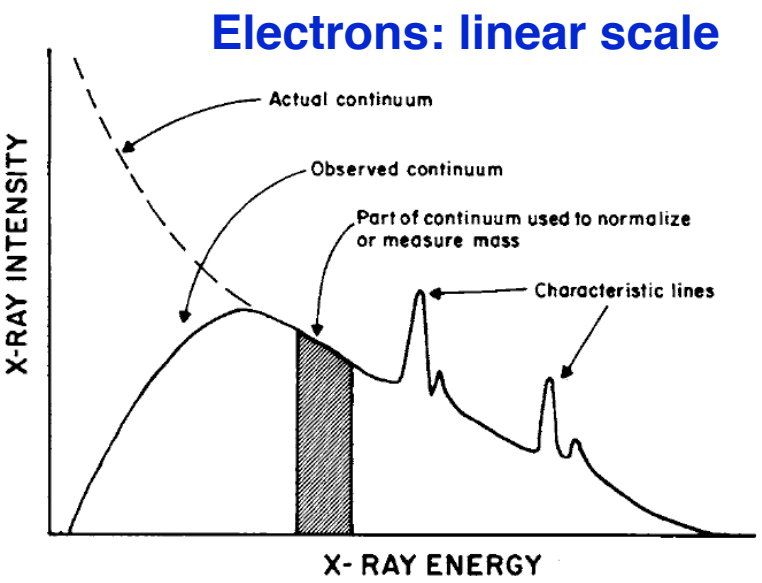

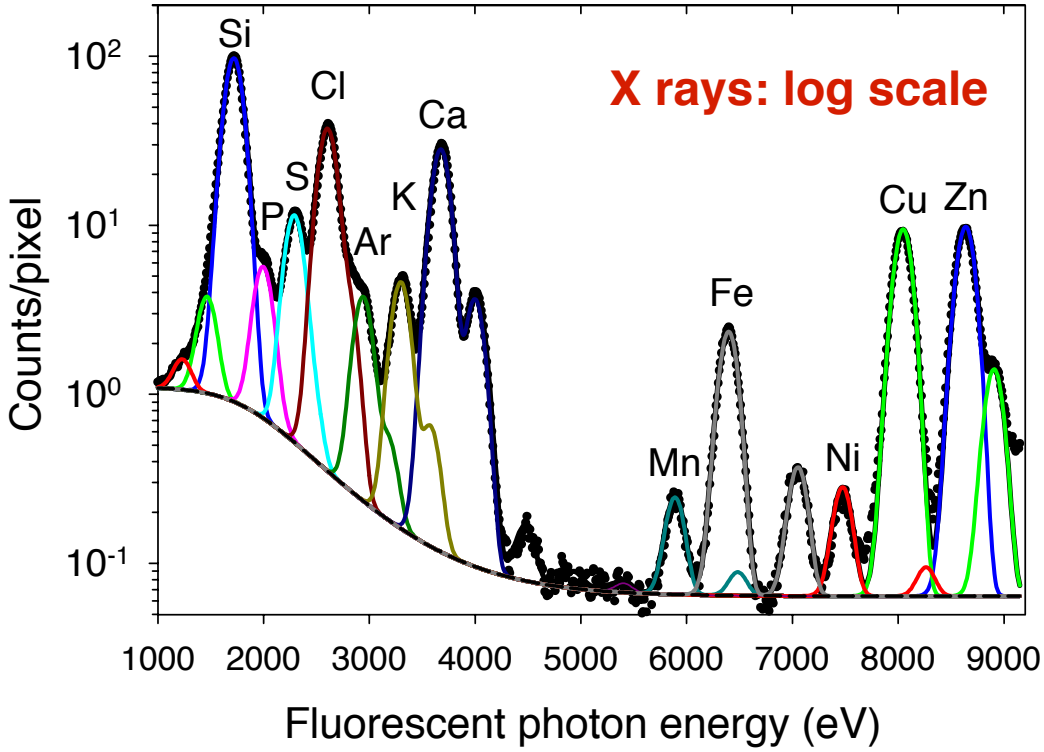

LeFurgey and Ingram, *Environmental Health Perspectives* **84**, 57 (1990)

Twining *et al.*, *Anal. Chem.* **75**, 3806 (2003). Analysis approach: Vogt, Maser, and Jacobsen, *J. Phys. IV* **104**, 617 (2003).

Example x-ray spectrum and fit

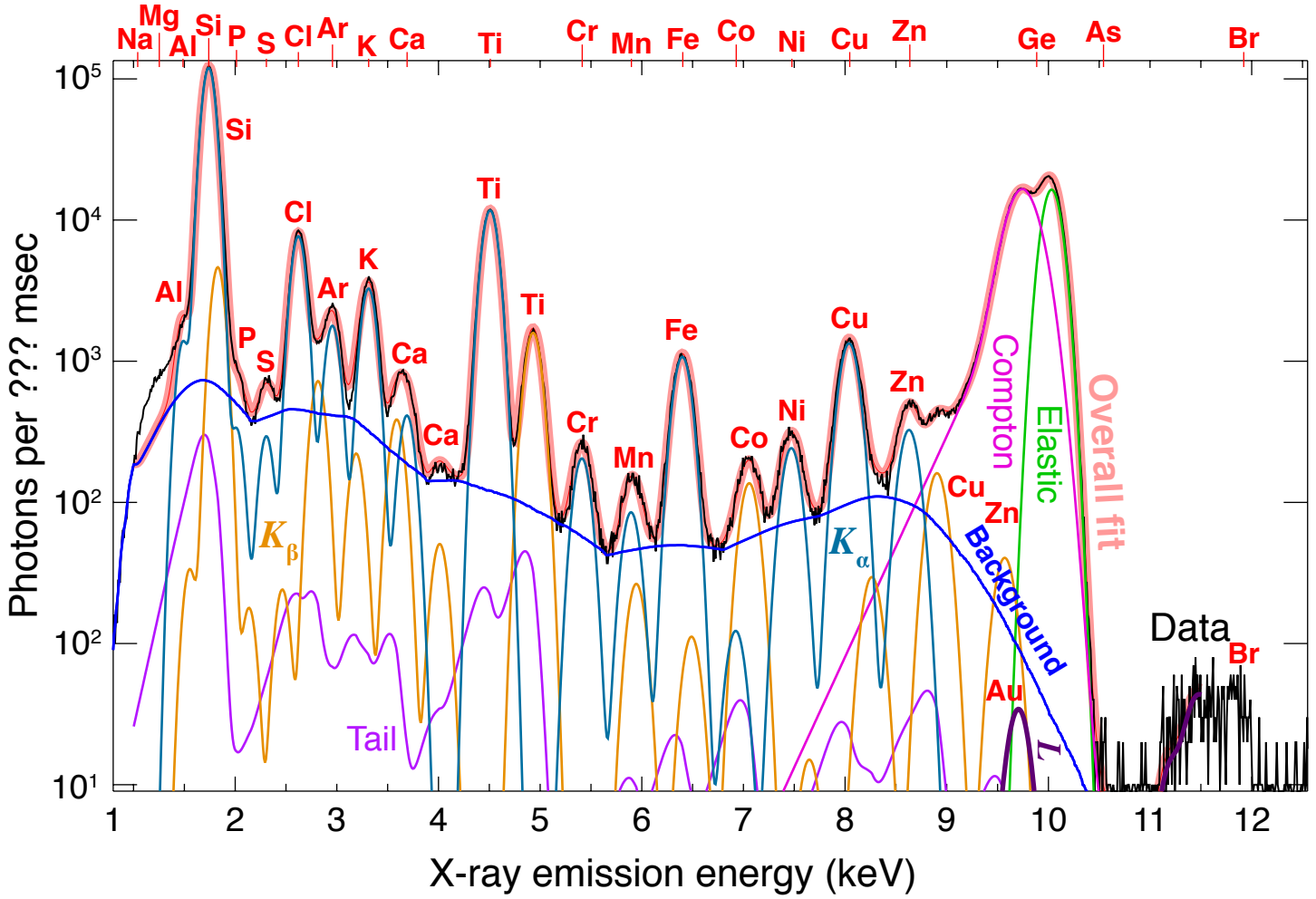

Spectrum: Olga Antipova, APS. Fit: S. Vogt, *J. Phys. IV France* **104**, 635 (2003). See also Ryan and Jamieson, *Nucl. Inst. Meth. B* **77**, 203 (1993); and Solé *et al.*, *Spectrochimica Acta B* **62**, 63 (2007).

Electron probes in thick specimens

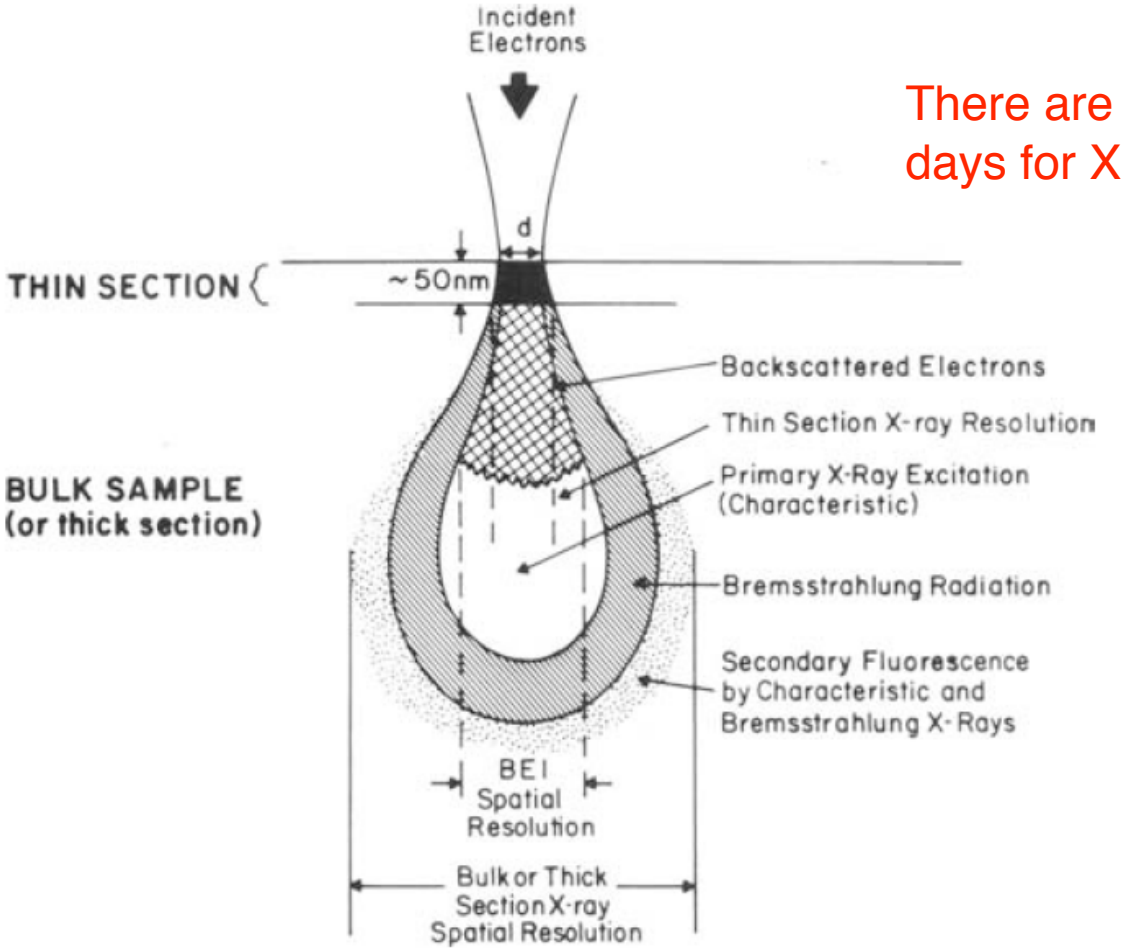

There are no cloudy days for X rays!

Electron beams broaden in thick specimens due to sidescattering; x-ray beams do not. LeFurgey and Ingram, *Environmental Health Perspectives* **84**, 57 (1990).

Global carbon cycle

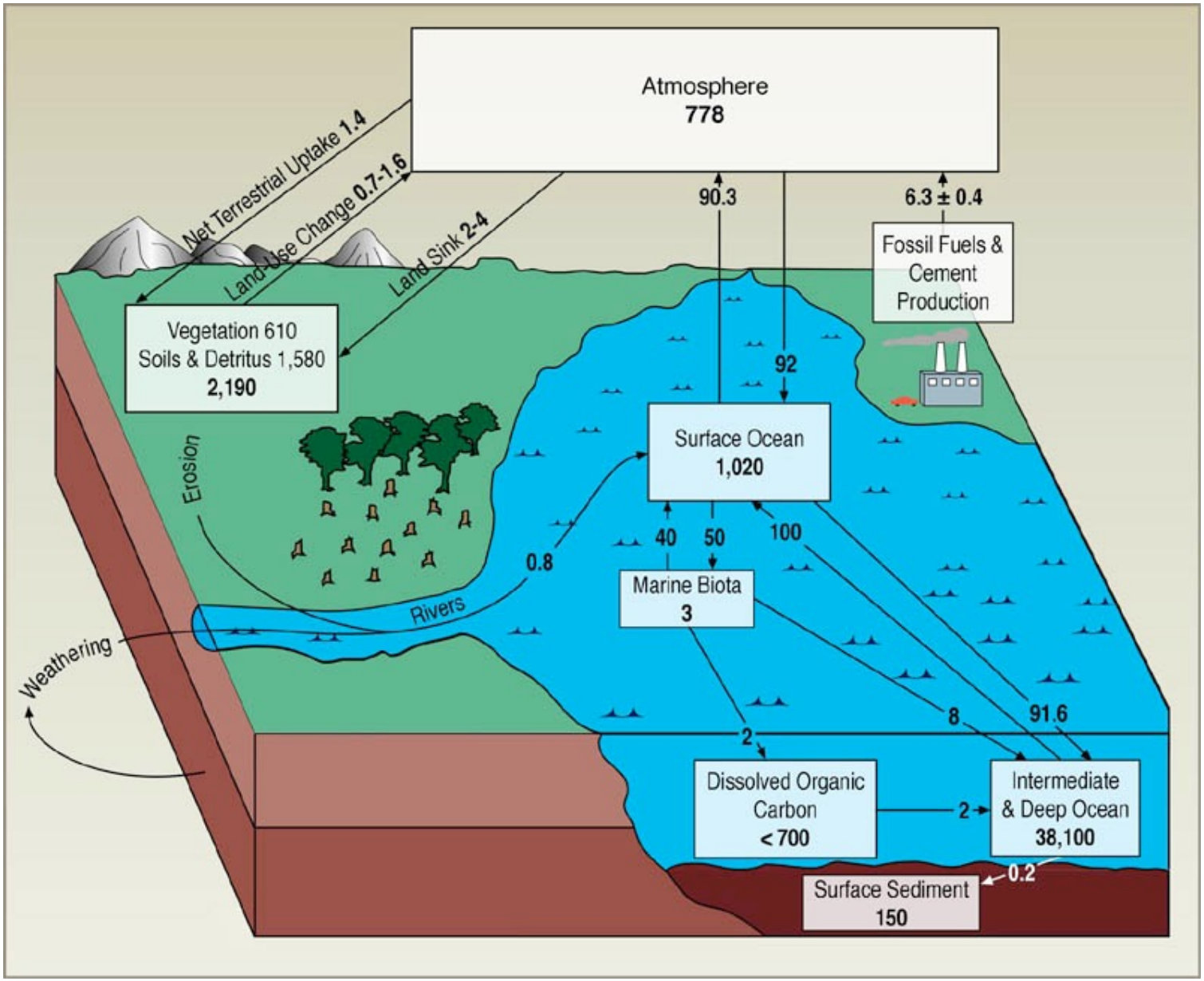

petagrams, petagrams/year (climatescience.gov)

Iron and carbon in the ocean

- Seed Southern Pacific with bioavailable iron to increase CO_2 uptake?
- Requires understanding of iron and carbon uptake in phytoplankton; combine fluorescence with phase contrast.

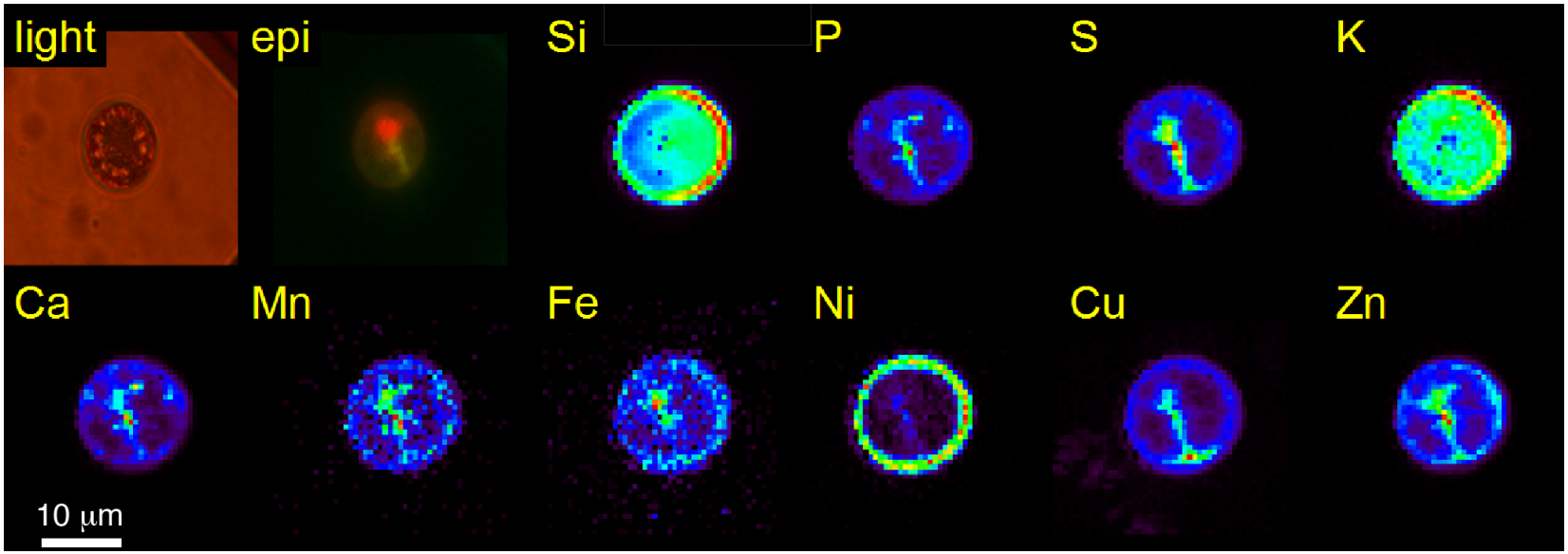

B. Twining, S. Baines, N. Fisher, J. Maser, S. Vogt, C. Jacobsen, A. Tovar-Sanchez, and S.Sañudo-Wilhelmy, *Anal.. Chem.* **75**, 3806 (2003)

Cruising the Southern Pacific

Quantitative 3D fluorescence of a diatom

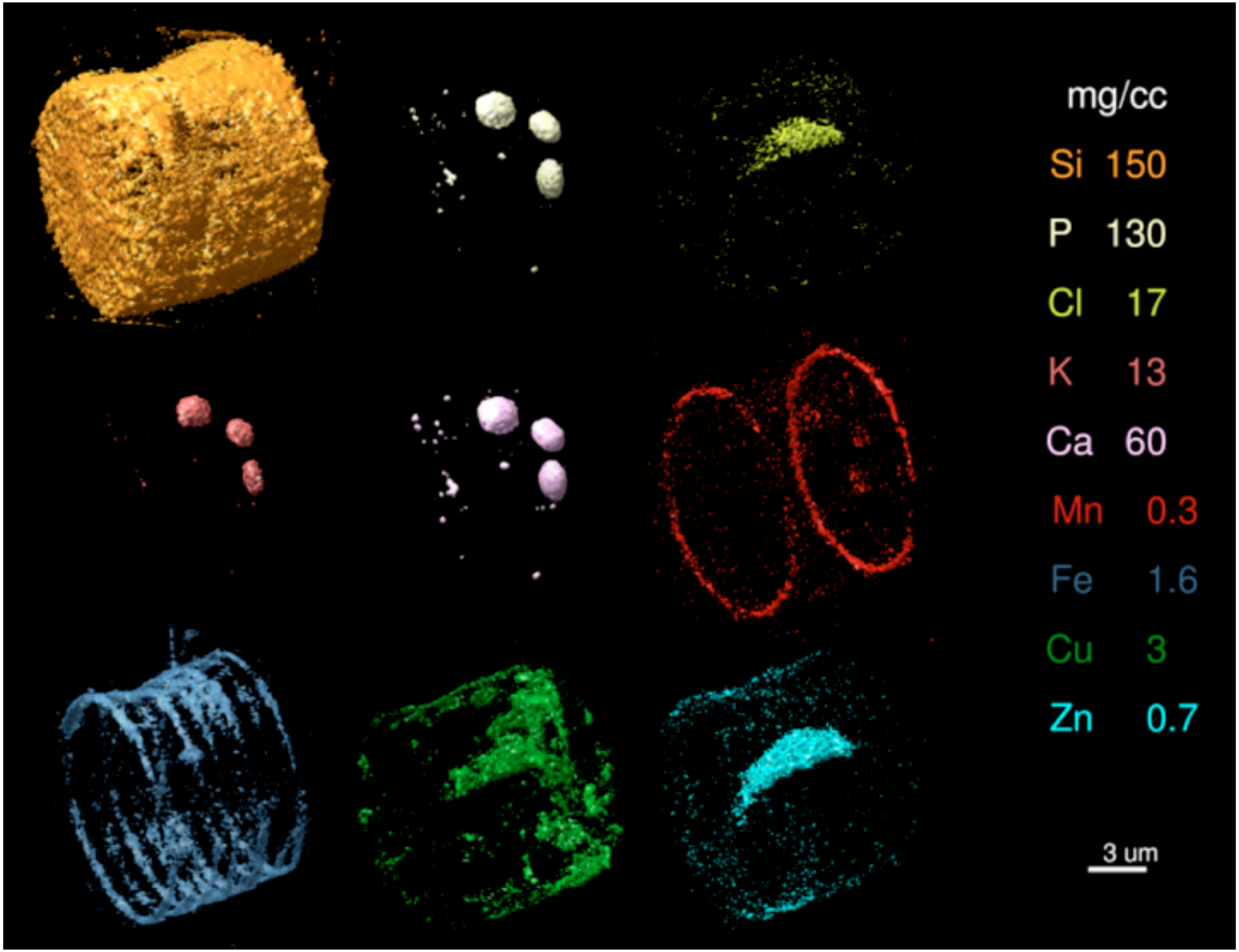

M. de Jonge, C. Holzner, S. Baines, B. Twining, K. Ignatyev, J. Diaz, D. Howard, A. Miceli, I. McNulty, C. Jacobsen, S. Vogt, *Proc. Nat. Acad. Sci.* **107**, 15676 (2010)

Fluorescence tomography

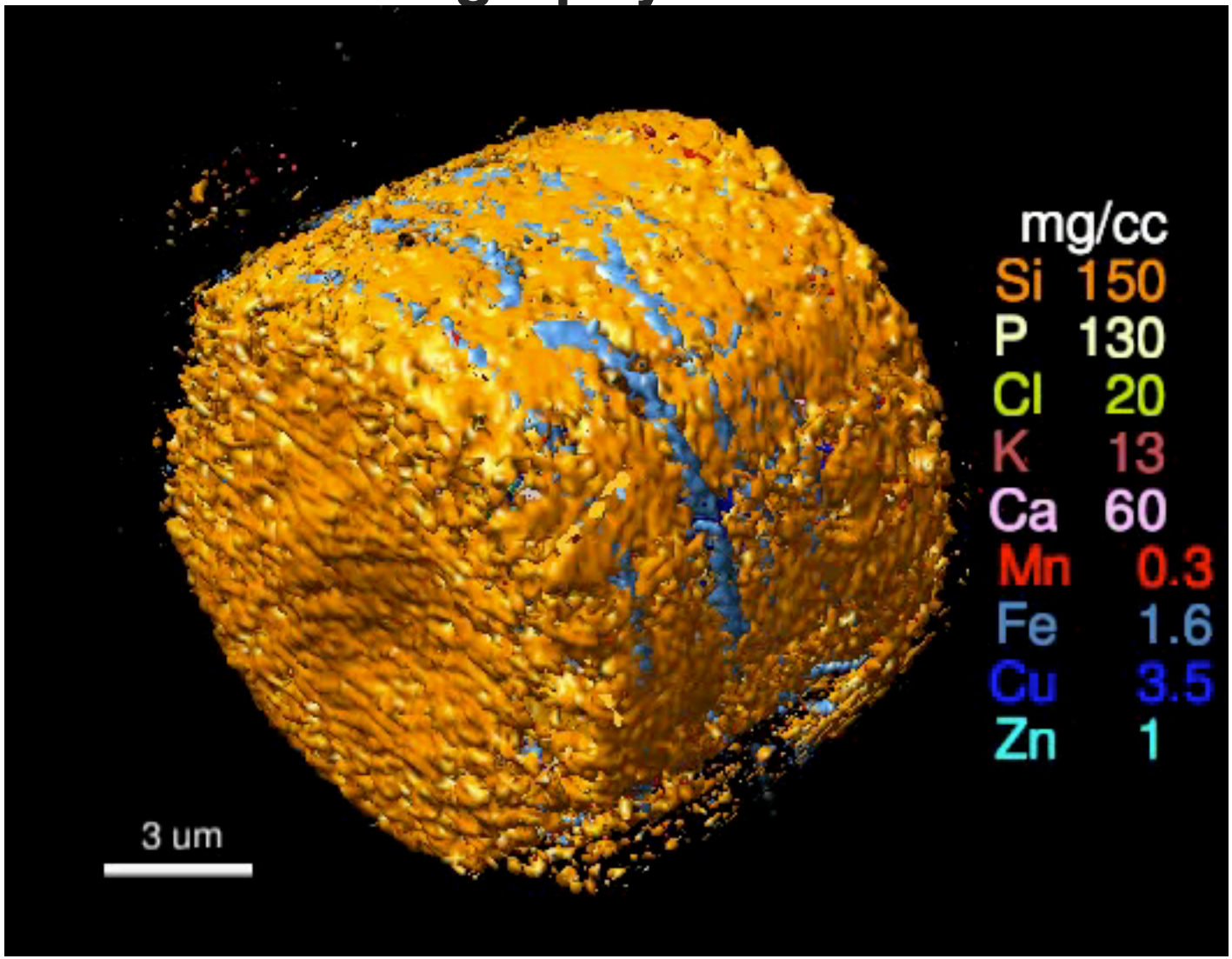

de Jonge *et al.*, *Proc. Nat. Acad. Sci.* **107**, 15676 (2010).

X-ray fluorescence microscopy

- Energy dispersive detectors: 3.65 eV per electron-hole pair separation in Si.
- 10 keV photon produces 2740 electrons. Fluctuations: $(2740)^{1/2}$=52, so uncertainty is (52/2740)*10,000 eV=190 eV.
- Detector at 90°: minimize elastic scattering.

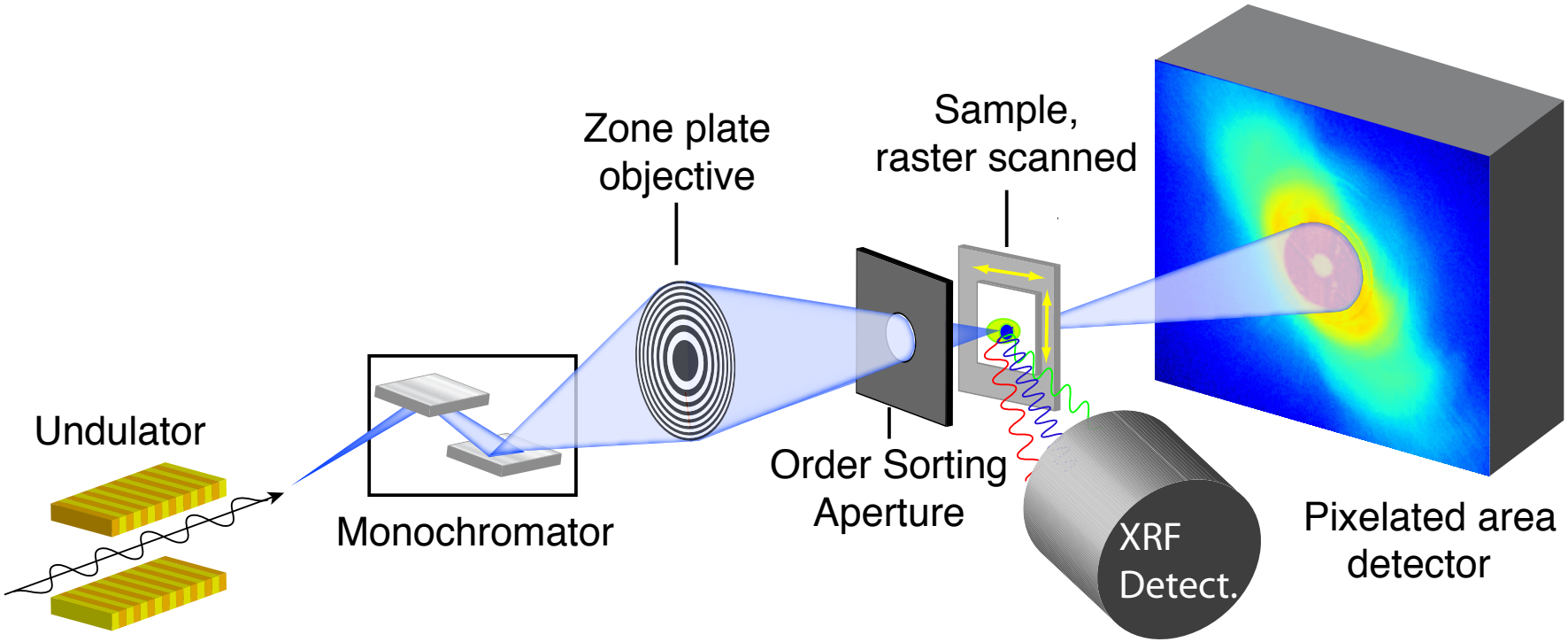

Combined x-ray ptychography and fluorescence

- *Chlamydomonas reinhardtii*, frozen in <0.1 msec from the living state, imaged whole under cryogenic conditions.
- 80 nm resolution in fluorescence, 18 nm resolution in ptychography
- Deng, Vine, Chen, Jin, Nashed, Peterka, Vogt, and Jacobsen, *Scientific Reports* **7**, 445 (2017)

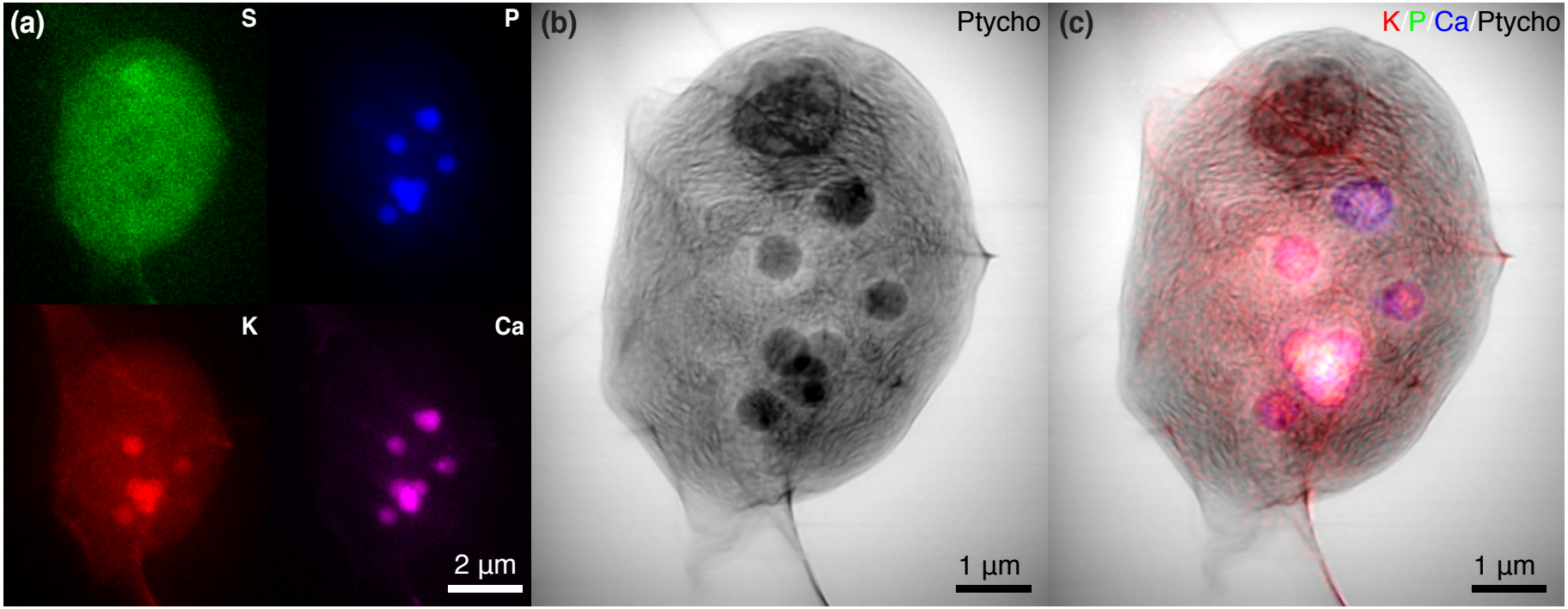

Frozen hydrated alga in 3D

- Deng, Lo, Gallagher-Jones, Chen, Pryor Jr., Jin, Hong, Nashed, Vogt, Miao, and Jacobsen, *Science Advances* **4**, eaau4548 (2018)
- 3D resolution of about 100 nm

Removing/re-adding in turn:

Cl
S
K
P
Ca

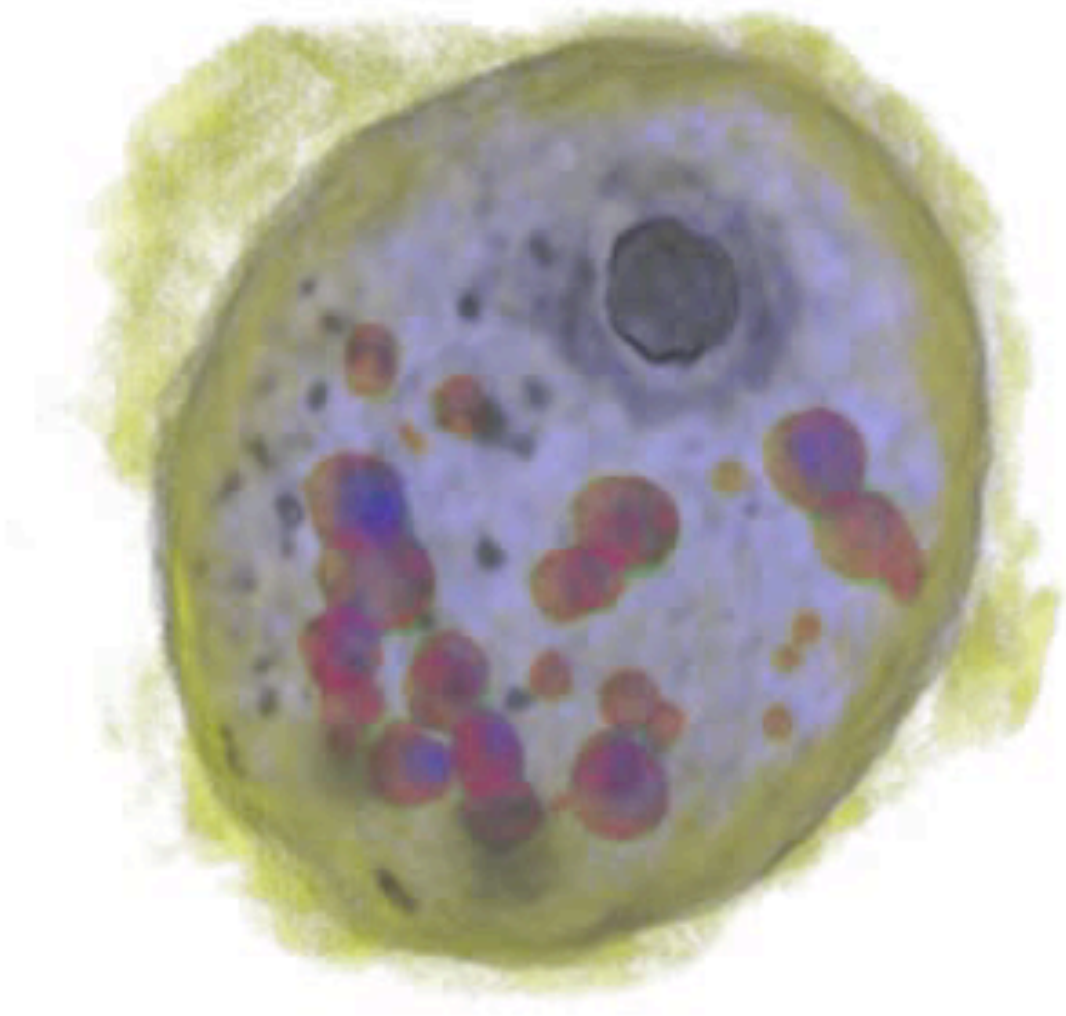

Going beyond the depth of focus (DOF)

- Classical optics: depth of focus goes like DOF~5(transverse resolution)$^2/\lambda$
- Past work: 5•(1 μm)^2 @ 25 keV: DOF=10 cm
- Future: 5•(30 nm)^2 @ 25 keV: DOF=90 μm
- Tomography normally ignores this, and assumes one records a pure projection through the specimen with no diffraction effects (or multiple scattering).

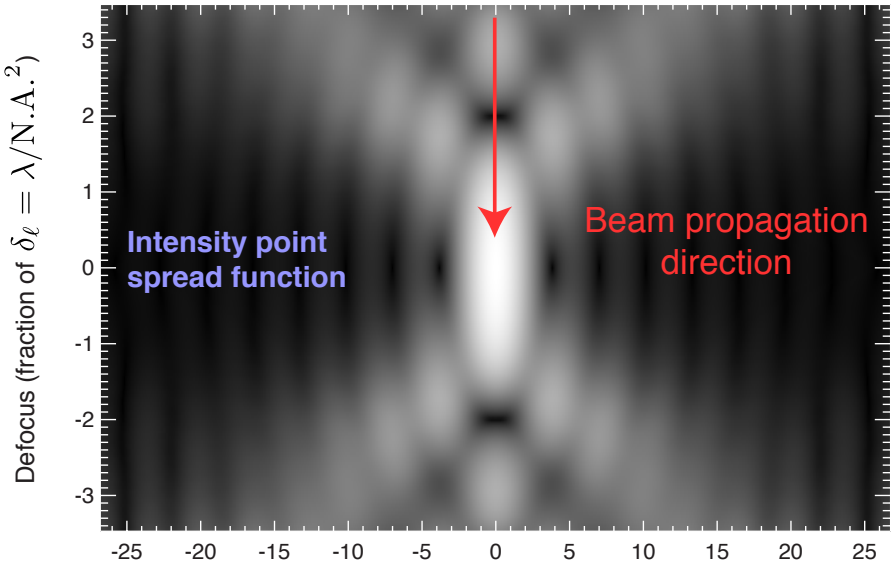

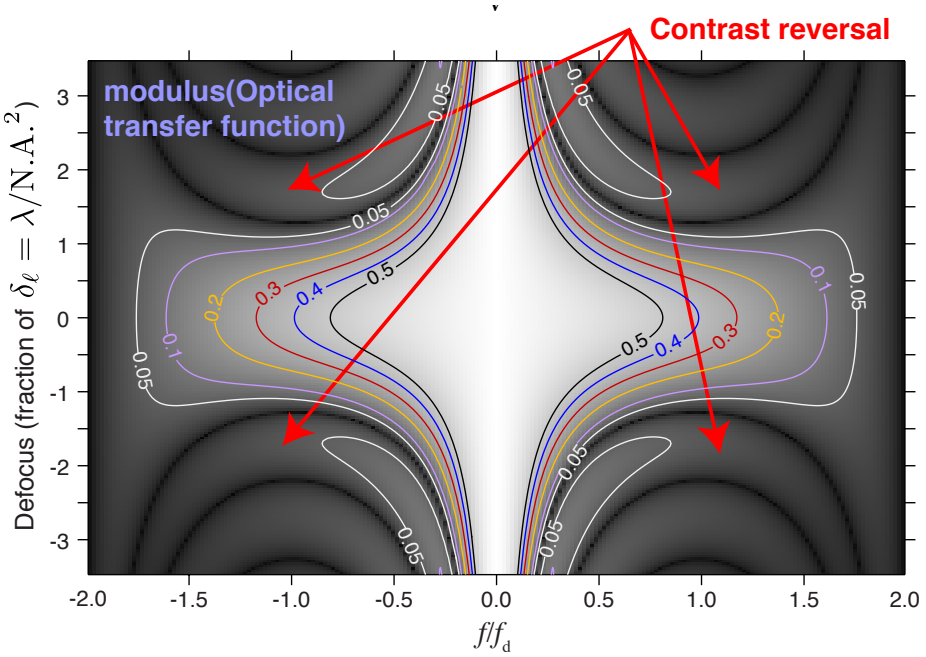

The multislice method

- Multislice method: Cowley and Moodie, *Proceedings of the Physical Society of London B* **70**, 486 (1957); *Acta Crystallographica* **10**, 609 (1957).
- Visible light: beam propagation method. Van Roey *et al.*, *JOSA* **71**, 803 (1981).
- Accounts for multiple scattering effects.
- It even reproduces mirror reflectivity and waveguide effects in x-ray optics! Li and Jacobsen, *Optics Express* **25**, 1831 (2017).

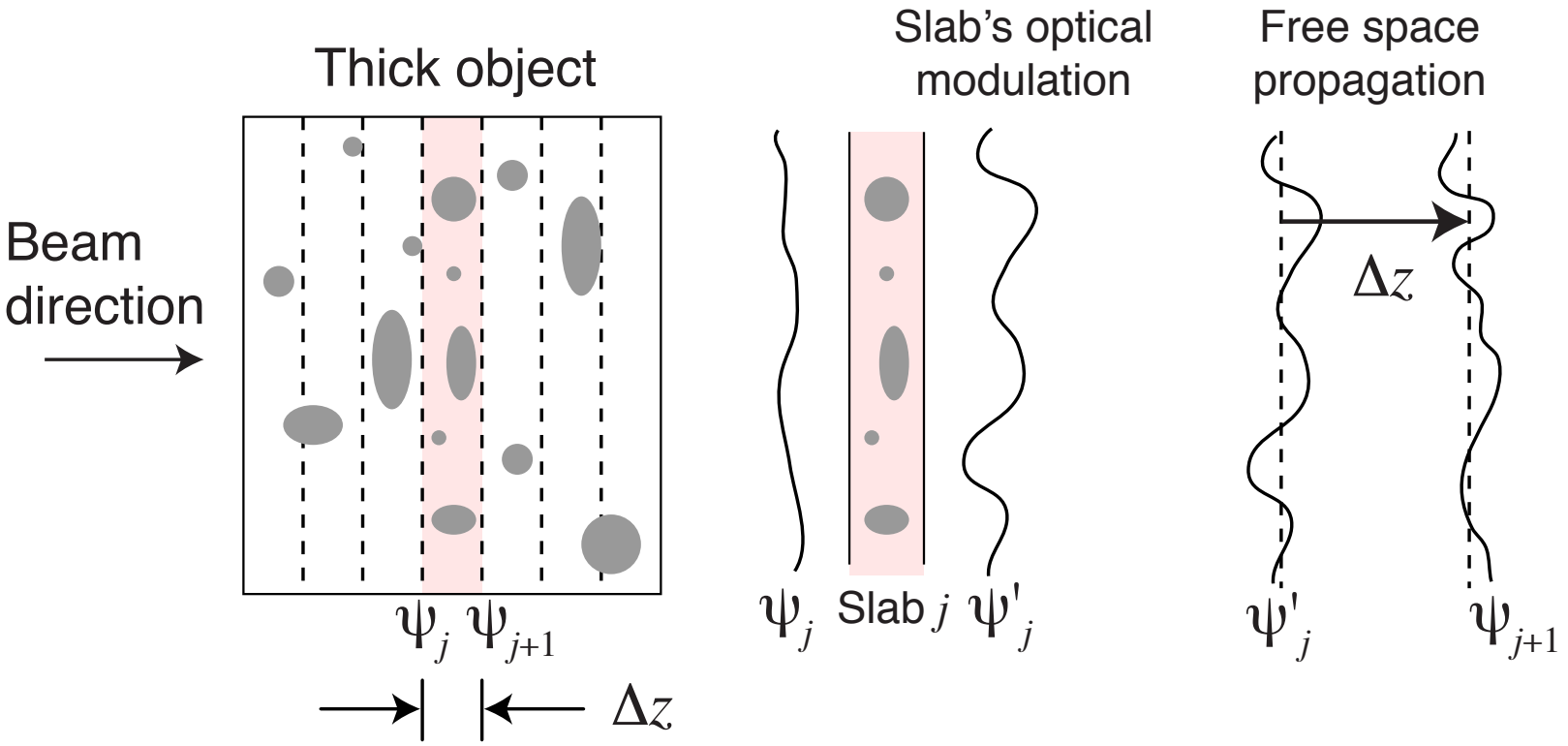

Beyond the depth of focus, and Kierkegaard

- Søren Kierkegaard (1813-1855): “life must be lived forwards, but it is best understood backwards”
- Wavefield through a simulated cell: Thibault, Elser, Jacobsen, Shapiro, and Sayre, *Acta Cryst. A* **62**, 248 (2006).

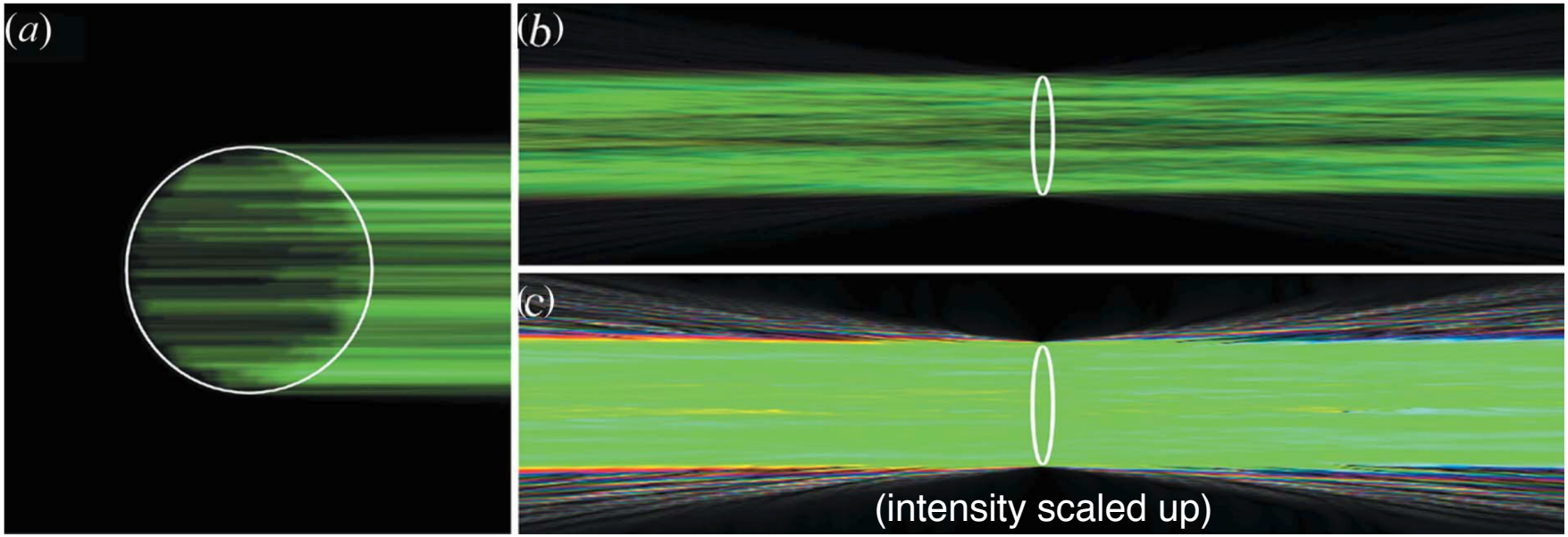

Forward multislice propagation of a wave through a simulated cell

Backward propagation of the correctly-phased far-field wavefield

Numerical optimization of cost functions

- If you know the forward model (multislice), you can define a cost function:

$$C = |I_{\text{measured}} - I_{\text{predicted}}| + \lambda_n R_n$$

- From a present guess of the object, calculate $I_{\text{predicted}}$. Adjust guess based on derivatives (gradient descent), including regularizers R. Iterate.
- No need for phase unwrapping.
- Examples of optimization approach for visible light diffraction tomography:
  - Kamilov *et al.*, *IEEE Transactions on Computational Imaging* **2**, 59 (2016).
  - Review talk on Monday morning by Tomasz Kozacki!

Multislice on continuous 3D objects

- Gilles, Du, Nashed, Jacobsen, and Wild, “3D X-ray imaging of continuous objects beyond the depth of focus limit,” *Optica* **5**, 1078 (2018).
  - 200k core hours for 256^3 with 23x23 probe positions, 70 viewing angles
  - Beyond pure projection approximation: important to rotate over 360° not 180°

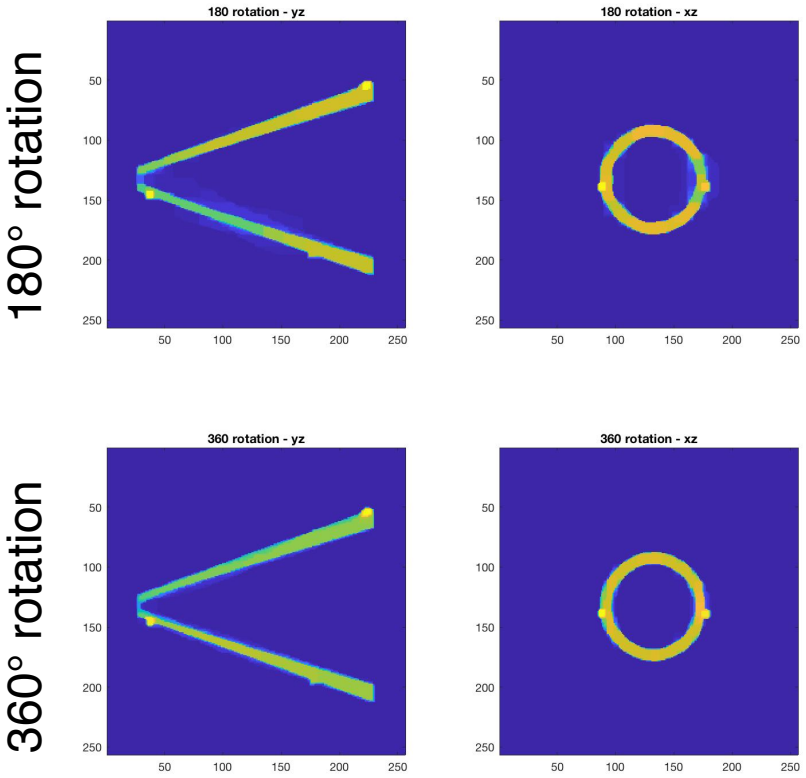

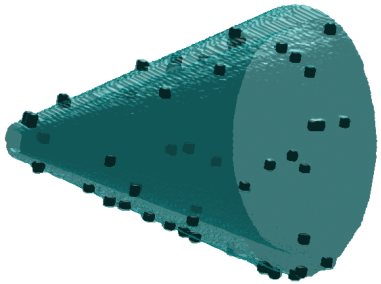

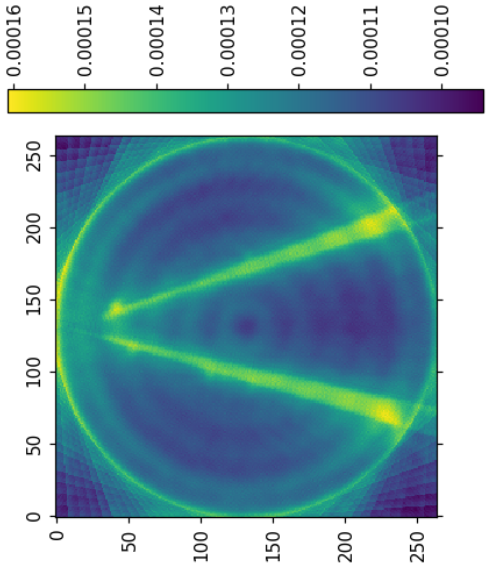

Standard ptychography reconstructions used as projections in tomography

Automatic for the people

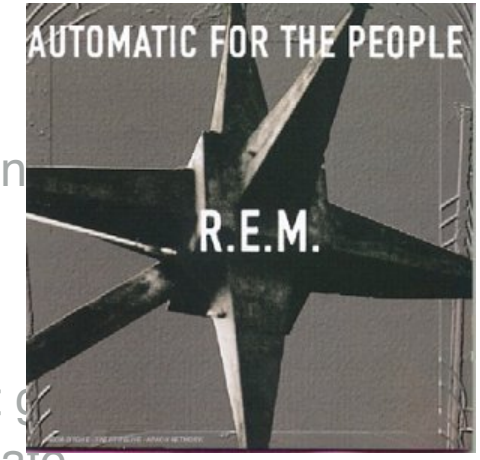

- If you know the forward model, you can define a cost function

$$C = |I_{\text{measured}} - I_{\text{predicted}}| + \lambda_n R_n$$

- From a present guess of the object, calculate $I_{\text{predicted}}$. Adjust g
  derivatives (gradient descent), , including regularizers R. Iterate.
- Calculating derivatives on complex sequences of mathematical operations can be tedious!
- Let's let a computer do the work: calculate derivatives of operations expressed in computer code. Automatic Differentiation!
- Several toolkits available: TensorFlow (from Google), AutoGrad…
- Better performance on high performance clusters: Horovod version of TensorFlow (from Uber) which uses MPI instead of TCPIP for internode communication.

TensorFlow

HOROVOD

Automatic differentiation is competitive!

- Y. Nashed, T. Peterka, J. Deng, and C. Jacobsen, *Procedia Computer Science* **108C**, 404 (2017). doi:10.1016/j.procs.2017.05.101
- PIE: Rodenburg and Maiden. AD: Tensor Flow's Automatic Differentiation
- **Sync: synchronize solutions from subregions at every iteration**
- Async: solve subregions (per computational node) and stitch together at the end

Simulation: 160x160 scan points with 90% overlap, 128x128 detector pixels (1.56 TBytes)

See also S. Kandel, S. Maddali, M. Allain, S. Hruszkewycz, C. Jacobsen, and Y. Nashed, *Optics Express* (accepted)

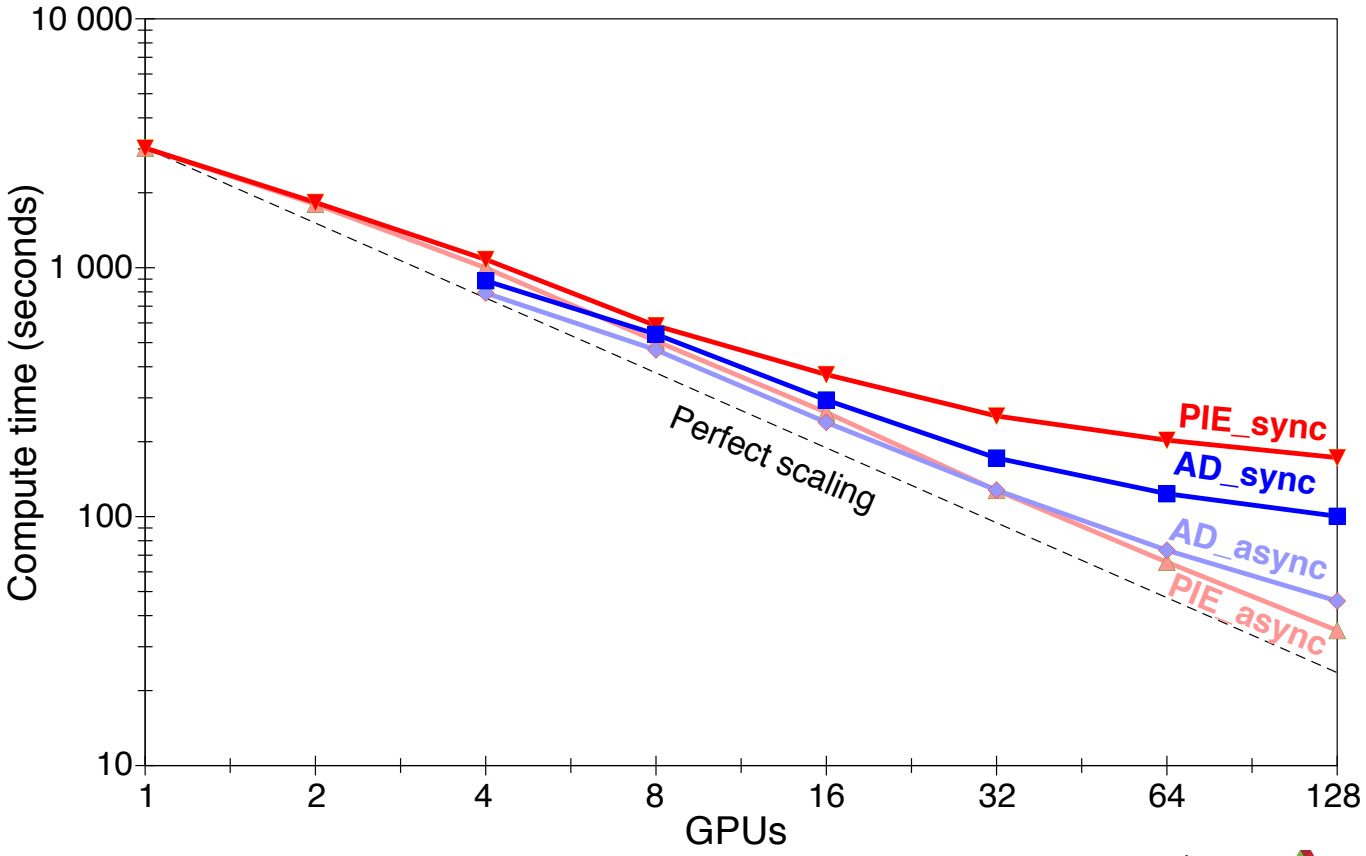

Recent activities in Automatic Differentiation

- Saugat Kandel: One framework can solve multiple inverse problems (far field, near field, Bragg diffraction). *Optics Express* (accepted).
- Sajid Ali and Ming Du: alternative forward models based not on Fresnel propagation, but the finite difference approximation to the Helmholtz equation.
- Ming Du *et al.*: use Automatic Differentiation in TensorFlow to reconstruct 3D objects beyond the Pure Projection Approximation. 23x23 probe positions, 500 viewing angles, regularizers included. 16,500 core hours (46 clock hours) for $(256)^3$.

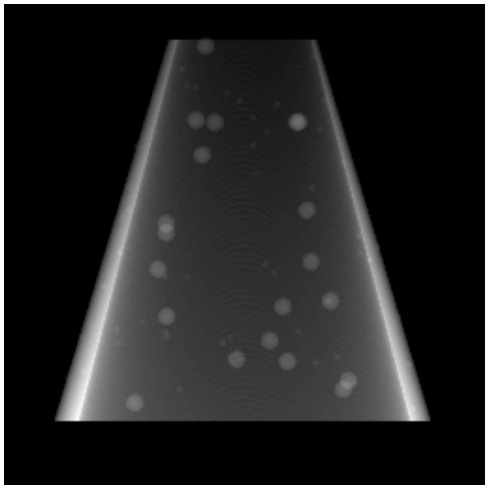

Projection through true object

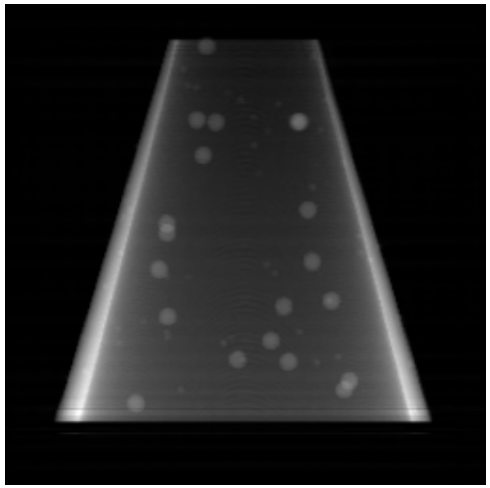

Projection through 3D reconstruction

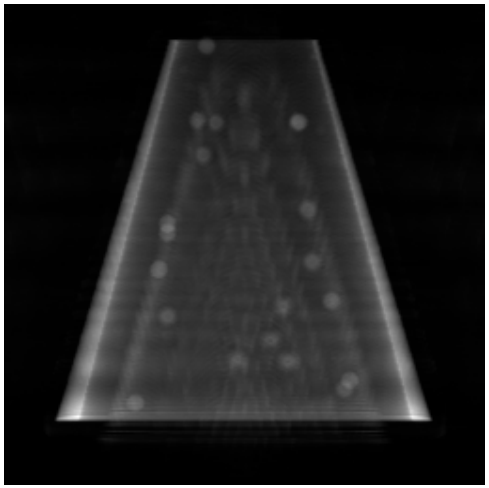

Conventional pure projection imaging

Poisson and Gaussian statistics

- Poisson distribution: if the average value over many, many tests is $\bar{n}$, what's the probability P of seeing n on one particular test?

$$P(n, \bar{n}) = \frac{\bar{n}^n}{n!} \exp(-\bar{n})$$

- Gaussian distribution: same meaning for n, $\bar{n}$, and P, but valid only for large $\bar{n}$:

$$P(n, \bar{n}) = \frac{1}{\sqrt{2\pi\bar{n}}} \exp\left[-\frac{(n-\bar{n})^2}{2\bar{n}}\right]$$

"Bell curve"

Comparing Poisson (exact) and Gaussian

- The Gaussian approximation works well for even very small values of $\bar{n}$

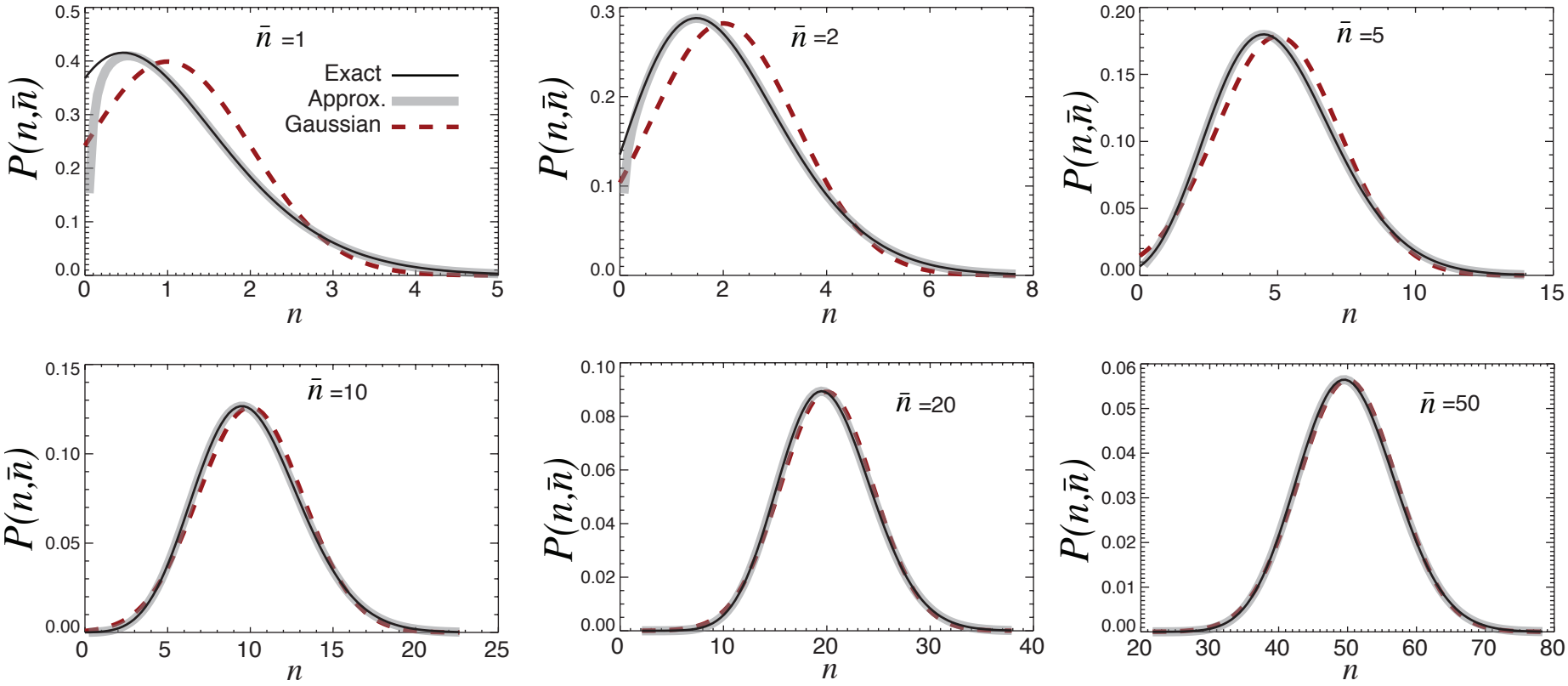

Signal to noise and required number of photons

- Simple statistics on $\bar{n}$ incident photons:

$$\mathrm{SNR} = \frac{\mathrm{Signal}}{\mathrm{Noise}} = \frac{\bar{n}|I_f - I_b|}{\sqrt{(\sqrt{\bar{n}}I_f)^2 + (\sqrt{\bar{n}}I_b)^2}} = \sqrt{\bar{n}}\frac{|I_f - I_b|}{\sqrt{I_f + I_b}} = \sqrt{\bar{n}}\Theta$$

where Θ=contrast parameter, I_f=intensity of feature, I_b=intensity of background. Also account for absorption in overlaying layers.

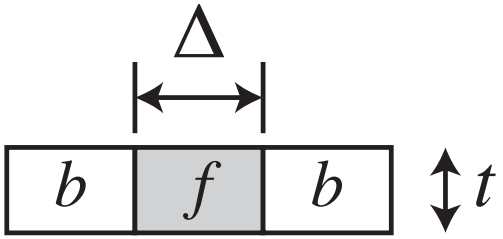

- Thus required number of incident photons $\bar{n}$ is

$$\bar{n} = \frac{\mathrm{SNR}^2}{\Theta^2}$$

- See e.g., Glaeser, *J. Ultrastruct. Res.* **36**, 466 (1971); Sayre *et al.*, *Ultramicroscopy* **2**, 337 (1977); Sayre *et al.*, *Science* **196**, 1339 (1977)

What about imaging in 3D?

- Rainer Hegerl and Walter Hoppe, *Zeitschrift für Naturforschung* **31**(a), 1717 (1976):

> A three-dimensional reconstruction requires the same integral dose as a conventional two-dimensional micrograph provided that the level of significance and the resolution are identical. The necessary dose *D* for one of the *K* projections in a reconstruction series is, therefore, the integral dose divided by *K*.

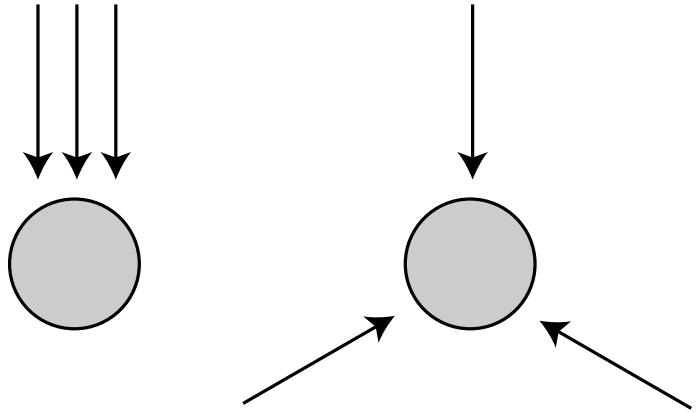

- Originally controversial; now embedded in practice of single particle electron microscopy, medical x-ray tomography.

Calculating dose

- SI units for ionizing radiation: 1 Gray=1 J/kg=100 rad
- Lambert-Beer law with inverse absorption length μ(=1.3 mm for protein at 8.98 keV):

$$I = I_0 e^{-\mu x} \qquad \text{with} \qquad \mu = 2\frac{\rho N_A}{A} r_e \lambda f_2$$

- Energy per thickness with inverse absorption length μ:

$$\frac{dE}{dx} = h\nu \frac{dI}{dx} = h\nu\, \mu\, I_0 e^{-\mu \cdot 0} = I_0\, h\nu\, \mu$$

- Energy per mass (note: I0 is effectively $\overline{n}$):

$$\frac{dE}{dm} = \frac{dE}{dx}\frac{1}{\text{Area} \cdot \rho} = h\nu\, \mu\, I_0 \frac{1}{\text{Area} \cdot \rho} = h\nu\, \frac{I_0\, \mu}{\text{Area} \cdot \rho}$$

Dose numbers

- G factor: number of bonds broken per 100 eV. G~5 for many organic molecules (room temp.)
- Quick estimate to break 1 bond per atom:

$$\frac{(20\ \text{eV/atom}) \cdot (N_A\ \text{atoms/mol}) \cdot (1.6 \times 10^{-19}\ \text{J/eV})}{(12\ \text{g/mol}) \cdot (10^{-3}\ \text{kg/g})} = 1.6 \times 10^{8}\ \text{Gray}$$

- Representative dose in crystallography:

$$\frac{10^{14}\ \text{photons}}{(50\ \mu\text{m})^2} \frac{(8979\ \text{eV/photon}) \cdot (1.6 \times 10^{-19}\ \text{J/ev})}{(1300\ \mu\text{m}) \cdot (1.35\ \text{g/cm}^3) \cdot (10^{-4}\ \text{cm}/\mu\text{m})^3 \cdot (10^{-3}\ \text{kg/g})} = 3.3 \times 10^{7}\ \text{Gray}$$

- "Henderson limit" [Henderson, *Q. Rev. Biophys.* **28**, 171 (1995)]: 2×10^7 Gray is when diffraction spots fade.
- X-ray microscopy: doses of 10^6-10^8 Gray are common, depending on resolution

Dose versus resolution for transmission x-ray imaging

- Calculation of radiation dose using best of phase, absorption contrast and 100% efficient imaging

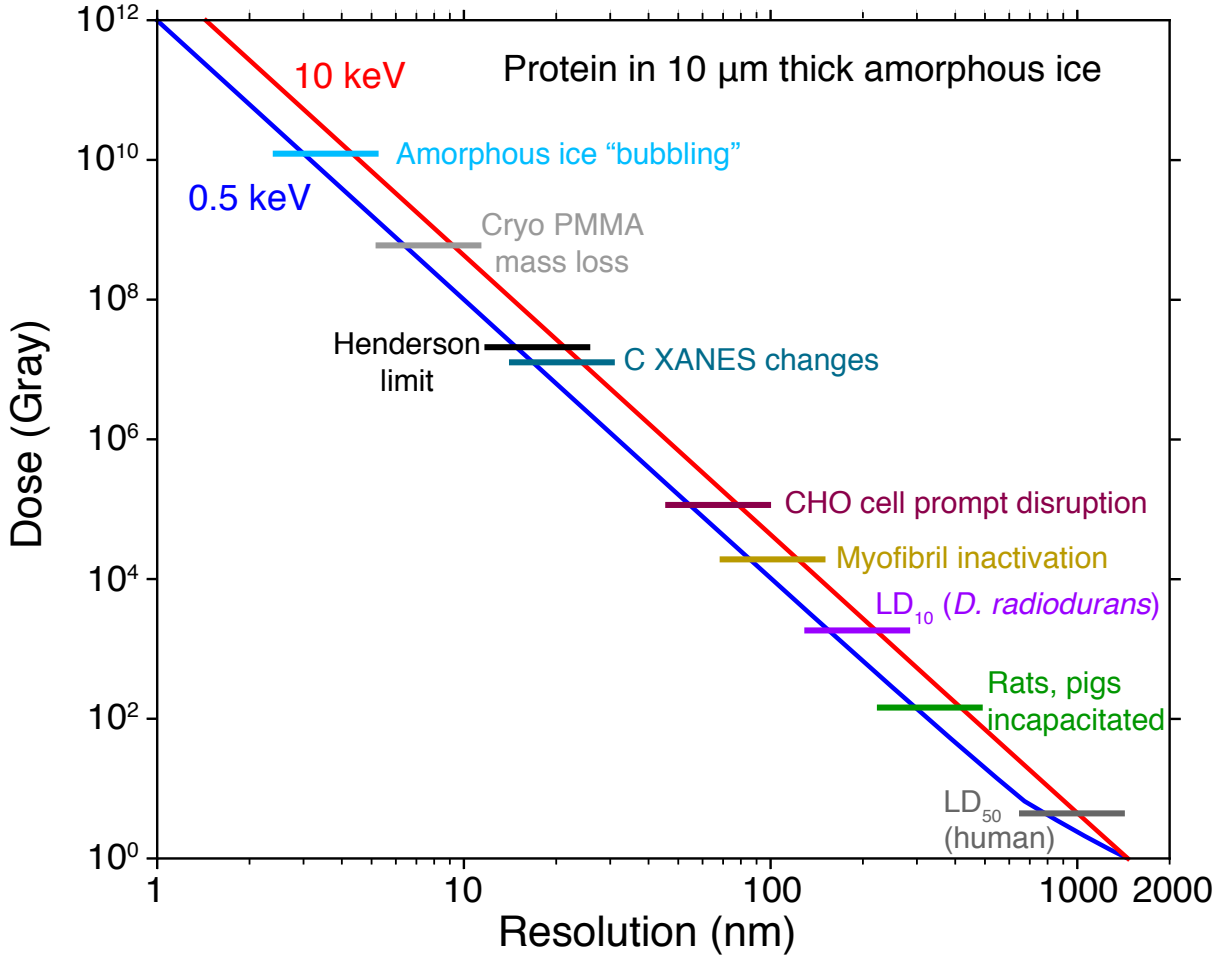

Du and Jacobsen, *Ultramicroscopy* **184**, 293-309 (2018).

X-ray and electron microscopy are complementary

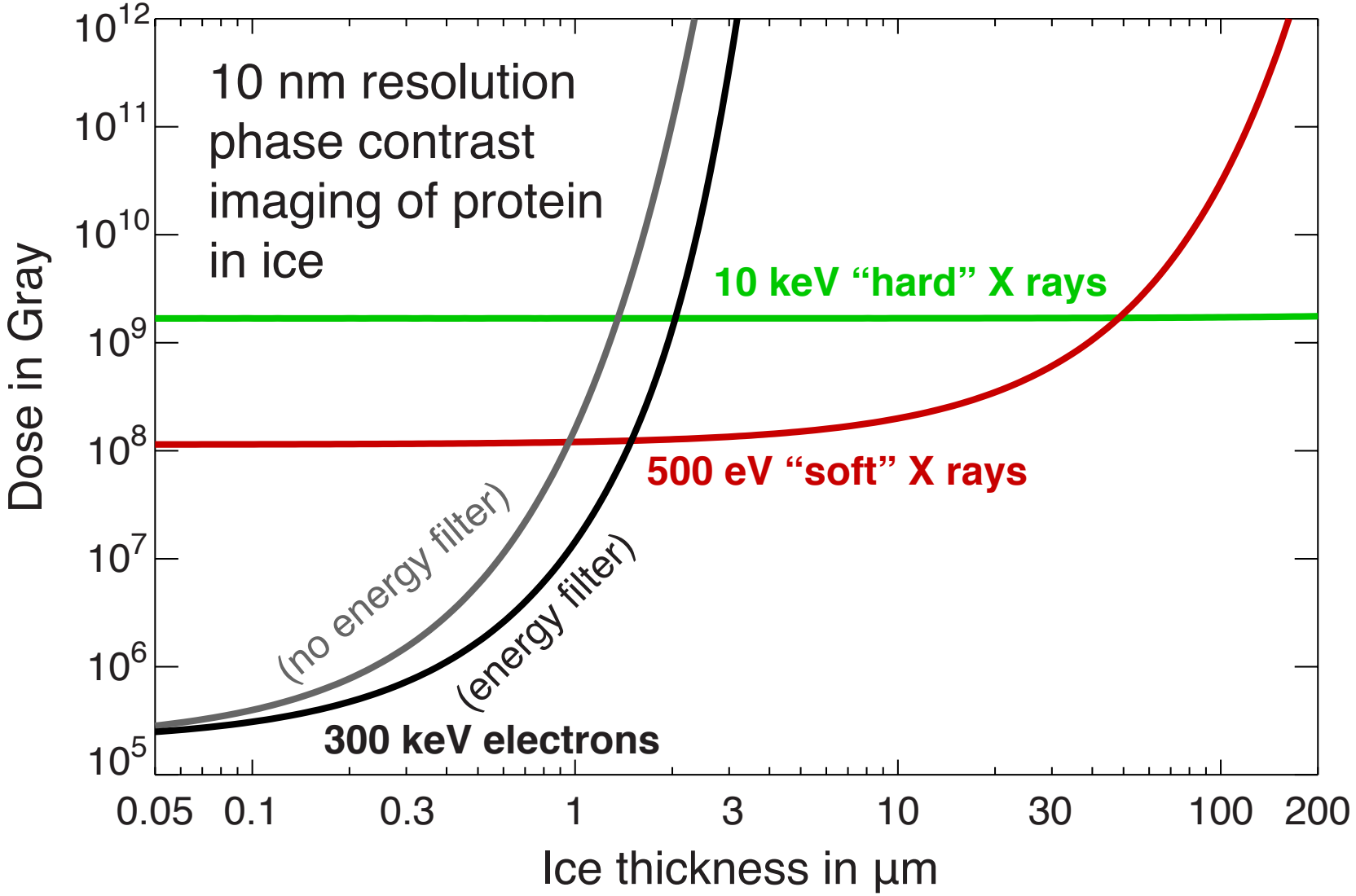

Ming Du and Chris Jacobsen, *Ultramicroscopy* **184**, 293-309 (2018). doi:10.1016/j.ultramic.2017.10.003

X-ray microscopy of initially living cells

- Radiation dose in high resolution x-ray, electron microscopy is ~10^6-10^8 Gray
- 5 Gray (really 5 Sievert) kills people!
- Chinese hamster ovarian (CHO) fibroblasts in culture medium with periodic reflow.
- "Red for dead" fluorescent dyes used to confirm viability over hours with no x-ray exposure.
- Imaged in a soft x-ray scanning transmission microscope (NSLS X1A)

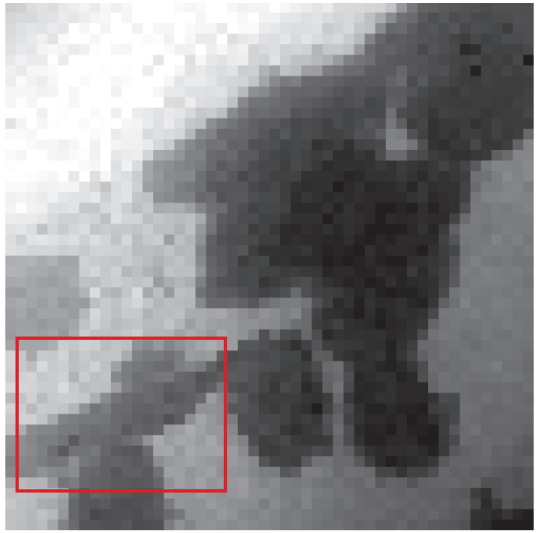

10 μm
6.0×10^2 Gray, ET=2 minutes

Experiment by V. Oehler, J. Fu, S. Williams, and C. Jacobsen, Stony Brook using specimen holder developed by Jerry Pine and John Gilbert, CalTech. In Kirz, Jacobsen, and Howells, *Quarterly Reviews of Biophysics* **28**, 33 (1995).

1 Gray=1 Joule/kg absorbed
1 Sievert=1 Gray•RBE (relative biological effectiveness of radiation type)

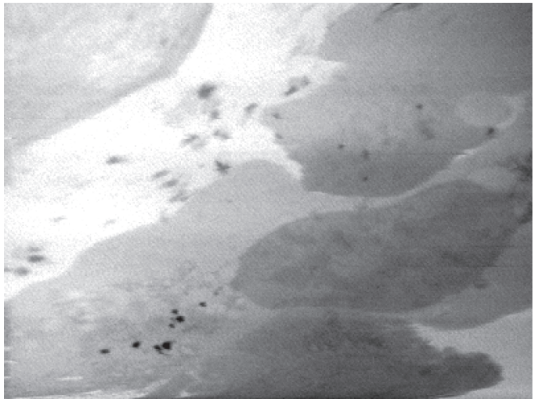

5 μm
1.2×10^5 Gray, ET=9.5 min

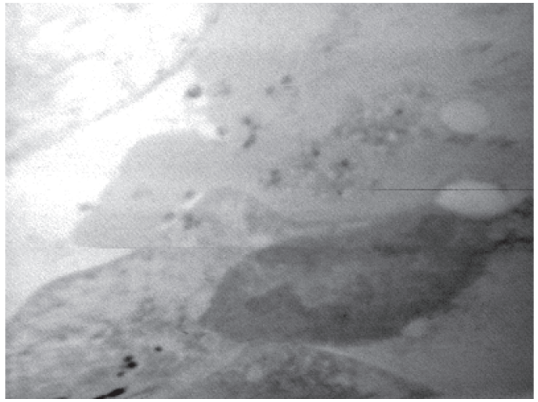

5 μm
2.4×10^5 Gray, ET=17 min

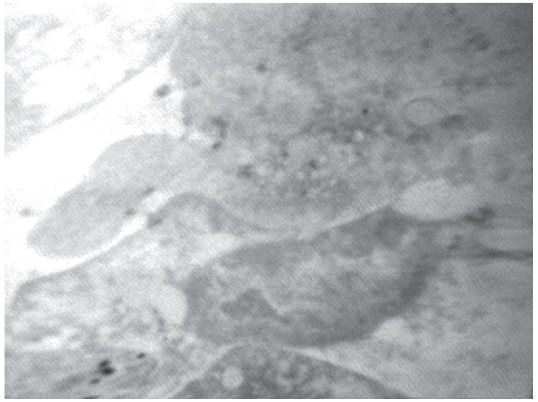

5 μm
3.7×10^5 Gray, ET=24.5 min

Wet, fixed samples: one image is OK

- Chromosomes are among the most sensitive specimens.
- *V. faba* chromosomes fixed in 2% glutaraldehyde. S. Williams *et al*., *J. Microscopy* **170**, 155 (1993)
- Repeated imaging of one chromosome shows mass loss, shrinkage

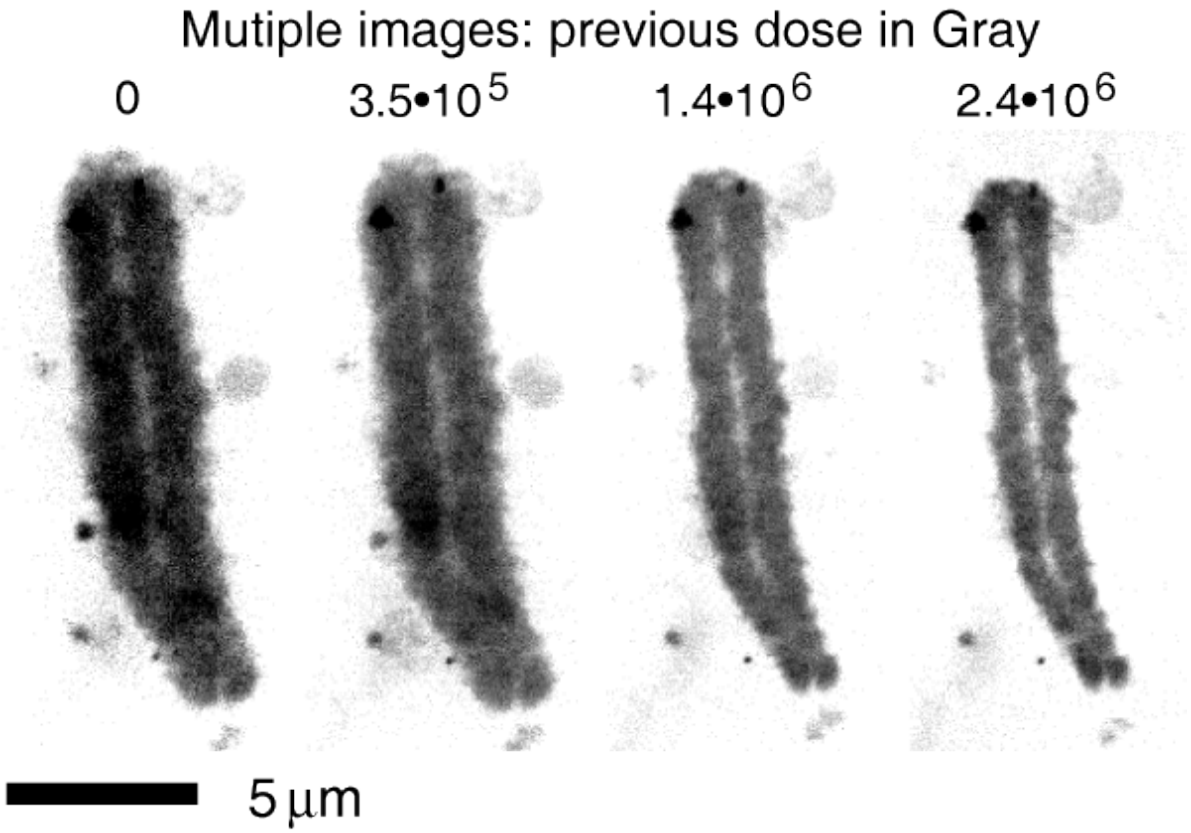

Cryo crystallography

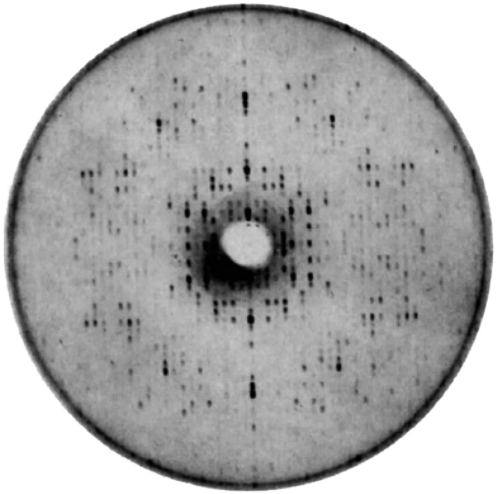

25°C

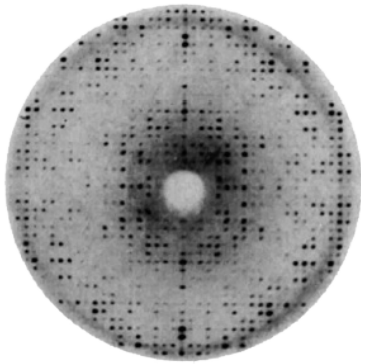

-75°C

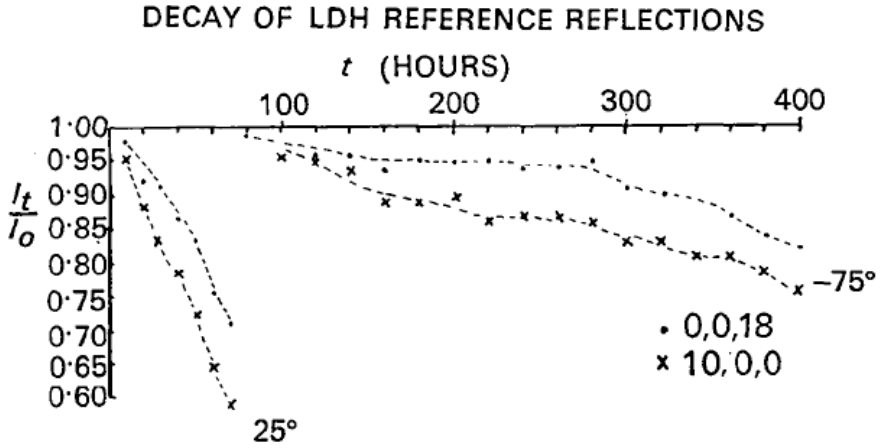

Fig. 5. The ratio I_t/I_0 for two reference reflections plotted as a function of exposure time for a typical native and frozen crystal. I_t represents the intensity at time t. Results for 0,0,18 and 10,0,0 are shown with dots and crosses respectively.

Acta Cryst. (1970). B**26**, 998

Crystallographic Studies on Lactate Dehydrogenase at -75°C

BY DAVID J. HAAS* AND MICHAEL G. ROSSMANN

Crystals of lactate dehydrogenase (LDH) were frozen by equilibration in a sucrose–ammonium sulfate solution, and then dipping into liquid nitrogen. The rate of radiation damage for frozen crystals was tenfold less than for crystals at room temperature. The physical properties of frozen crystals are discussed. Analysis of 3·5 Å data collected at −75°C for native LDH and two heavy atom derivatives showed that these derivatives retained their isomorphism in the frozen state.

See also Low, Chen, Berger, Singman, and Pletcher, *PNAS* **56**, 1746 (1966)

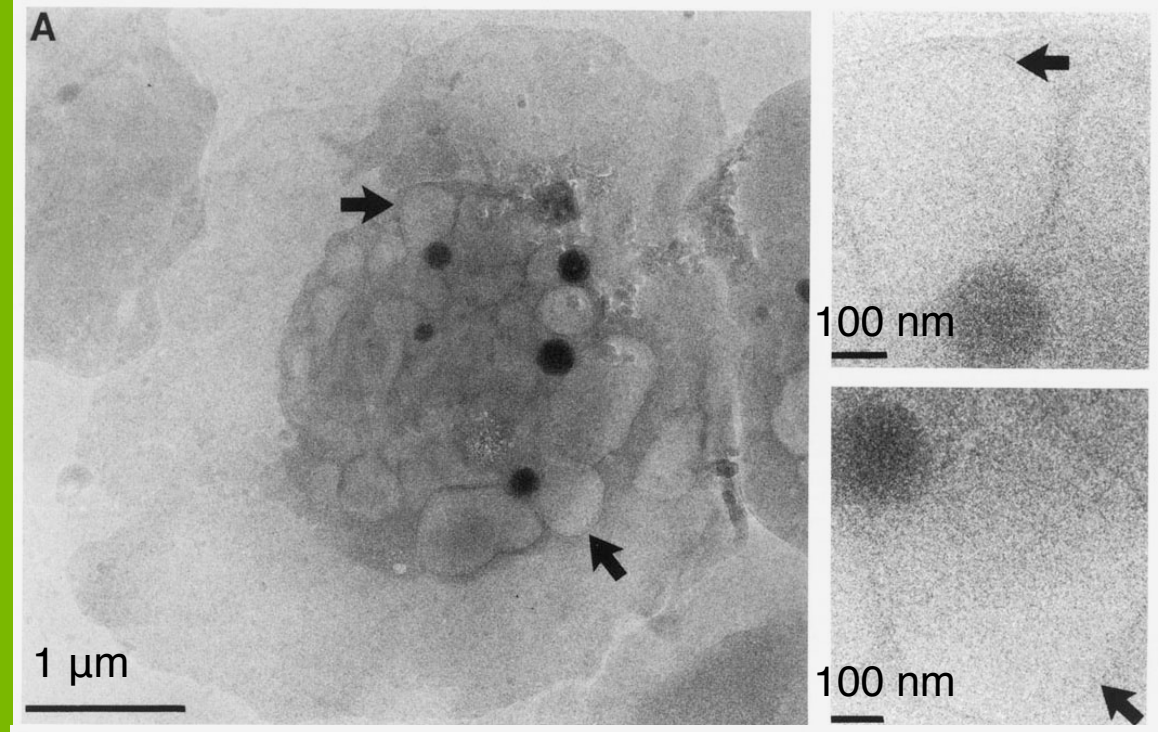

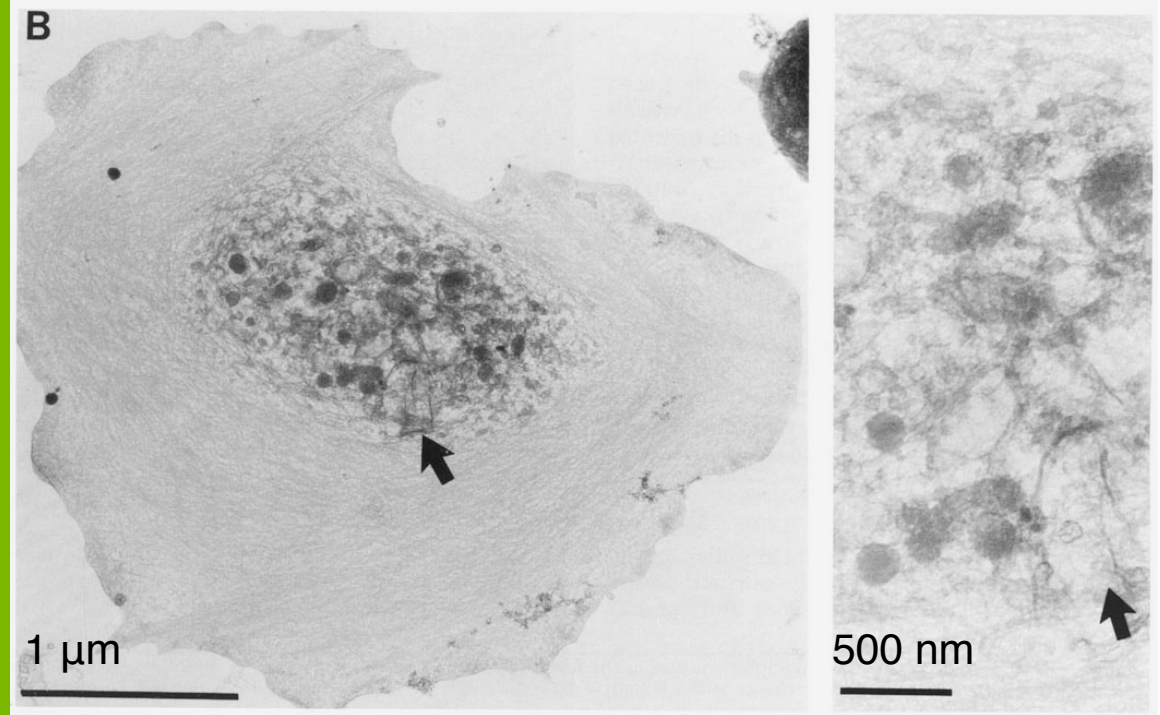

Frozen hydrated

- Human blood platelets
- 1 MeV transmission electron microscope (JEOL-1000)
- O'Toole, Wray, Kremer, and McIntosh, *J. Struct. Bio.* **110**, 55 (1993)

2% glutaraldehyde fix
1% OsO_4 postfix
critical-point dry

Argonne NATIONAL LABORATORY

Cryo preservation keeps chemistry intact

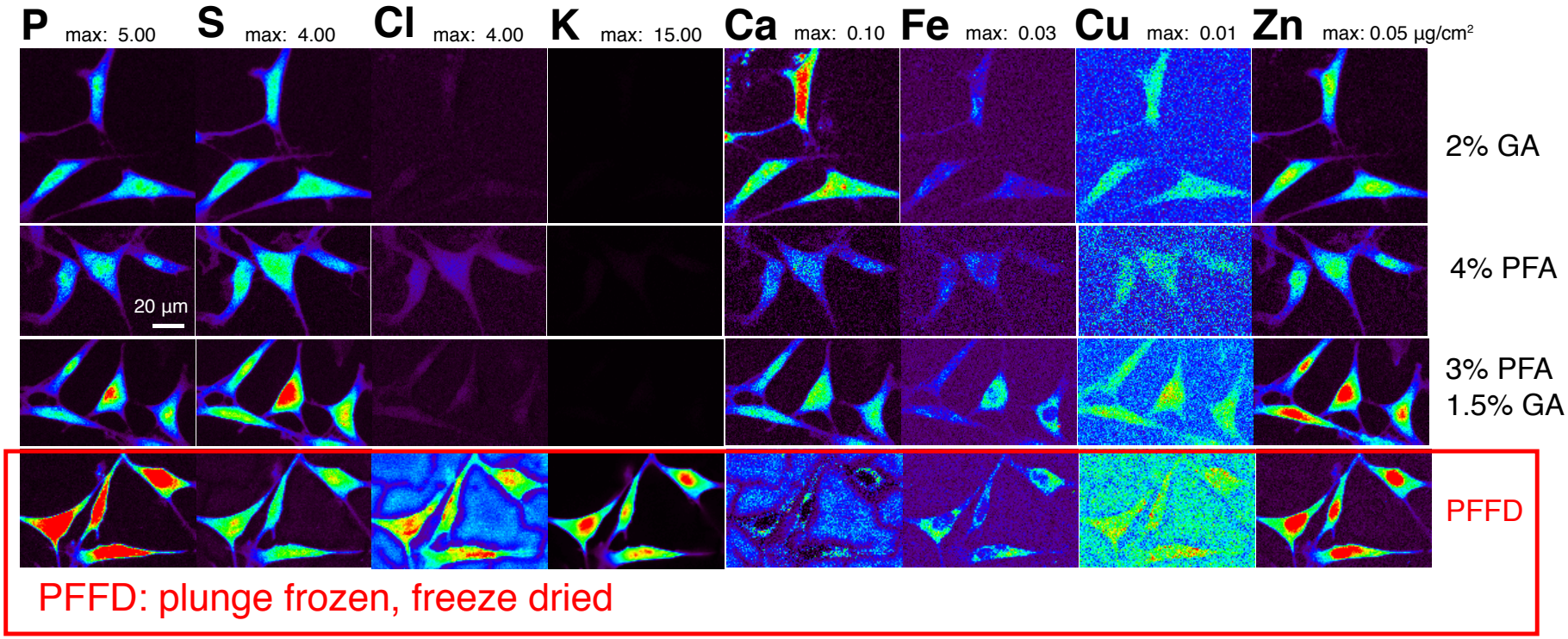

- Jin, Paunesku, Lai, Gleber, Chen, Finney, Vine, Vogt, Woloschak, and Jacobsen, *J. Microscopy* **265**, 81 (2017).
- See also Perrin, Carmona, Roudeau, and Ortega, *J. Analyt. Atom. Spectr.* **30**, 2525 (2015).

Metals in cell division

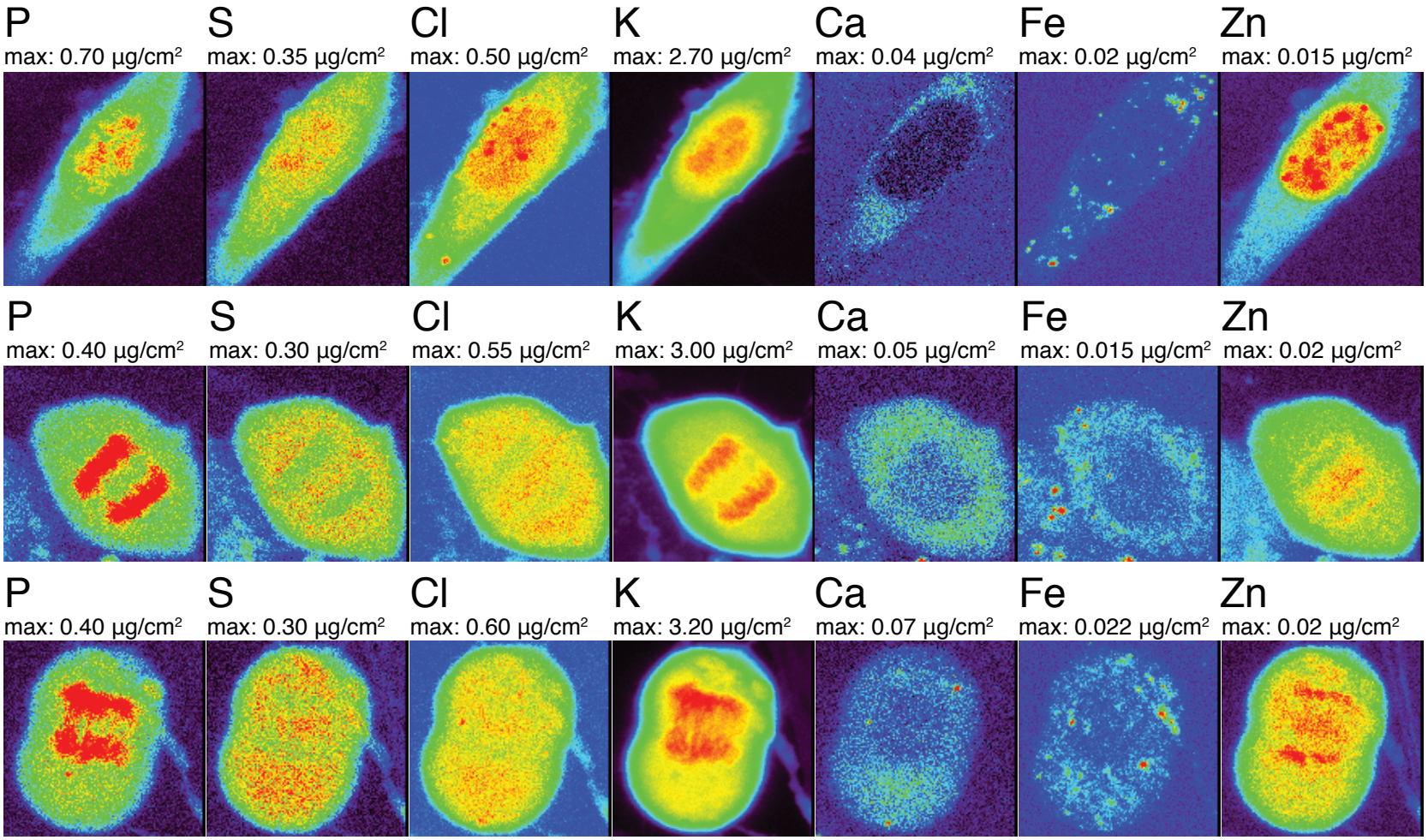

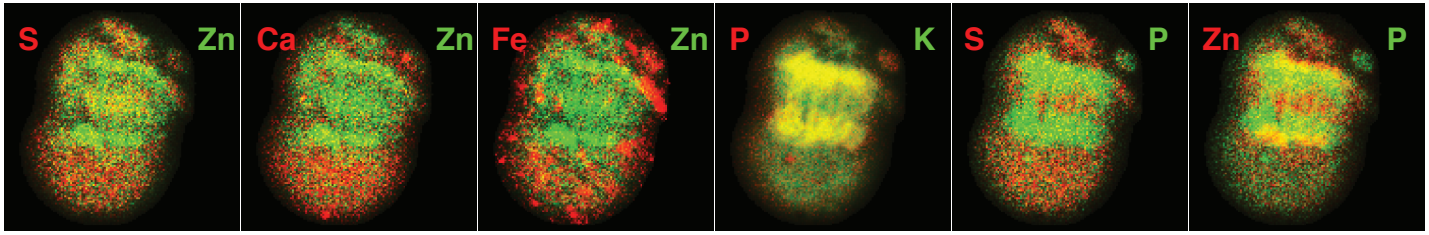

Qiaoling Jin, Everett Vacek,
Si Chen, Barry Lai,
Tom O'Halloran,
Chris Jacobsen

Radiation damage resistance in cryo microscopy

Frozen hydrated fibroblast image after exposing several regions to ~10^{10} Gray

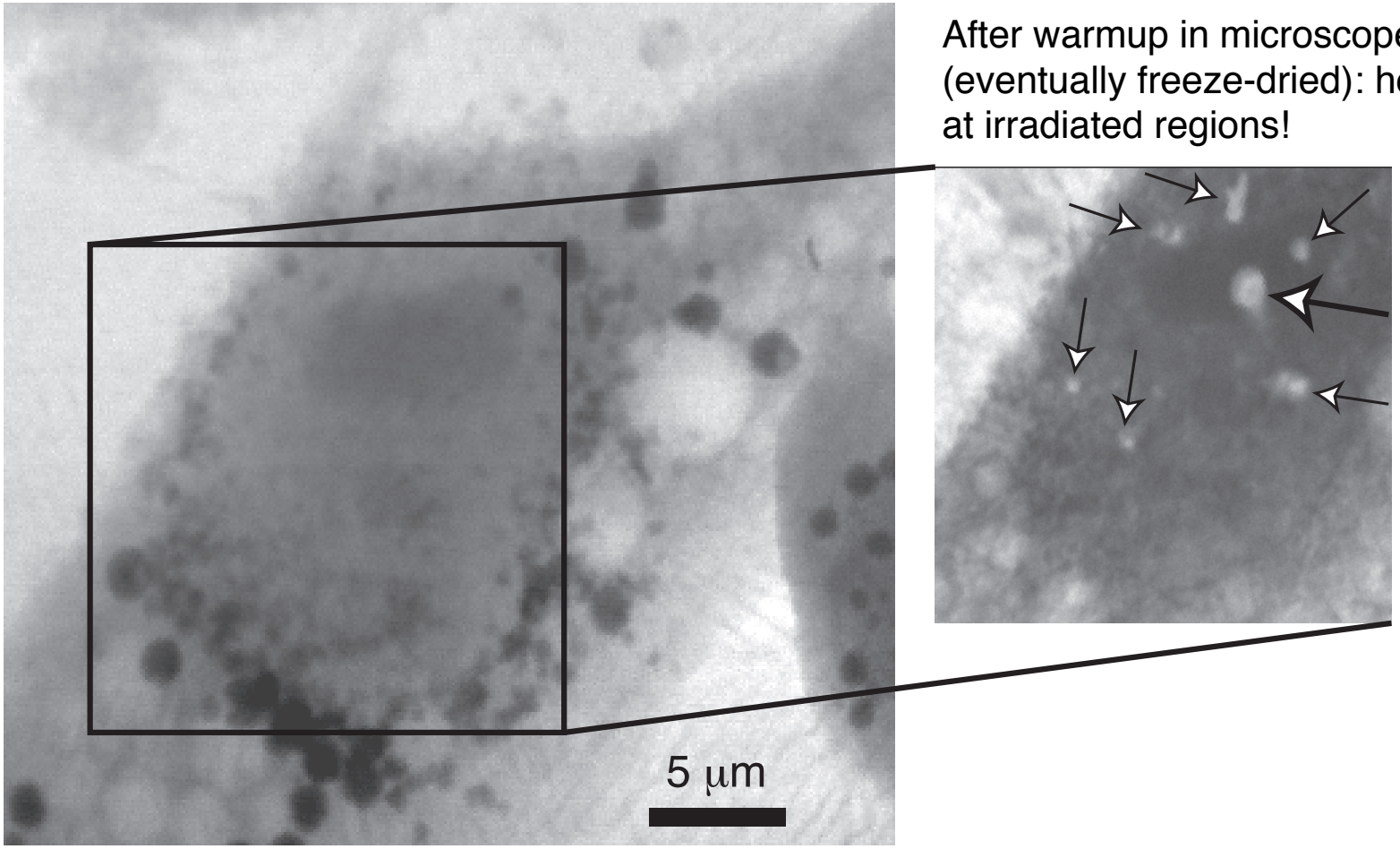

After warmup in microscope (eventually freeze-dried): holes at irradiated regions!

Maser *et al.*, *J. Micros.* **197**, 68 (2000)

Radiation damage studies: poly (methyl methacrylate) or PMMA

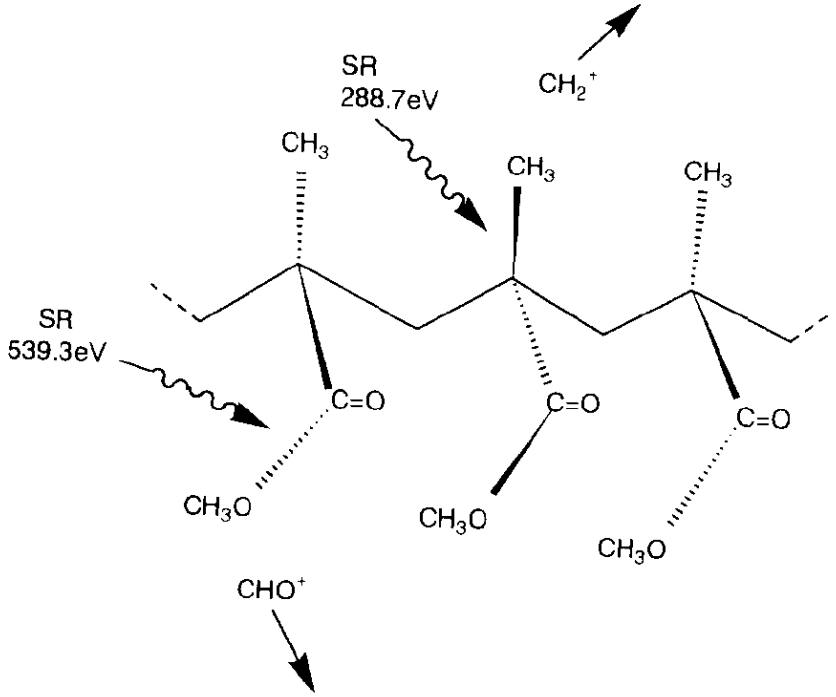

Tinone *et al.*, *Appl. Surf. Sci.* **79**, 89 (1994)

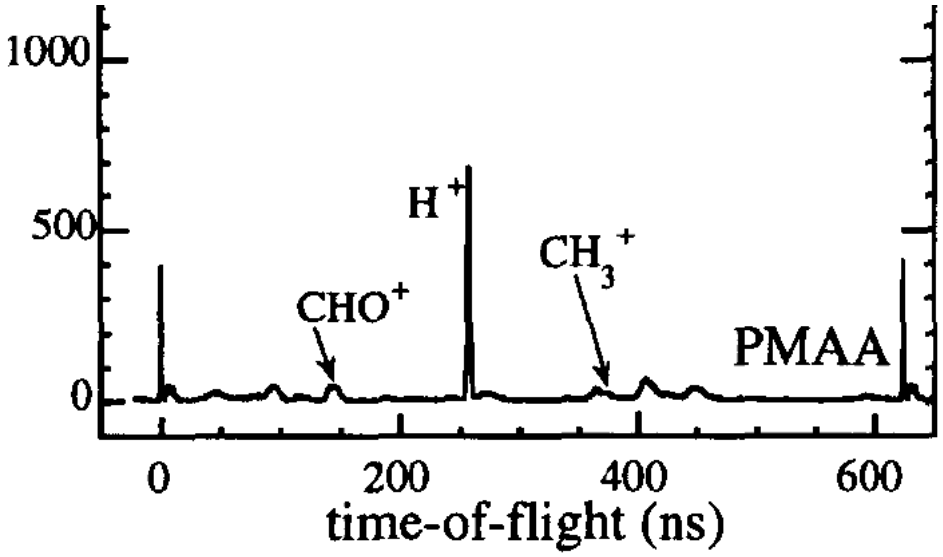

Tinone *et al.*, *J. Electron Spect. Rel. Phen.* **80**, 117 (1996).

PMMA at room, LN2 temperature

- Beetz and Jacobsen, *J. Synchrotron Radiation* **10**, 280 (2003)
- Repeated sequence: dose (small step size, long dwell time), spectrum (defocused beam)
- Images: dose region (small square) at end of sequence

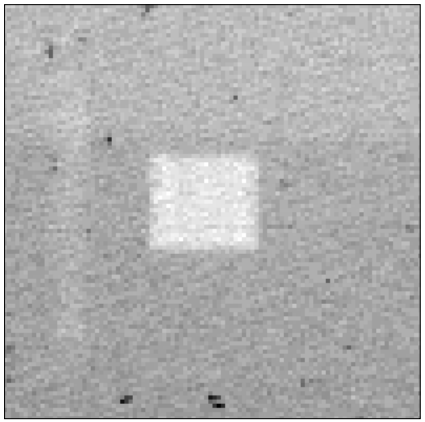

Room temperature: mass loss immediately visible

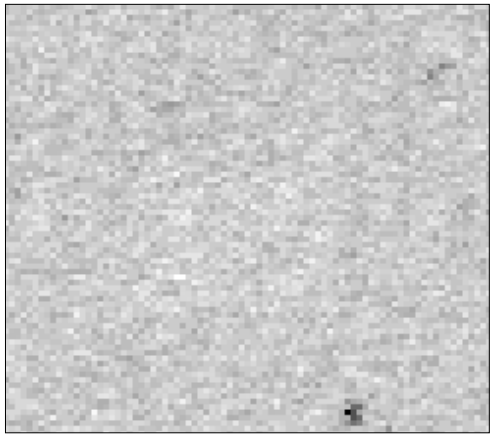

LN_2 temperature: no mass loss immediately visible

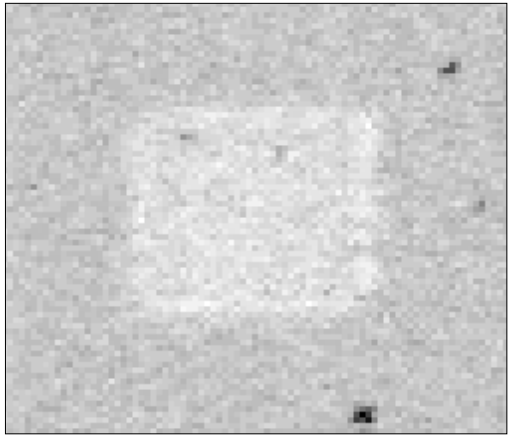

After warm-up: mass loss becomes visible

PMMA at 300 K and 110 K: chemistry and mass

LN_2 temp: protection against mass loss, but not against breaking bonds (at least C=0 bond in dry PMMA)

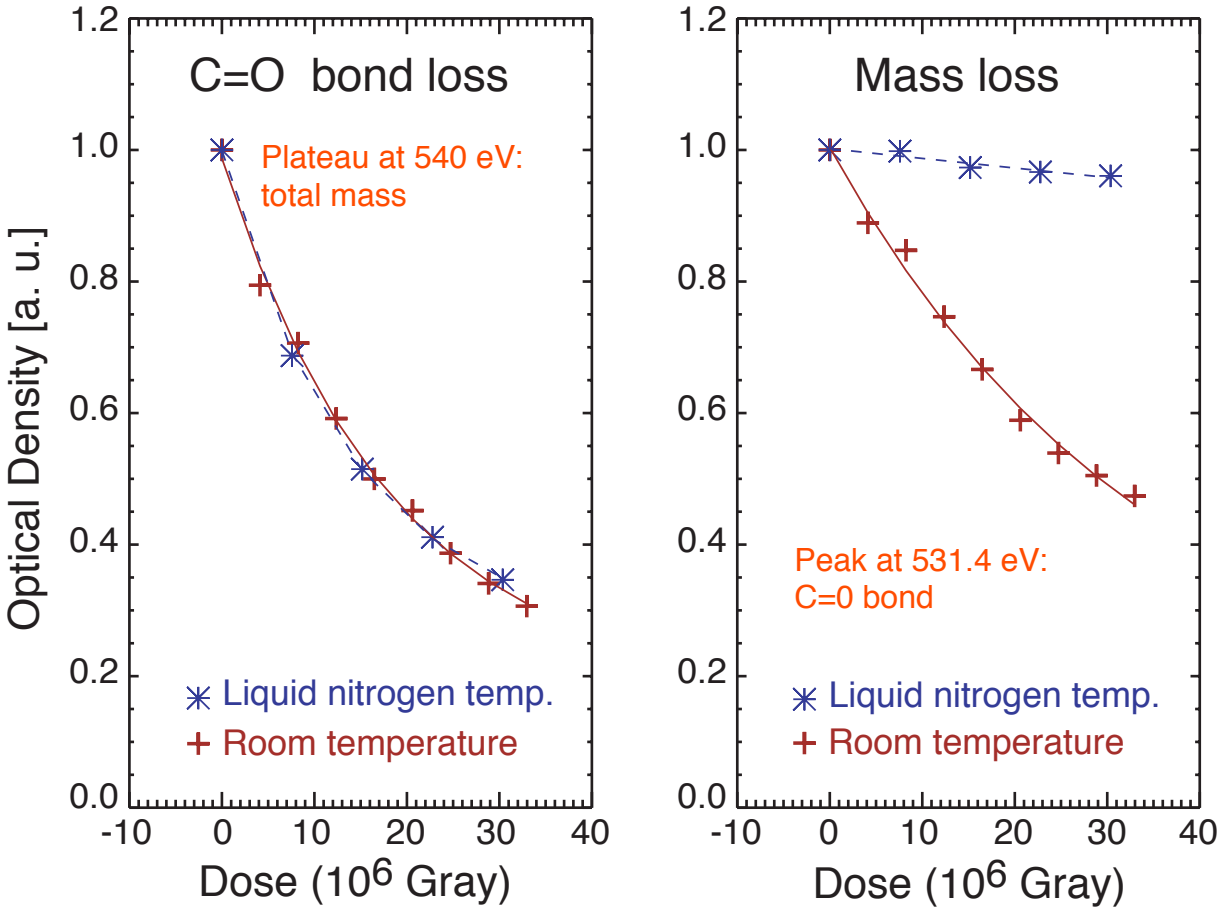

Beetz and Jacobsen, *J. Synchrotron Radiation* **10**, 280 (2003)

The Ramen noodle model of radiation damage

Macromolecular chains with no “encapsulating” matrix
(dry, room temperature wet)

The Ramen noodle model of radiation damage

Macromolecular chains in an “encapsulating” matrix
(frozen hydrated)

The Ramen noodle model of radiation damage

Actual noodles *were* harmed during the filming of this movie

Dose versus resolution for transmission x-ray imaging

- Calculation of radiation dose using best of phase, absorption contrast and 100% efficient imaging

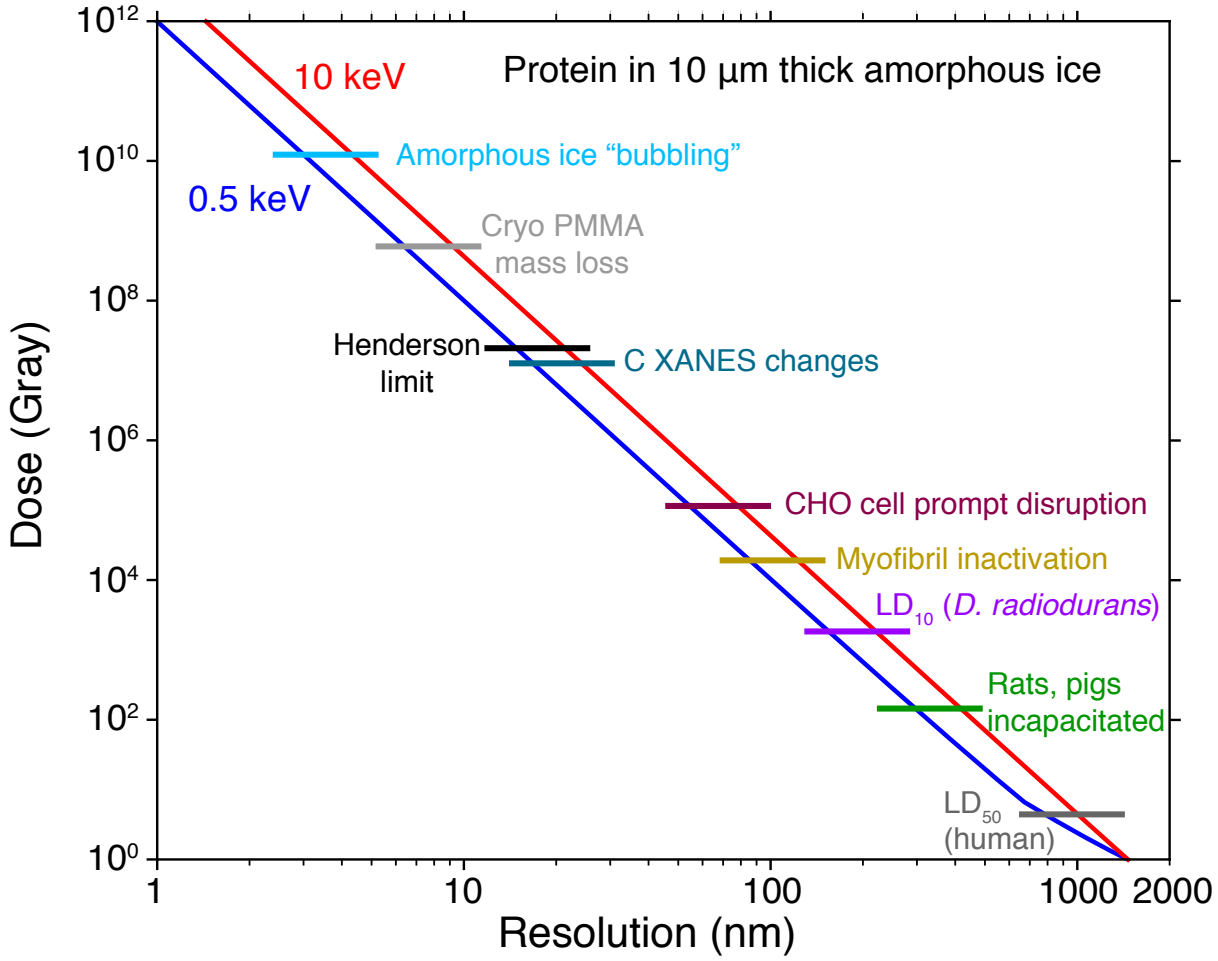

Du and Jacobsen, *Ultramicroscopy* **184**, 293-309 (2018).

Achievable resolution?

- Howells *et al.*, *J. Electron Spectroscopy and Related Phenomena* **170**, 4 (2009)